Royal Netherlands
Meteorological Institute
Ministry of Infrastructure and the Environment

Advanced Delta Change method

Extension of an application to CMIP5 GCMs

P. Kraaijenbrink

De Bilt, 2013 | Internal report; IR 2013-04

Advanced Delta Change method:

Extension of an application to CMIP5 GCMs

Trainee report

Royal Netherlands Meteorological Institute

Version 2

April 2013

Philip Kraaijenbrink MSc – 3132102

Master student Physical Geography

Utrecht University

Supervisors:

Jules Beersma (KNMI)
Maarten Zeylmans van Emmichoven (UU)

Royal Netherlands
Meteorological Institute
Ministry of Infrastructure and the Environment

Universiteit Utrecht

Royal Netherlands Meteorological Institute
PO Box 201, 3730 AE De Bilt, The Netherlands

Visiting address: Wilhelminalaan 10, De Bilt
Telephone +31 30 22 06 911
www.knmi.nl

Utrecht University
P.O. Box 80020, 3508 TA Utrecht, The Netherlands

Visiting adress: Budapestlaan 4, Utrecht
Telephone + 31 30 253 3550
www.uu.nl

PREFACE

This document is the final report of my scientific internship at the Royal Netherlands Meteorological Institute. At the department of climate services I have continued the trainee work of Astrid Ruiter, a fellow student. The internship has functioned as the final five months of my master in Physical Geography at Utrecht University, after which I will directly obtain my master degree.

Daily supervision of the internship has been performed by Jules Beersma of the KNMI. I want to thank him for his useful explanations of the sometimes hard to grasp methodology and his patience, every time I knocked at his door. Furthermore I want to thank my colleague Adri Buishand for providing insights in problems and solutions during his co-supervision. At last, I want to thank Maarten Zeylmans van Emmichoven, my supervisor from Utrecht University, for his support and, very importantly, for pointing out the vacancy of this internship as I enjoyed both the work and working environment.

TABLE OF CONTENTS

LIST OF FIGURES

LIST OF TABLES

LIST OF APPENDICES

1. INTRODUCTION

1.1. Importance of future precipitation data

During and after the industrialization and development of the world since the 19th century, a great rise in world population together with urbanisation has put stress on the environment and its space. Besides our imprint on flora and fauna, the more and more densely populated areas encounter threats from natural processes that thereby become classified as natural hazards. In the Netherlands, which comprises mainly a densely populated delta, the predominant threatening natural process is that of river flooding. Due to this threat, water management and flooding risk mitigation have already been practised here for multiple centuries. Hence most rivers in the Netherlands have been diked, anthropogenic barrages and the like have been placed and the famous "Dutch Waterworks" provide an innovative barrier against the sea (van de Ven & Lowlands, 2004) .

In the last decades the increase in knowledge about the future climate, a climate that will most likely be characterized by an increase in temperature and (extreme) precipitation (Alley et al., 2007), gives rise to concern in the Netherlands about possible future increases in river discharge and flooding risks. To assess these risks and to determine a new design discharge for the coming decades, i.e. the extreme river discharge for which protective measures such as dikes are designed to withstand (Bouwer et al., 2010), hydrological modelling is required that is based on data about the future climate. This data can in principle be obtained from global climate models (GCMs), however the output of the GCMs cannot be used directly for hydrological modelling because of the coarse spatial resolution and systematic biases in temperature and precipitation. To solve this issue methods have been developed that are able to project the GCM climate change signal onto historical time series that have a smaller, more suitable, spatial scale. One of these methods is the so called delta change method.

1.2. The delta change method

The delta change method is a transformation that scales historical precipitation time series to obtain series that are representative for a future climate. Usually historical time series are used for the transformation. The coefficients required in the transformation are obtained from the GCM climate change signal. For precipitation this signal is essentially the relative difference in precipitation between a control period of the GCM, i.e. the same period as the historical time series, and a future period. As the historical data and GCM data is usually present on very different spatial scales, a linkage between the two scales is required. This is performed by the use of a common grid to which the observation data is aggregated and the GCM data is interpolated.

The classic delta change method comprises a linear transformation of mean precipitation values, which may result in an unrealistic change of the precipitation distribution compared to the changes that occur in the GCMs. However, detailed insight in the change of the extremes in the precipitation distribution is valuable for research and modelling, as many environmental processes trigger only at extreme low or high precipitation amounts, e.g. flooding, erosion and vegetation stress. To accommodate this, a revised version of the delta change method was developed by Van Pelt (Van Pelt et al., 2012), which is called the advanced delta change (ADC) method. This revised method focuses primarily on increasing detail in the high end of the distribution as it is aimed at aiding hydrological modelling of extreme discharge events in the Netherlands. The principal difference with the original delta change method is that the revised method uses a non-linear transformation based on the 60% and 90% quantiles of the precipitation distribution (Fig. 7). Furthermore, biases in these quantiles in the control period of the GCM compared with the observation series are corrected for.

Van Pelt has applied the ADC method to observation data of 134 sub-basins of the Rhine basin, which were defined for hydrological simulations with the Hydrologiska Byråns Vattenbalansavdelning (HBV). model (Bergström & Singh, 1995) . To determine the transformation coefficients Van Pelt used multiple GCMs that belong to the Coupled Model Intercomparison Project Phase 3 (CMIP3). Her study showed that using a non-linear transformation is a feasible method to yield small scale daily data that incorporates the relative change of the precipitation distribution, which could be used for modelling the effects of climate change on hydrological extremes.

1.3. CMIP5 GCMs and RCPs

Relatively recently, numerous new GCMs were developed as part of the Coupled Model Intercomparison Project Phase 5 (CMIP5). With this project (Taylor et al., 2012) a new method of climate forcing is introduced in the models, the so called representative concentration pathways (RCPs). Previously GCMs were driven by greenhouse gas concentration estimates that were based on anthropogenic emissions as well as albedo differences due to land use changes. These scenarios were defined in the IPCC Special Report on Emission Scenarios (SRES) and correspond to specific combinations of future technological, economic and political conditions (Nakićenović et al., 2000). The new approach is to not directly prescribe certain emission scenarios as drivers, but a predetermined future path of radiative forcing in W/m^2 by using the RCPs (Fig. 1). However, these paths were determined with certain scenarios in mind. The forcing estimates are based on greenhouse gases and other forcing agents, but do not include direct impacts of for example land use or mineral dust (IIASA, 2013).

There are four main RCPs defined up to the year 2100, each developed by an independent research group using integrated assessment analysis and modelling. Temporal extensions to the year 2300 are made using simple algorithms to drive long-term earth-system simulation experiments. The RCPs have a suffix that indicates the radiative forcing in W/m^2 by the year 2100 as reported by the modellers. A concise description per RCP is provided in Table 1.

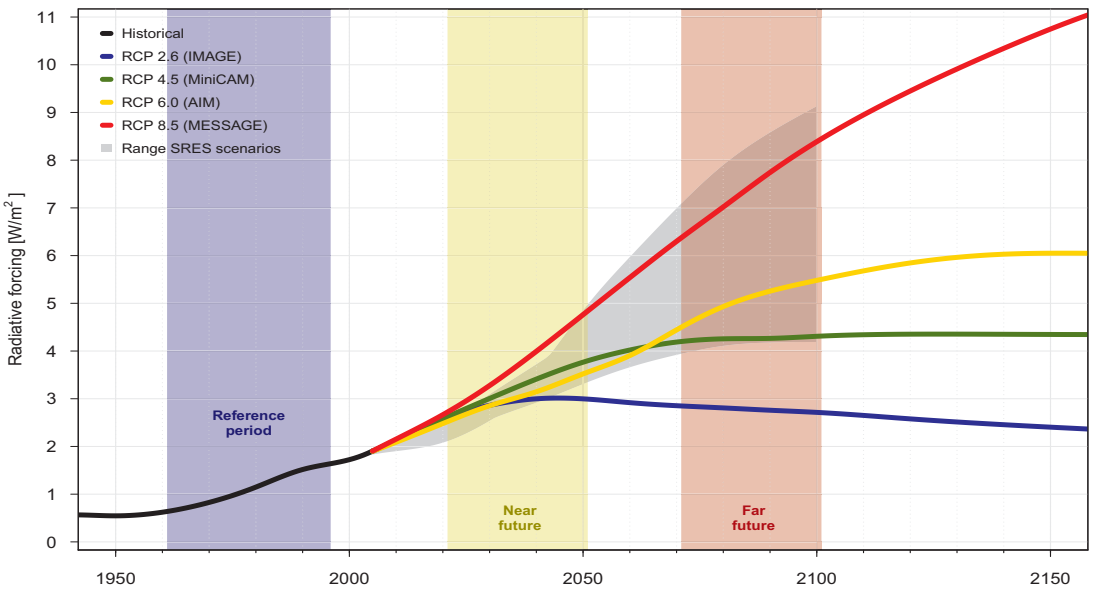

Figure 1: The predetermined radiative forcing paths of the four Representative Concentration Pathways (IIASA, 2013), the modelled forcing range of the SRES scenarios (after Alley et al., 2007) and the three time periods used in this study.

RCP 2.6	A "peak" scenario: its radiative forcing level first reaches a value around 3.1 W/m^2 mid-century, returning to 2.6 W/m2 by 2100. In order to reach such forcing levels, greenhouse gas emissions are reduced over time.
RCP 4.5	A stabilization scenario where total radiative forcing is stabilized before 2100 by employment of a range of technologies and strategies for reducing greenhouse gas emissions.
RCP 6.0	A stabilization scenario where total radiative forcing is stabilized after 2100 without overshoot by employment of a range of technologies and strategies for reducing greenhouse gas emissions.
RCP 8.5	Characterized by increasing greenhouse gas emissions over time representative for scenarios in the literature leading to high greenhouse gas concentration levels.

Table 1: Description of the four main representative concentration pathways (IIASA, 2013).

1.4. Prior trainee research

This research is a continuation of trainee research conducted by Ruiter (Ruiter, 2012). Ruiter applied the ADC method to the same observation data of the 134 HBV Rhine sub-basins as Van Pelt (Van Pelt et al., 2012) and to 15 HBV sub-basins of the Meuse River. To determine the transformation coefficients 38 RCP 4.5 model runs for the far future period (2071-2100, fig. 1) were used that originate from 15 different CMIP5 GCMs.

Before bulk-applying the ADC method, Ruiter first examined the effect of interpolation of GCM data to the common grid. It was shown that the effect of the interpolation to a common grid can be significant for individual quantiles, but that it is negligible for quantile factors, which are ratios between future and control quantiles. As the advanced delta change method is primarily based on quantile factors the effect of interpolation to a common grid is therefore classified as insignificant. The optimal common grid that Ruiter defined to encompass both the Rhine and Meuse basins is presented in Figure 4.

Ruiter showed that the CMIP5 models yield different results in future precipitation changes compared to the CMIP3 models used by Van Pelt. The overall changes in the precipitation distribution were lower for the CMIP5 climate model simulations (RCP4.5) than for the CMIP3 simulations based on SRES scenario A1B (Nakićenović et al., 2000). This difference was concluded to be at least partly caused by the difference in climate forcing of the RCP and the SRES scenario. However, there is now reason to believe that Ruiter mistakenly switched the summer and winter results in the data tables and quantile plots that she presented. Considering this, the differences between Ruiter's results and those of Van Pelt appear to be rather limited.

1.5. Problem definition, research aim and outline

This trainee research aims at the obtainment of ADC transformed data for the Rhine and Meuse HBV sub-basins using all available CMIP5 GCMs and RCPs. This in order to provide daily precipitation and temperature data that is representative for future periods to Deltares and RWS-Waterdienst for hydrological modelling. Furthermore eight runs of the EC-EARTH model are examined, a model that is co-developed by the KNMI. These runs play a prominent role for the upcoming new KNMI climate scenarios (currently denoted as KNMI Next or KNMI `13) that are developed specifically for the Netherlands. By making use of the CMIP5 and EC-EARTH GCM simulations in combination with the ADC method it is also planned to produce a corresponding set of climate scenarios for the major Dutch rivers, i.e. the Rhine and Meuse.

The Czech University of Life Sciences and the Bundesanstalt für Gewässerkunde in Germany have expressed interest in applying the ADC method and other parties are expected to gain interest as well. Therefore another focus of this research is to develop a generic method that provides a multitude of end-users easy access to the ADC method. To provide this it is aimed to perform all steps that in principle have to be performed only once, i.e. the calculation of the ADC method coefficients for all GCMs, and to

distribute the coefficient data to the end-users. To obtain a high degree of serviceability the coefficients need to be determined for a large area, which introduces two new issues, denoted in the next paragraph.

Ruiter's work (Ruiter, 2012) provides a framework for the main aims of this research. However, as her work could not be fully completed during the time of her internship, several issues remain with the framework that require solutions. In Ruiter's study:

- Transformation coefficients were spatially smoothed by using an overall median. This method is unfeasible if the focus area is enlarged to provide other users with the ADC coefficients to an area that climatologically varies significantly.
- The same observation data was used in the transformation and the ADC method's bias correction. This is not possible if the focus area is enlarged for other users, as their historical data of choice is unknown.
- Temperature transformations were not yet included, while they are a required input for the hydrological models besides precipitation.
- Only the far future period (2071-2100) has been considered while many impact modellers are interested in the near future (2021-2050) as well in order to use short term projections.

With respect to these aims and issues, this research aims to answer the following research questions and sub questions:

- What are the ranges in precipitation and temperature changes for the near and far future?
- What are differences in precipitation changes between winter and summer half years?
- Are there differences between different RCPs in terms of transformed precipitation?
- What is the difference between the Rhine and the Meuse basins?

- How to generically convert the method in order for it to be used by other users easily?
  - How to apply spatial smoothing to the transformation coefficients over a large climatologically varying area?
  - Which input dataset must be used to be able to perform bias correction for a large area?

The outline of the remainder of this report is as follows. The methodology section deals with the study area, used data, newly developed methods and provides a concise elaboration on the workings of the ADC method by Van Pelt (2012). The subsequent results section is split in two main parts. The first part presents graphs regarding method validation and accuracy. The second part presents the hard results of the transformations using graphs, tables and brief descriptions of relevant climate change. The discussion section further elaborates on the results, their implications and relation with previous findings and makes conclusive statements.

2. METHODOLOGY

2.1. Study area and period

The principal study area, i.e. the area for which datasets are transformed, is the same as used by Ruiter (Ruiter, 2012), i.e. it comprises both the Rhine and Meuse basins (Fig. 2). The river Rhine, with a total length of 1230 km, is the longest river of Western Europe. The Rhine originates in the Swiss Alps, and has a total basin area of approx. 185 000 km^2. It is fed by glacier melt, snow melt and rainfall, which causes an average discharge at Lobith of 2200 m^3s^{-1}. The Meuse river originates on the plateau of Langres in northeast of France and is primarily a rainfall fed river with an average discharge of 350 m^3s^{-1}. The total Meuse basin area upstream of Borgharen is about 21000 km^2 (Van Stokkom et al., 2005).

To accommodate the distribution the ADC method and its transformation coefficients to a large group of potential end-users a secondary focus area is used in this research for which the coefficients are determined. This area extends from 14° W to 36° E in longitude and from 32° N to 62° N in latitude and encompasses most of Europe (Fig. 3).

The periods of interest are two future periods and a reference period. These are respectively 2021-2050 (near future), 2071-2100 (far future) and 1961-1995. Their temporal positioning with respect to the climate forcing paths is denoted in Figure 1.

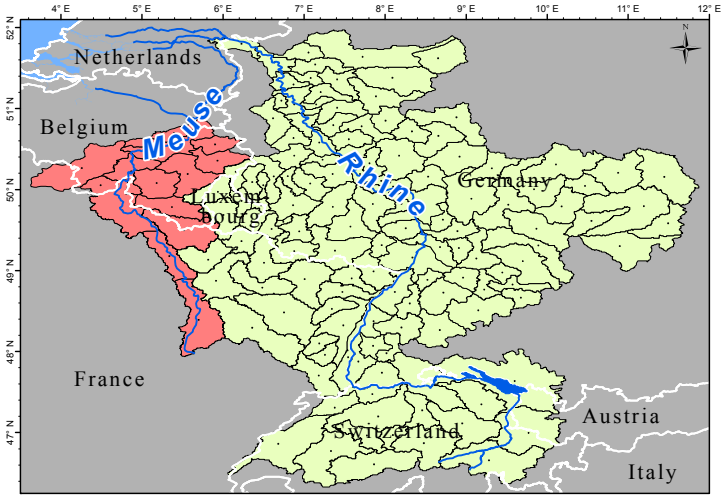

Figure 2: Location of the principle study area and the HBV sub-basins of the Rhine and Meuse.

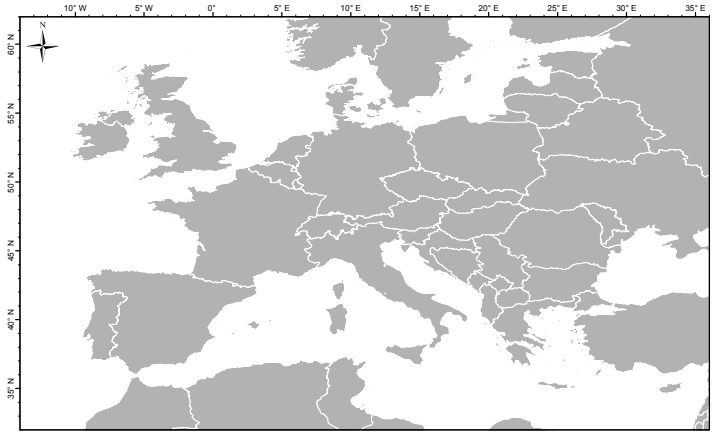

Figure 3: The secondary focus area for which the transformation coefficients are determined.

2.2. Observation data

This study uses three observation datasets. For the Rhine basin the CHR-OBS dataset is used (Eberle et al., 2002; Kew et al., 2011; Perrin et al., 2010; Wit & Buishand, 2007). This dataset consists of area-average daily mean precipitation and temperature observations aggregated to the 134 HBV sub-basins of the Rhine basin and covers the period 1961-1995. New precipitation data for the HBV sub-basins of the Rhine that is based on the HYRAS gridded dataset are processed; however, analysis has not yet been performed and the results for the Rhine in this report comprise transformations of CHR-OBS data solely.

For the Meuse basin data of the French and Belgium meteorological surveys is used that is interpolated to the 15 HBV sub-basins used for the Meuse (Buishand & Leander, 2011; Leander, 2009). The timeframe used from this dataset is 1967-2007. There is no temperature data available for 1961-1966, and therefore this timeframe differs slightly from the chosen reference period. Its use is justified by the assumption that the average climate does not differ significantly from that of the reference period.

To determine the transformation coefficients for the large area a precipitation dataset is required that can be used for bias correction needed in the ADC method. For this the E-OBS 0.25° gridded dataset is used (Haylock et al., 2008). It comprises interpolated data from meteo-stations and covers most of Europe and parts of North Africa. It is generally accurate, although some areas that have sparse data availability suffer more from smoothing due to the interpolation procedure than areas with large data densities. Examples of areas with limited data availability are parts of Eastern Europe and North Africa.

Model (n=31)	**Model runs**	**RCP 2.6**	**RCP 4.5**	**RCP 6.0**	**RCP 8.5**	**Total**
ACCESS1-0	1	-	1	-	1	2
ACCESS1-3	1	-	1	-	1	2
bcc-csm1-1	1	1	1	1	1	4
bcc-csm1-1-m	1	1	1	1	1	4
BNU-ESM	1	1	1	-	1	3
CanESM2	5	5	5	-	5	15
CCSM4	3	3	3	3	3	12
CMCC-CESM	1	-	-	-	1	1
CMCC-CM	1	-	1	-	1	2
CMCC-CMS	1	-	1	-	1	2
CNRM-CM5	1	1	1	-	1	3
CSIRO-Mk3-6-0	10	10	10	10	10	40
FGOALS-s2	3	1	3	1	3	8
GFDL-CM3	1	1	-	1	1	3
GFDL-ESM2G	1	1	1	1	1	4
GFDL-ESM2M	1	1	1	1	1	4
GISS-E2-R	1	-	1	-	-	1
HadGEM2-CC	3	-	1	-	3	4
HadGEM2-ES	4	4	4	4	4	16
inmcm4	1	-	1	-	1	2
IPSL-CM5A-LR	4	4	4	1	4	13
IPSL-CM5A-MR	1	1	1	1	1	4
IPSL-CM5B-LR	1	-	1	-	1	2
MIROC-ESM	1	1	1	1	1	4
MIROC-ESM-CHEM	1	1	1	1	1	4
MIROC5	3	3	3	1	3	10
MPI-ESM-LR	3	3	3	-	3	9
MPI-ESM-MR	3	1	3	-	1	5
MRI-CGCM3	1	1	1	1	1	4
NorESM1-M	1	1	1	1	1	4
EC-EARTH-v2.3	8	-	-	-	8	8
Total	69	46	57	30	66	**199**

Table 2: List of the GCMs used in this study, their number of available runs as well as the RCPs available for those runs. See IIASA (2013) for more information regarding the models and their developers

2.3. Global climate model data

In this study GCMs are used that are part of CMIP5. Only daily precipitation and temperature output of the models is used. The timeframes extracted from the GCM data are 1961-1995, 2021-2050 and 2071-2100. It was aimed to use all possible models, runs and available RCPs for the model runs. However, only runs are used for which all the selected timeframes could be obtained entirely with no missing data or errors present and for which both precipitation and temperature were available. All together there are 30 different CMIP5 models used that have a total of 191 runs, with between 30 and 58 runs per RCP.

Furthermore a set of runs from the KNMI co-developed model EC-EARTH release 2.3-extra is used (Hazeleger et al., 2010). Although there are EC-EARTH runs that are part of CMIP5, the runs from the version used here are not. Version 2.3-extra has 8 runs or members that were driven by the 8.5 W/m^2 pathway. A list of all the used models, runs per model and RCPs per model is presented in Table 2.

2.4. Common grid definition

The common grid defined by Ruiter (Ruiter, 2012) has an optimal cover of and spatial distribution over the HBV sub-basins of the Rhine and the Meuse and is therefore used, with a very minor alteration, as basis for the common grid used in this study. The grid with cells of 1.2° latitude by 2° longitude uses 14 gridcells to cover the Rhine and Meuse basins. As this study enlarges the area for which the ADC coefficients are determined, the grid is extended to encompass the entire focus area. The minor alteration is related to the latitudinal size of the cells, namely a change into 1.25°. This small change is introduced to simplify the aggregation of the bias correction dataset E-OBS and to improve the aggregation accuracy, as exactly 5 by 8 E-OBS cells fit one common grid cell and therefore no interpolation of the E-OBS data is required. The new common grid, Ruiter's grid cells and both basins are all presented in Figure 4.

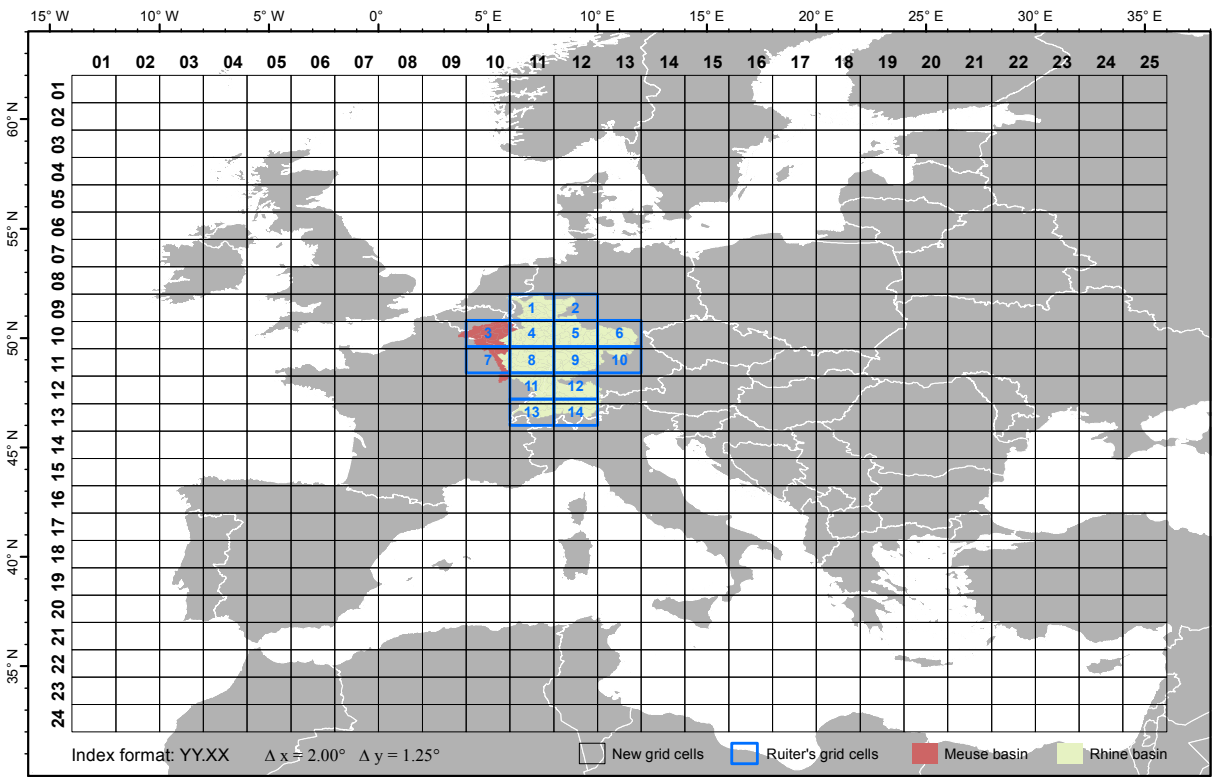

Figure 4: The common grid definition and cell indexes used in this study, Ruiter's grid definition and cell indexes (Ruiter, 2012) as well as the location of the Rhine and Meuse basins.

2.5. Aggregation of E-OBS to the common grid

As already mentioned in section 2.4, 40 E-OBS cells fill a common grid cell exactly. Its aggregation to the common grid is therefore performed by summing the precipitation values of the 40 cells. As the precipitation unit of the data is mm and it is on a latitude-longitude grid, the values are first converted to absolute volumes by multiplying them by the cell surface areas.

The E-OBS dataset is only available for land areas, i.e. sea cells are set to not available (NA) using a sea-mask that is based on the GTOPO30 dataset (pers. comm. E. van den Besselaar and A. Klein Tank, KNMI). Furthermore, cells for which interpolated data could not be determined are NA as well. Despite the absence of precipitation values for these E-OBS cells, a common grid precipitation value is calculated as long as one of the 40 E-OBS cells has precipitation values present. For such common grid cells the representativity of the grid cell value is reduced, as its value is based on samples that only represent a fraction of the cell. To quantify this loss in accuracy this fraction is determined and distributed along with the ADC transformation coefficients for possible accuracy assessments of a cell by end-users (Fig. 5).

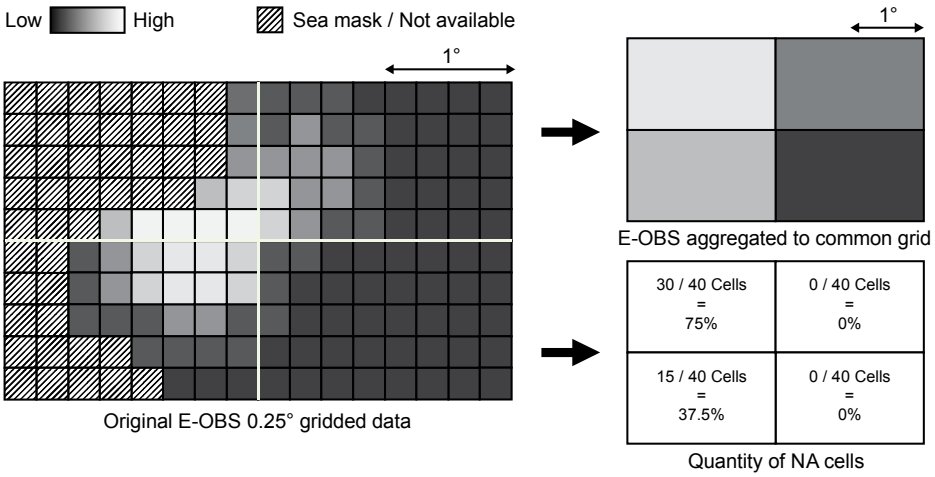

Figure 5: Schematic representation of the E-OBS aggregation.

2.6. Spatial smoothing

Due to the enlargement of the focus area, it now covers various climatological areas and therefore a new smoothing method is required for the transformation coefficients. It is chosen to use a 2D moving window operator (Burrough et al., 1998) based on eight neighbours (Fig. 6) that calculates the median value of nine common grid cells and assigns it to the center cell. Important to note is that cells that lie on the outer edge of the common grid or near the coast experience edge effects, i.e. less cells are available to determine the median. Therefore the accuracy of the determined coefficients is reduced for those cells. This is not always a noticeable issue, as cells that that represent a coastline (Fig. 10) have a reduced accuracy already.

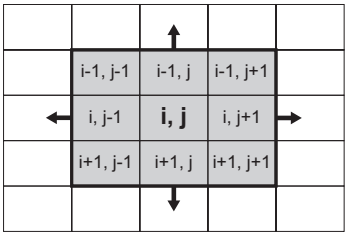

Figure 6: Schematic representation of the used moving window operator.

2.7. Advanced delta change method

As already mentioned in the introduction, the advanced delta change method (Van Pelt et al., 2012) comprises a non-linear transformation of daily observed precipitation series by using a climate signal from a GCM. Both datasets must be on the same spatial scale and therefore an aggregation of the daily observation values to the common grid is performed using an area-weighted mean. The daily GCM data, both the control and future period, are interpolated to the same grid by bilinear interpolation using CDO (Max Planck Institute for Meteorology, 2012).

The ADC method does not act on the daily values itself, but rather on 5-day precipitation sums. This is performed as extreme discharge events depend on multiple days of extreme precipitation. In practise, the use of 5-day sums results in 73 non-overlapping sums in a 365-day year. For leap years an extra five day sum is introduced that covers 24-29 February. A specific month is assigned to each five day sum, not entirely analogous to Gregorian calendar months. Namely, the months January up to November are each assigned to consecutive groups of six 5-day sums while December is assigned to the remaining group of seven 5-day sums. Figures 8 and 9 present flowcharts that denote all steps of the ADC method that are explained in this section as well as the different temporal scales involved in each step. All calculations for the ADC method are performed in developed R-scripts (R Development Core Team, 2008).

For the transformation of the observed 5-day precipitation sums (P) two different equations are used, i.e. for precipitation sums that are smaller or larger than their 90% quantile (P_{90}). This quantile is determined per calendar month and per common grid cell over the entire reference period; hence there are twelve different P_{90} values per grid cell.

The two transformation equations are:

$$P^{*} = aP^{b} \quad \text{for} \quad P^{O} < P_{90}^{O} \tag{1}$$

$$P^{*} = \overline{E^{F}} \Big/ \overline{E^{C}} \cdot (P^{O} - P_{90}^{O}) + a(P_{90}^{O})^{b} \quad \text{for} \quad P^{O} > P_{90}^{O} \tag{2}$$

where P^{*} represents the transformed 5-day sums, P the observation 5-day sums, P_{90} the 90% quantile and a and b are the transformation coefficients. The superscripts ^{O}, ^{C} and ^{F} denote whether the variable represents respectively the observation time series, the GCM control series or the GCM future series. For 5-day precipitation sums that exceed the P_{90} of their month an excess value (E) is determined, which is the part of the precipitation that is above P_{90} (Fig. 7). It is calculated by:

$$E = P - P_{90} \tag{3}$$

The mean future and control excesses in Equation 2 are, similarly to P_{90}, determined on a monthly basis per grid cell over the entire period by:

$$\overline{E^{C}} = \frac{\sum P^{C} - P_{90}^{C}}{n^{C}} \quad \text{and} \quad \overline{E^{F}} = \frac{\sum P^{F} - P_{90}^{F}}{n^{F}} \tag{4}$$

The linear scaling of the transformed precipitation with the ratio of future and control excess in Equation 2 expresses a change in the slope of the extreme value plot of the 5-day maximum precipitation amounts (appendix in Van Pelt, 2012). I also avoids unrealistically high transformed precipitation values that may occur when Equation 1 is used for $P > P_{90}$ and $b > 1$.

The transformation coefficients a and b are derived from the 60% and 90% quantiles by:

$$b = \frac{\log\{g_2 \cdot P_{90}^{F} / (g_1 \cdot P_{60}^{F})\}}{\log\{g_2 \cdot P_{90}^{C} / (g_1 \cdot P_{60}^{C})\}} \tag{5}$$

$$a = P_{60}^{F} / (P_{60}^{C})^{b} \cdot g_1^{1-b} \tag{6}$$

The calculation of the transformation coefficients requires bias correction factors g_1 and g_2 that address systematic differences between the P_{60} and P_{90} of the observations and the GCM control series (Fig. 7) to ensure a proper reproduction of the relative changes in these quantiles during the transformation. The correction factors are determined by:

$$g_1 = P_{60}^{O} / P_{60}^{C} \tag{7}$$

$$g_2 = P_{90}^{O} / P_{90}^{C} \tag{8}$$

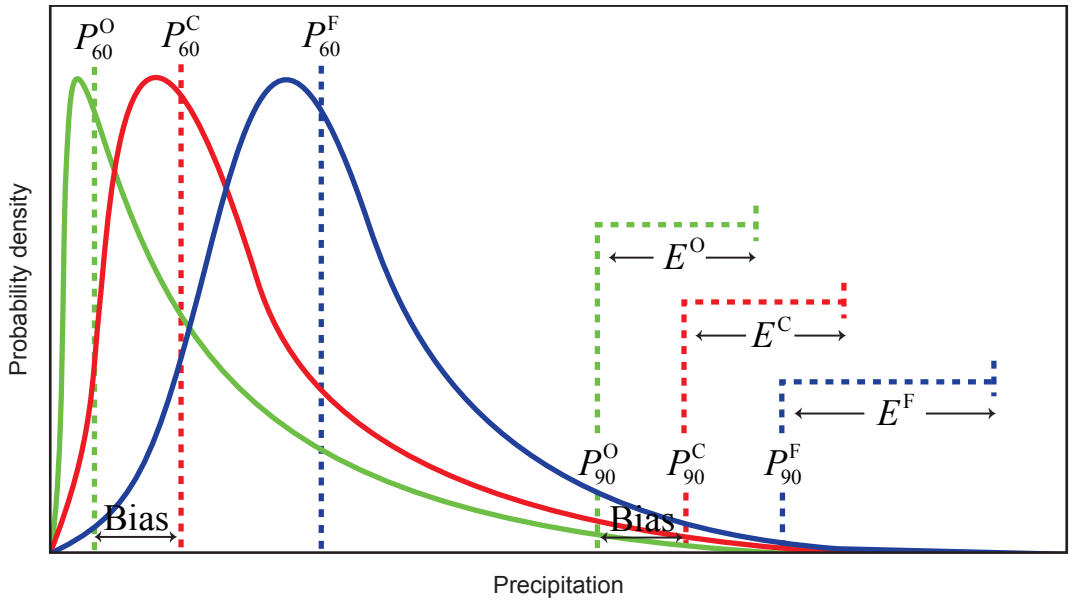

Figure 7: Schematic probability distribution of observation, control and future precipitation with the quantiles, excesses and biases denoted (after Van Pelt et al., 2012).

To reduce sampling variability in the transformation coefficients, the P_{60} and P_{90} are smoothed temporally by using a weighted mean with weights of 0.25, 0.5 and 0.25 on respectively the previous, current and next month. The mean excesses ($\overline{E^C}$ and $\overline{E^F}$) are smoothed temporally in a similar manner.

There is also noise present in the parameters spatially (van Pelt et al., 2012). This is especially an issue for the *b* coefficient that has a relatively large influence in the transformation and could cause considerable and unrealistically large differences in transformation results of neighbouring common grid cells. Therefore spatial smoothing is applied using the moving window operator that is described in section 2.6. The ratio between the control and future mean excesses used in Equation 2 is smoothed spatially as well.

When the 5-day precipitation sums are transformed a change factor can be determined for each sum that is subsequently applied to its corresponding five days of daily observations. The individual days within the five day groups are thereby transformed with an equal change factor. This change factor (R) is determined by:

$$R = P^{*} \big/ P \tag{9}$$

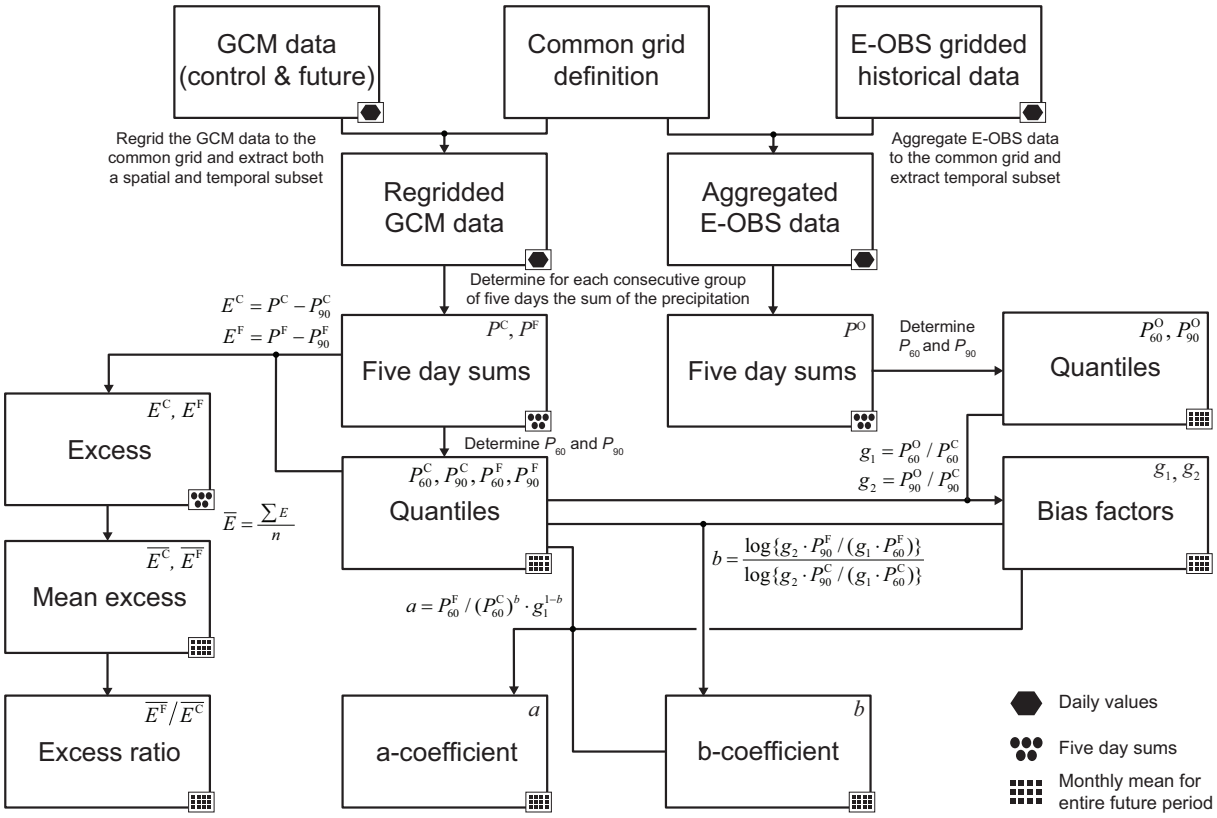

Figure 8: Flowchart of the parameter calculation steps of the advanced delta change method.

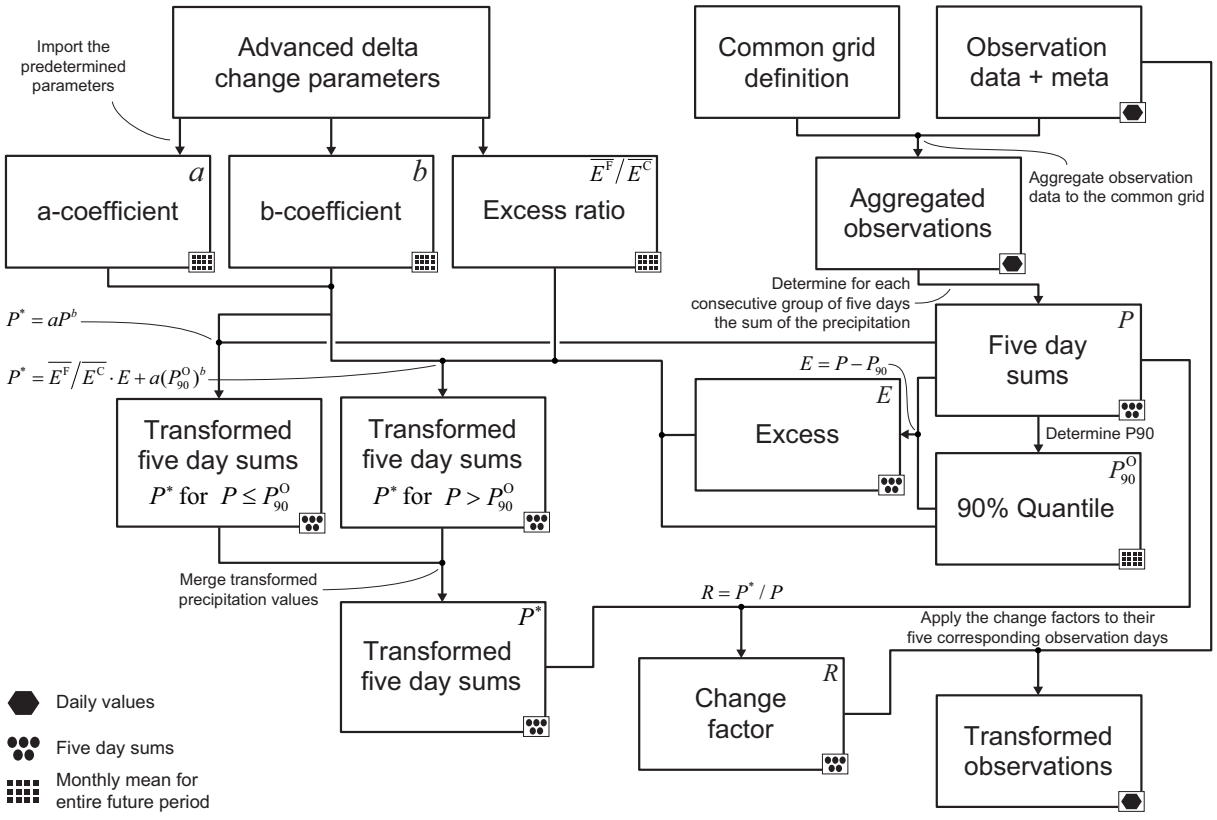

Figure 9: Flowchart of the transformation of the observation time series, or application of the coefficients.

2.8. Temperature transformation

For hydrological modelling purposes transformed temperature data is required besides the transformed precipitation data. To accommodate in this need, temperature data for the HBV sub-basins of the Rhine and Meuse are transformed to represent future temperatures. The temperature transformation, conversely to that of precipitation, is linear in nature and has the form (Van Pelt et al., 2012):

$$T^* = \frac{\sigma^{\mathrm{F}}}{\sigma^{\mathrm{C}}}(T - \overline{T^{\mathrm{O}}}) + \overline{T^{\mathrm{O}}} + \overline{T^{\mathrm{F}}} - \overline{T^{\mathrm{C}}} \tag{10}$$

where T^* represents the transformed temperature; T the observed temperature; $\overline{T^{\mathrm{O}}}$, $\overline{T^{\mathrm{C}}}$ and $\overline{T^{F}}$ the monthly mean of respectively the observed, control and future temperature; σ^{C} and σ^{F} the standard deviations of the daily control and future temperature calculated per calendar month.

The means and standard deviations are, similarly as for the precipitation transformation, determined for each common grid cell by aggregation of the observations and bilinear interpolation of the GCM temperatures. Furthermore, similar temporal smoothing is applied to the standard deviations. The transformation however operates on daily values and as a result the transformation does not requires the use of a change factor, i.e. the transformation is applied directly to daily values on the sub-basin scale (*T)* by using the common grid scale means ($\overline{T^{\mathrm{O}}}$, $\overline{T^{\mathrm{C}}}$, $\overline{T^{F}}$) and standard deviations (σ^{C}, σ^{F}).

3. RESULTS

3.1. Guide to the section

This section presents plots together with concise elaborations of the patterns that are observable in the plots. There are a few principles used throughout this section:

- The numbering of the text labels on the scatter plots represents the different GCM runs processed in this study. Tables are included as appendix A that contain summaries of the results and also link the numbers in the scatter plot with the corresponding model runs.
- The month definitions used here are those presented in section 2.7. The definitions of winter and summer used in the remainder of this report are:
  Winter = October + November + December + January + February + March
  Summer = April + May + June + July + August + September
- The figures presented in this section do not encompass all entities that can be presented, i.e. all basins, seasons and future periods, unless there are characteristics that are worth mentioning. The main focus is on the far future as its results are more distinct. The near future counterparts of the figures are generally included as appendices and no further references are made to these figures in the remainder of this section.

3.2. Grid cell usability

The E-OBS aggregation process (section 2.5) yields information about the usability of the common grid cells by quantification of the amount of available E-OBS cells for the aggregation to a common grid cell. It also provides indirect accuracy information for the interpolated GCM data. Namely, in the coastal areas the common grid cells, as a result of the interpolation, comprise a mixture of land and sea characteristics that can be quite different for precipitation and temperature. The map in which the common grid cell usability is quantified, is presented as Figure 10.

3.3. Total range of used transformation coefficients

The range of and relation between the transformation coefficients a and b that are used in the precipitation transformation of both the Rhine and Meuse basins are presented in Figure 11. As the plot shows, values for a range from near-zero to about 6 and for b from about 0.5 to 2.6. The values for the summer months show more variance than those for the winter months, i.e. the whole right tail of b values larger than approx. 1.5 is found to comprise summer coefficients only. This is not shown on the plot but a similar dependency is denoted in Figure 17 that shows the mean coefficients per model run. The winter b coefficient is generally between approx. 0.8 and 1.2. The relation between the b coefficient and the separate quantiles is found to have relatively similar dependencies as the coefficient's relation with a (not shown here). The higher the b coefficient, the lower is the future quantile relative to its reference, although this dependency is more noticeable for lower quantiles such as P_{30}.

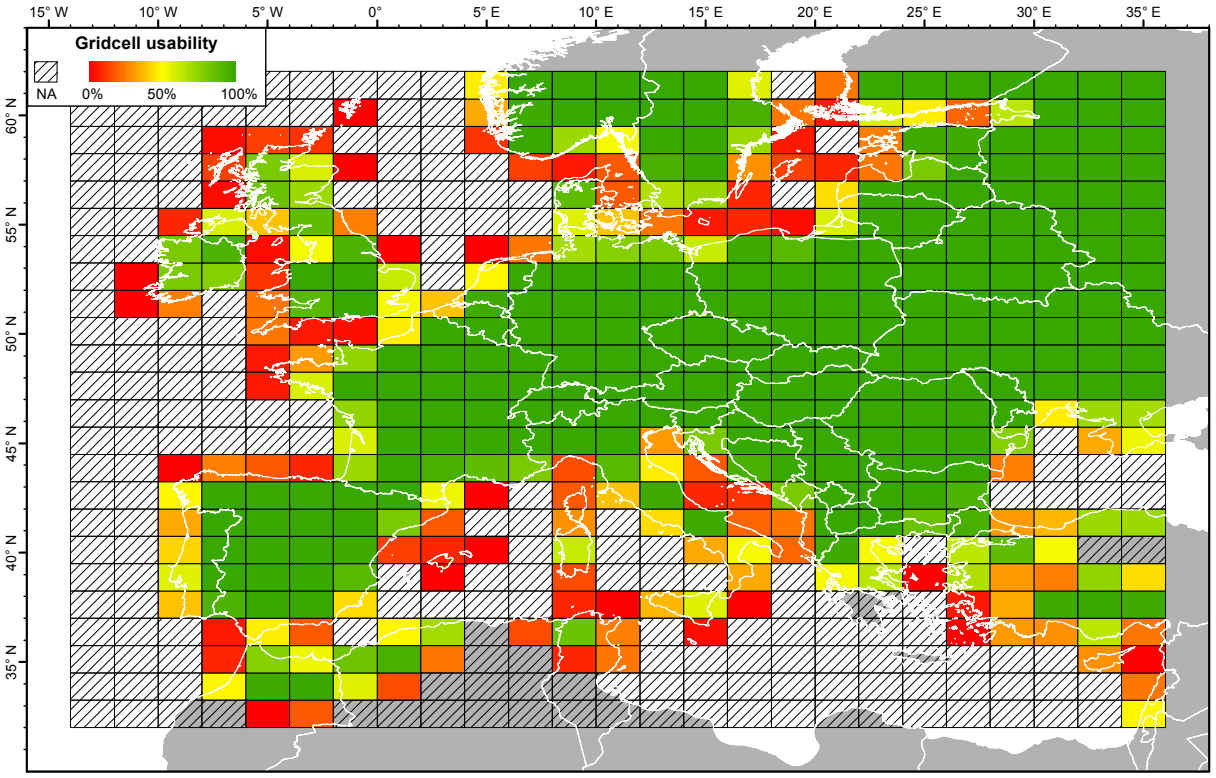

Figure 10: Map that quantifies the usability of the common grid cells, determined by the amount of available E-OBS 0.25° cells used in the E-OBS aggregation to each common grid cell.

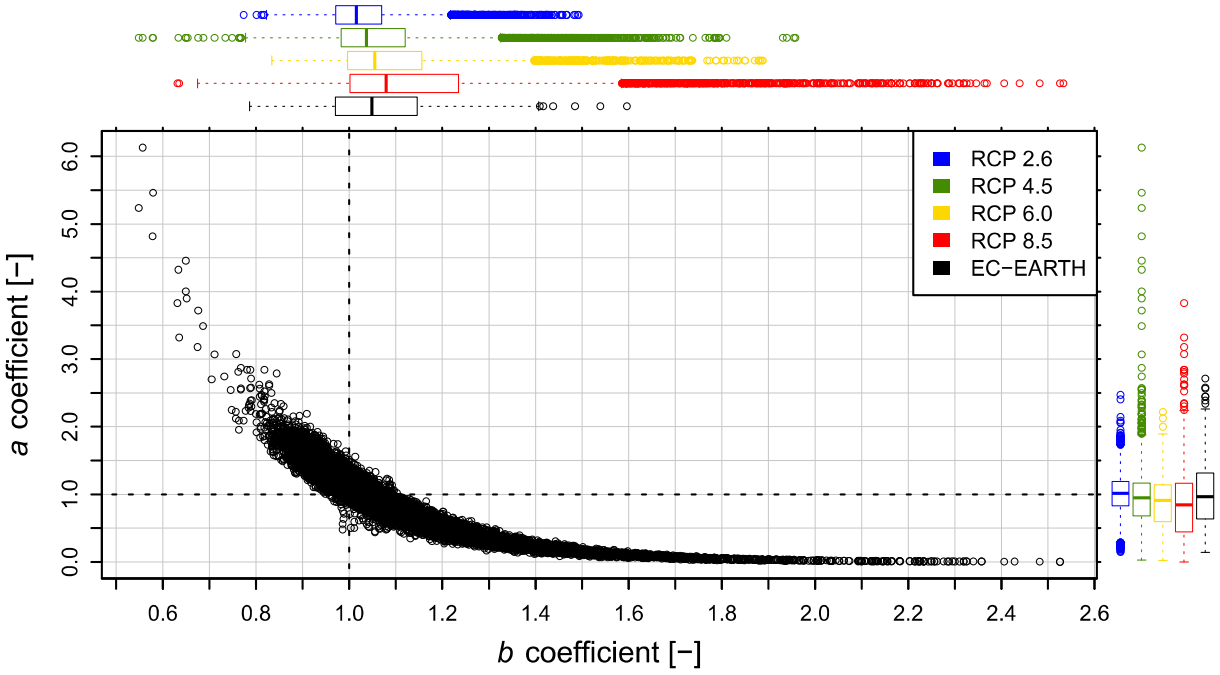

Figure 11: The transformation coefficients *a* and *b* that are used in the far future transformation of both the Rhine and the Meuse basin precipitation. The plot shows separate points for each possible combination of month, gridcell and model run ($n = 31044$). The coloured boxplots denote the coefficient distribution among the different RCPs with the outliers defined as values that exceed 1.5 times the interquartile range from the edge of a box.

3.4. Comparison of GCMs and transformed observations

To determine the accuracy of the ADC precipition transformation a comparison is made between the relative change in precipitation taken directly from the GCMs and that in the transformed observations. By plotting the quantile factors, i.e. the ratio between future/transformed and control/reference quantiles, of both datasets versus each other the accuracy of the reproduction of the GCM climate change within the transformed observations can be visualised (Figs. 12 and 13). When the points lie on the 1:1 line there is in theory a perfect reproduction of the climate signal due to the application of the bias correction. However, due to the temporal and spatial smoothing that is applied and the use of a different dataset than the dataset that is being transformed, the bias correction is likely to become less effective. Nevertheless, as the bias correction has a relatively minor overall influence on the transformation, the plots remain a good estimation of the accuracy of the reproduction. The more the points deviate from the 1:1 line, the larger the difference between the climate signals of the models and the transformations. The parallel gridlines represent 0.05 intervals, i.e. 5%, of absolute difference in the quantile factors of the GCM and transformed data.

Winter months

As can be noted in the plots of Figure 12, the 60% and 90% quantiles show a relatively good relation between the transformed observations and the GCM data. Maximum absolute differences between the quantile factors of the GCM and transformed observation found for P_{60} and P_{90} are in the order of 5%. The relative differences for the 30% quantile are much larger, up to about 25%. Most winter quantiles show a clear increase, i.e. the fall within the upper right quadrant of the plots.

In terms of differences between RCPs, it can be noted that for the 60 and 90% quantiles RCP 8.5 shows the largest positive differences. There is a large overlap with the other RCPs however. The eight EC-EARTH runs generally follow a similar pattern. Remarkably, the 30% quantile plots show no clear relation between RCP and the amount of change visible by the widely scattered colours, except for the largest positive changes (> 1.3) that appear to be dominated by RCP 8.5 runs.

Summer months

The quantile plots for the summer months (Fig. 13) show similar patterns to those of the winter months in terms of relative differences between GCM data and transformed observation data. The scale is however different as absolute quantile factor differences of about 10, 7 and 30% are found for P_{90}, P_{60} and P_{30} respectively. The quantile factor ranges for the summer months are clearly different as decreases in all quantiles seem to be most common. For P_{90} this is less noticeable, as for this quantile there is still a relatively large amount of values in the upper right quadrant and the apparent average is close to no change.

Again RCP 8.5 appears to have the strongest overall influence, as it comprises the smallest quantile factors. Conversely to the winter plots a clear trend in the RCP distribution over the quantile factors is apparent for P_{30}. The EC-EARTH runs fall in the relatively high end of the RCP 8.5 range for all quantiles, i.e. they have less negative change.

Rhine and Meuse basins

The differences in range between the Rhine and the Meuse basin are relatively small for all quantiles and both winter and summer. There are slight differences between the two basins regarding the absolute differences between GCM data and transformed observation data though, where the Meuse generally shows larger deviations from the 1:1 line.

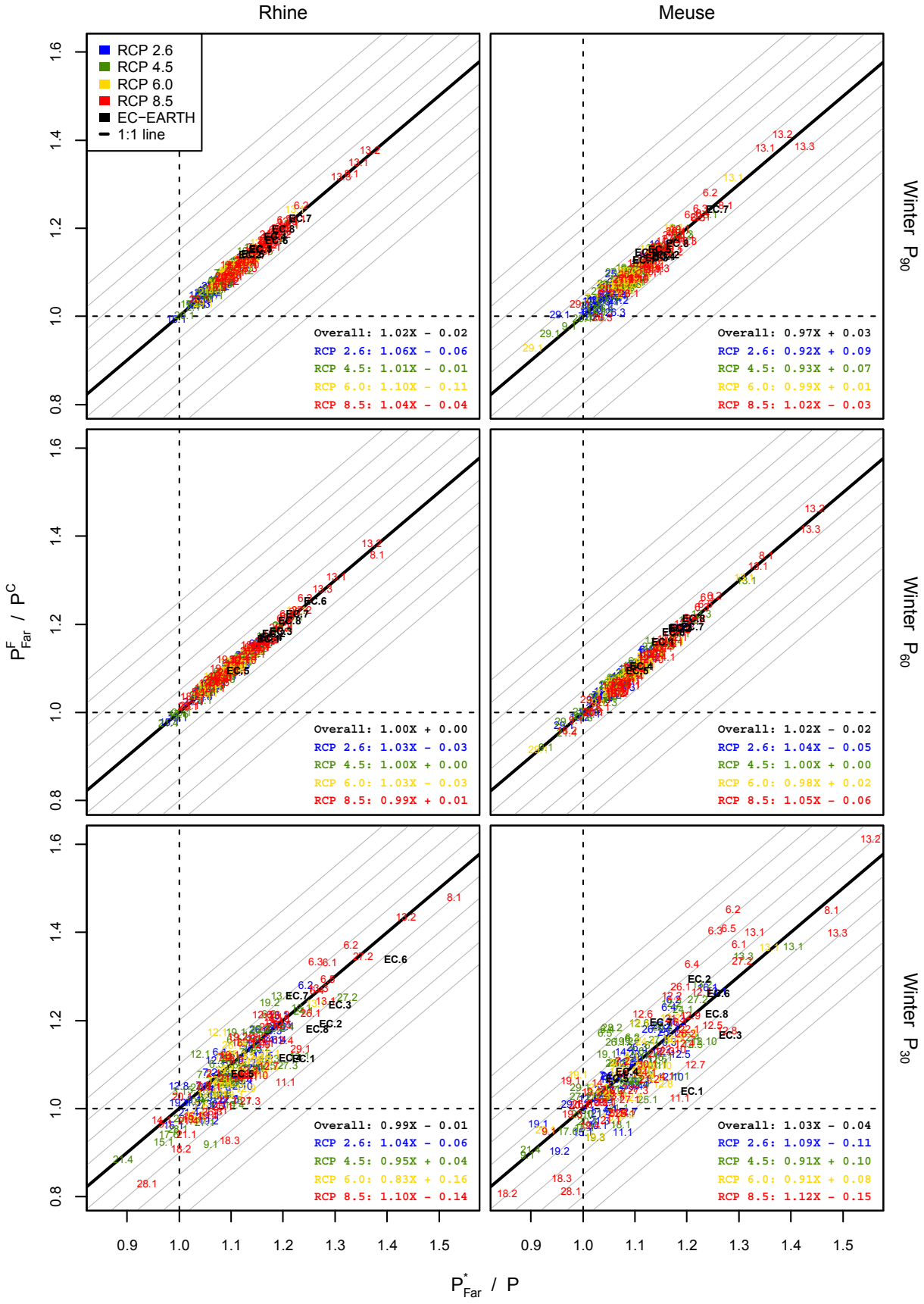

Figure 12: The 30%, 60% and 90% quantile factors of the transformed observations versus those of the GCM runs. The plot comprises the far future period and winter months only. On each plot the coefficients of a linear regression are presented for each RCP. The gridlines represent the absolute difference between quantile factors of the GCM and transformed observations with a 0.05 equidistancy.

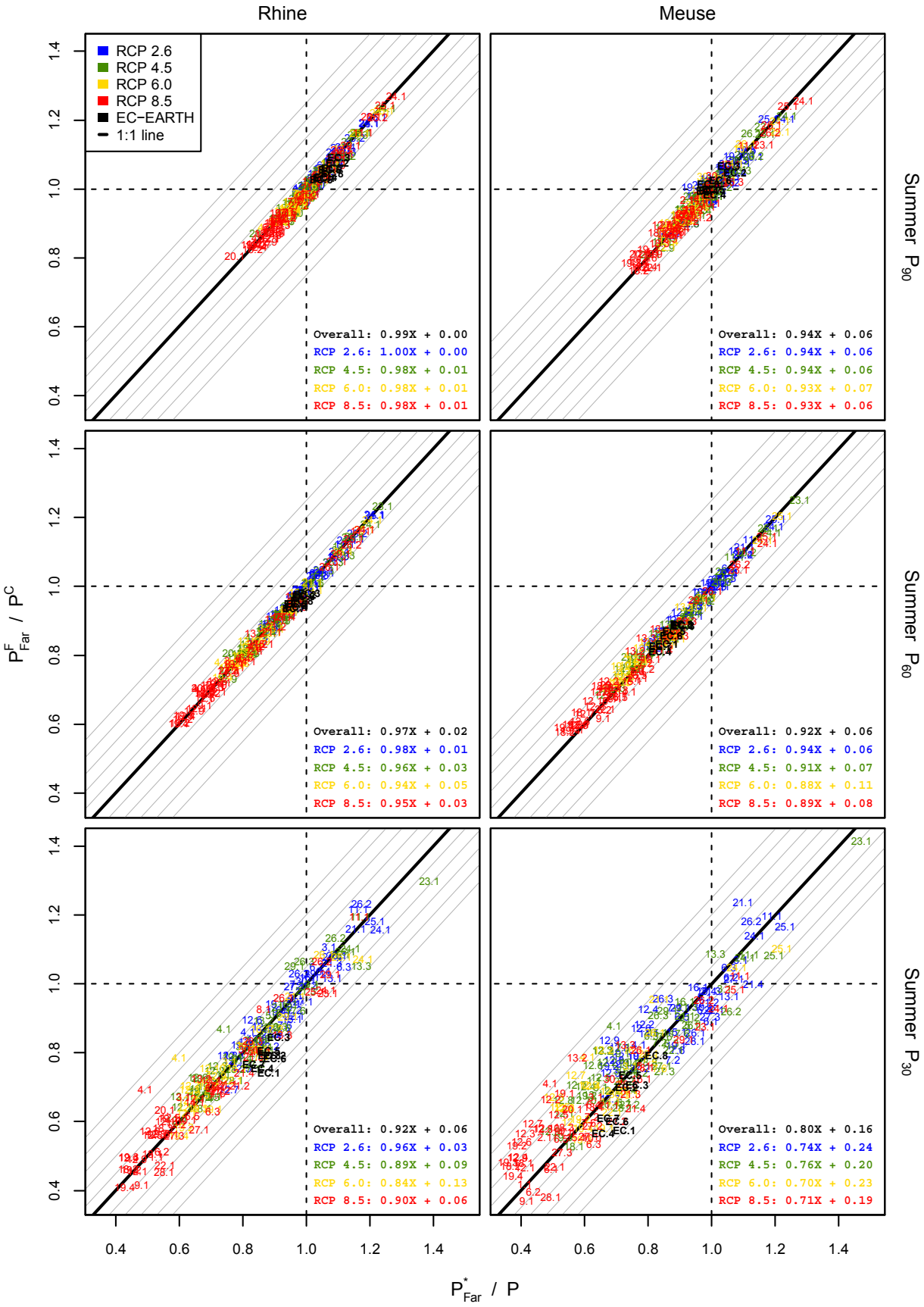

Figure 13: The 30%, 60% and 90% quantile factors of the transformed observations versus those of the GCM runs. The plot comprises the far future period and summer months only. On each plot the coefficients of a linear regression are presented for each RCP. Note the difference in axis scales with Figure 12. The gridlines represent the absolute difference between quantile factors of the GCM and transformed observations with a 0.05 equidistancy.

3.5. Seasonal changes in precipitation and temperature

Figure 14 shows the change in the precipitation's monthly mean and standard deviation for the Rhine basin in the far future. The standard deviations that are used represent the intra-month variation of the 5-day sums over the entire future and reference period.

The winter plot shows that all models have an increase in mean precipitation. The changes in the means clearly show a relation with the RCPs, the larger the forcing the larger the positive change. Winter standard deviations increase averagely with the same rate as the mean precipitation indicating a more or less constant coefficient of variation (CV) in this season.

The summer means are distributed over positive and negative change. Again a relation with forcing seems present, although not as evident as for the winter season. Namely, there appears to be a group of models that shows extreme negative change as well as a group that shows extreme positive change for all RCPS, i.e. there is a slight dichotomy between all runs. In terms of standard deviation, there is a clear difference with the winter changes. The change in standard deviation is larger than the change in mean precipitation, hence the CV increases. In the winter period the EC-EARTH runs seem to fit in well with the other RCP 8.5 runs, while in summer the change in mean is moderate compared to other RCP 8.5 runs.

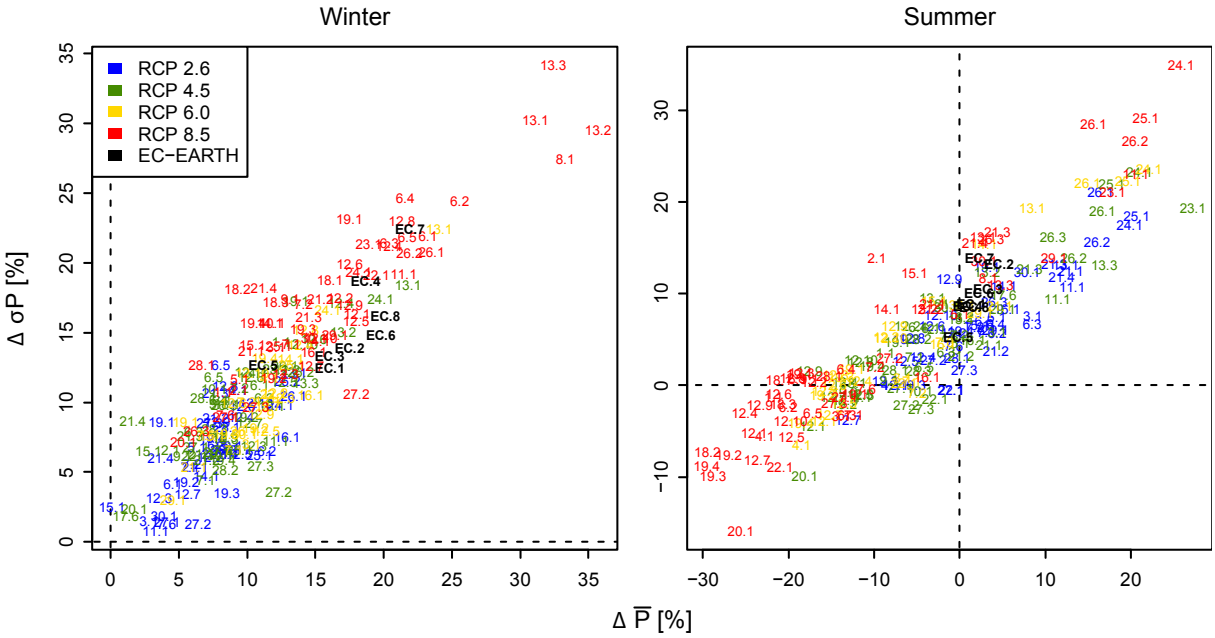

Figure 14: Mean seasonal changes in the monthly means and intra-month standard deviations of the precipitation 5-day sums for the entire Rhine basin in the far future.

Figure 15 shows the change in the temperature's monthly mean and standard deviation for the Rhine basin in the far future. Standard deviations are determined on an intra-month basis similarly as for precipitation, though this time using daily values. For both summer and winter an increase in forcing results in an increase of temperature. For the bulk of model runs the change in standard deviation appears to be opposite for the two seasons, as the winter variability generally decreases while summer variability increases. There are however some models that show a winter variability increase and a summer decrease. Note that these are not necessarily the same runs for winter and summer.

The winter change in standard deviation does not show a strong relation with the forcing. Summer variability on the other hand does seem to have a stronger relation to forcing. The eight EC-EARTH runs have a relatively small increase in temperature compared to the other RCP 8.5 runs (about 2 °C) for both the winter and summer periods.

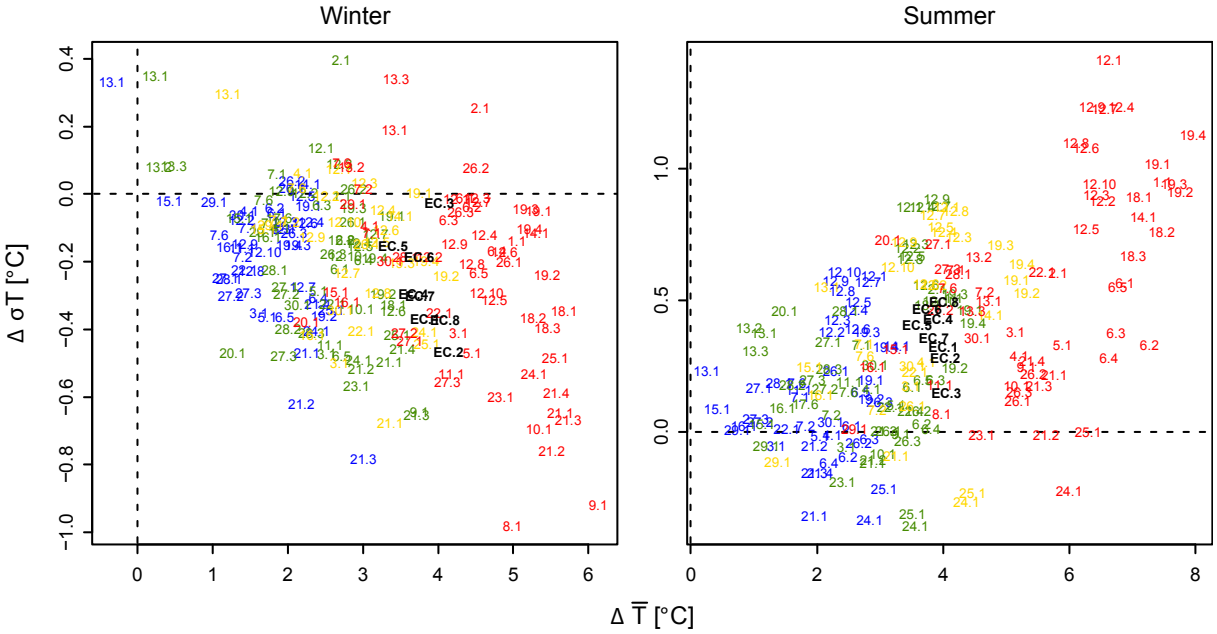

Figure 15: Mean seasonal changes in the monthly means and intra-month standard deviations of the daily temperatures for the entire Rhine basin in the far future.

3.6. Changes in precipitation of all model runs

Monthly changes in precipitation

The relative change of P_{30}, P_{60} and P_{90} per month of all model runs is visualized in Figure 16. The plots clearly show a general pattern of increasing quantile values for the winter months and decreasing values for the summer months. In the winter months, the bulk of the models show relatively similar changes for all quantiles, while for the summer months each quantile encounters different amounts of relative decreases. Especially P_{90} decreases considerably less than P_{30} and P_{60}, i.e. a clear non-linearity is present.

In the summer months, an increase in model variability is present that is especially the case for the period June to August. Note that the large hump of positive change in July, in contrast to most models that show negative change during these months, is primarily caused by the deviating results of a handful of models, primarily MIROC-ESM(-CHEM) and IPSL-CM5B-LR (see TFable 3).

Seasonal changes in precipitation

Seasonal changes in the quantiles and excesses as well as the transformation coefficients that were used to calculate these changes are shown in the boxplots of Figure 17. Here, similar patterns are present as in Figure 16, i.e. an average increase in winter quantile values and an average decrease in summer values. Furthermore, the difference in the degree of linearity of the changes in the three quantiles for both seasons is clearly noticeable. Monthly mean excesses seem to increase for the bulk of the models in both seasons, although approx. 5% more in the summer period.

The transformation coefficients are the foundation for the difference in transformed winter and summer precipitation and hence show differences between the two seasons of a similar magnitude. In the winter period *b* values are close to 1 while *a* values are primarily above 1. In summer the mean *b* coefficient can become large and is above 1 for most model runs. Conversely, the *a* coefficient is low and has values that are generally below 1.

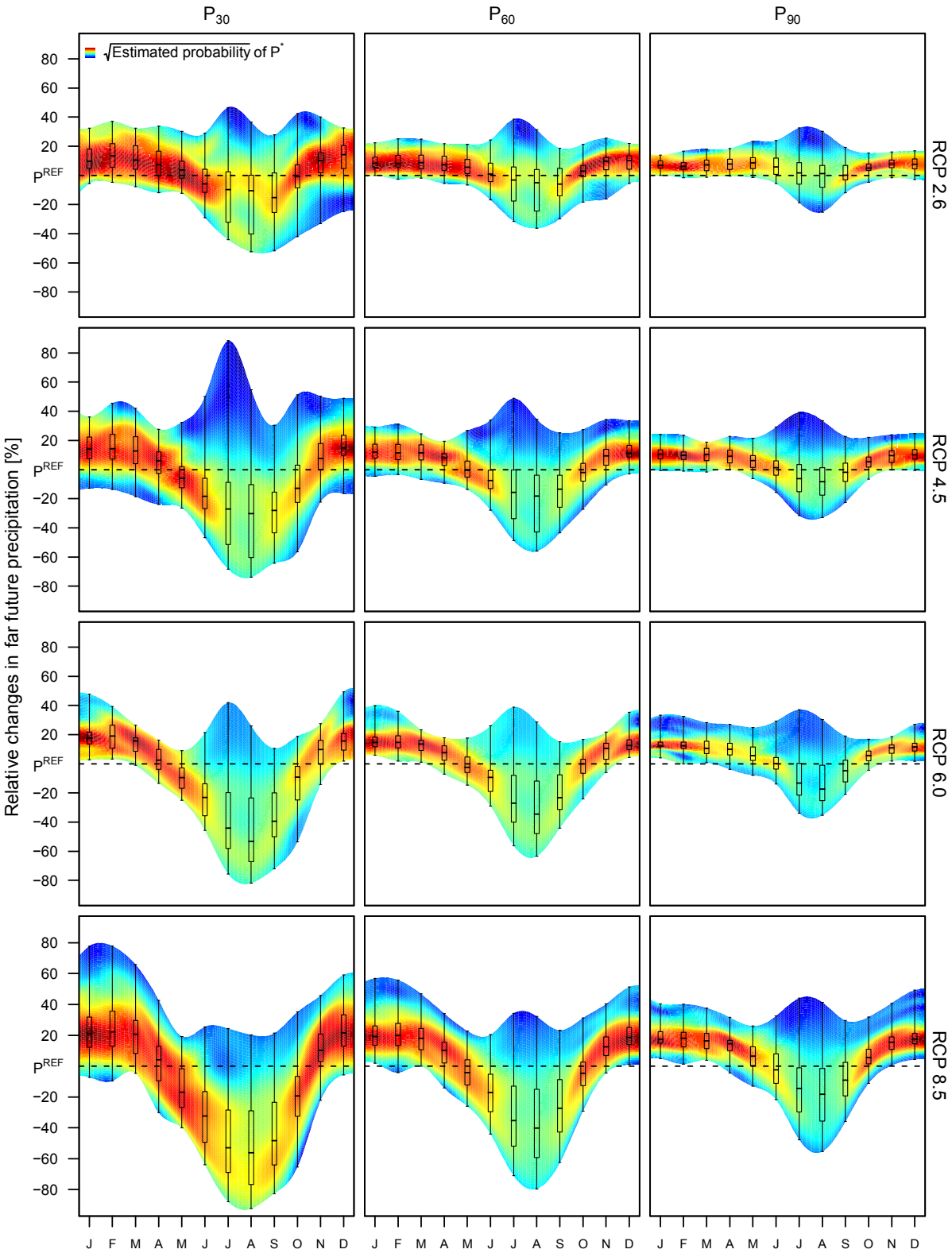

Figure 16: Total ranges of the relative changes in precipitation quantiles (P_{30}, P_{60} and P_{90}) per calendar month and RCP. The plotted values are averaged over the HBV sub-basins of both the Rhine and the Meuse and comprise far future data only. The boxplots denote the minimum, 1st quartile, median, 3rd quartile and maximum. The probability shading is constucted using monthly probability density functions that are estimated with a gaussian density model and are subsequently interpolated over months. Note that the square root of the probability is used to enhance the visible gradient at lower probabilities.

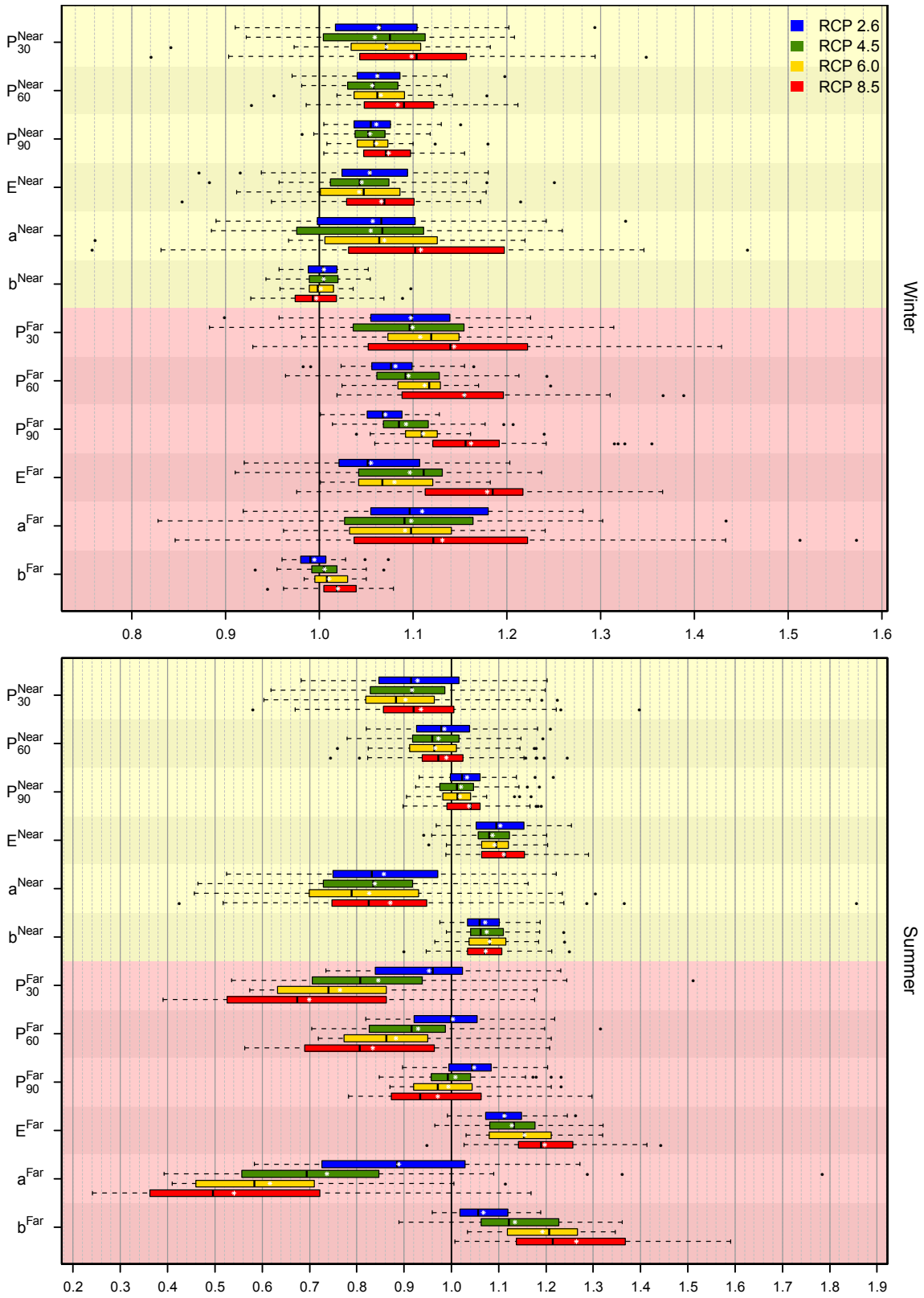

Figure 17: Relative change (by factors) of P_{30}, P_{60}, P_{90} and mean excess for the Rhine basin and both future periods. The transformation coefficients *a* and *b* comprise their values instead of change factors. All monthly values are averaged over the entire basin and subsequently over the specific season. The boxes are regular boxplots with the outliers defined as values that exceed 1.5 IQR from the edges of the box. Additionally, means are denoted by white stars. Note that the plots are a visualization of the data tables that are included as appendix A.

		RCP 2.6		RCP 4.5		RCP 6.0		RCP 8.5	
		Lowest	Highest	Lowest	Highest	Lowest	Highest	Lowest	Highest
Winter half year	P_{30}	0.903: HadGEM2-ES r1	1.265: FGOALS-s2 r1	0.853: CMCC-CM r1	1.420: FGOALS-s2 r1	0.923: MRI-CGCM3 r1	1.344: FGOALS-s2 r1	0.815: HadGEM2-CC r2	1.541: FGOALS-s2 r2
		0.918: HadGEM2-ES r2	1.253: GFDL-ESM2M r1	0.884: IPSL-CM5A-LR r4	1.295: FGOALS-s2 r3	0.957: HadGEM2-ES r1	1.205: CSIRO-Mk3-6-0 r3	0.905: CMCC-CM r1	1.479: FGOALS-s2 r3
		0.968: MRI-CGCM3 r1	1.208: MIROC5 r2	0.966: MPI-ESM-LR r1	1.250: CSIRO-Mk3-6-0 r10	1.009: HadGEM2-ES r3	1.184: GFDL-ESM2M r1	0.916: HadGEM2-CC r3	1.461: CMCC-CESM r1
	P_{60}	0.955: MRI-CGCM3 r1	1.200: FGOALS-s2 r1	0.917: CMCC-CM r1	1.325: FGOALS-s2 r1	0.908: MRI-CGCM3 r1	1.318: FGOALS-s2 r1	0.955: HadGEM2-CC r2	1.436: FGOALS-s2 r2
		0.980: HadGEM2-ES r2	1.194: GFDL-ESM2M r1	0.955: MRI-CGCM3 r1	1.230: FGOALS-s2 r3	1.019: HadGEM2-ES r1	1.180: GFDL-ESM2M r1	0.978: CMCC-CM r1	1.433: FGOALS-s2 r3
		1.010: GFDL-ESM2G r1	1.138: MIROC-ESM r1	0.968: IPSL-CM5A-LR r4	1.202: FGOALS-s2 r2	1.043: CSIRO-Mk3-6-0 r6	1.158: CSIRO-Mk3-6-0 r3	1.005: MRI-CGCM3 r1	1.354: CMCC-CESM r1
	P_{90}	0.948: MRI-CGCM3 r1	1.156: FGOALS-s2 r1	0.935: MRI-CGCM3 r1	1.245: FGOALS-s2 r1	0.903: MRI-CGCM3 r1	1.286: FGOALS-s2 r1	0.990: MRI-CGCM3 r1	1.413: FGOALS-s2 r3
		1.006: CNRM-CM5 r1	1.138: GFDL-ESM2M r1	0.977: CMCC-CM r1	1.188: FGOALS-s2 r3	1.023: CCSM4 r1	1.167: GFDL-ESM2M r1	1.033: MIROC5 r3	1.356: FGOALS-s2 r2
		1.007: CCSM4 r6	1.114: MIROC-ESM r1	1.003: inmcm4 r1	1.185: MIROC-ESM r1	1.033: MIROC5 r1	1.142: IPSL-CM5A-MR r1	1.039: CMCC-CM r1	1.316: FGOALS-s2 r1
	E	0.897: CCSM4 r6	1.223: HadGEM2-ES r4	0.869: MPI-ESM-LR r2	1.296: HadGEM2-ES r1	0.976: MRI-CGCM3 r1	1.206: HadGEM2-ES r1	1.018: MPI-ESM-LR r2	1.615: HadGEM2-CC r2
		0.923: NorESM1-M r1	1.214: CanESM2 r5	0.965: CCSM4 r1	1.248: ACCESS1-0 r1	0.995: MIROC5 r1	1.204: GFDL-CM3 r1	1.022: CSIRO-Mk3-6-0 r7	1.388: HadGEM2-ES r4
		0.927: MPI-ESM-LR r2	1.189: BNU-ESM r1	0.979: CNRM-CM5 r1	1.234: CMCC-CMS r1	1.002: bcc-csm1-1 r1	1.197: HadGEM2-ES r4	1.042: MIROC5 r3	1.382: FGOALS-s2 r3
	α	0.802: HadGEM2-ES r1	1.356: FGOALS-s2 r1	0.796: IPSL-CM5A-LR r4	1.498: FGOALS-s2 r1	0.906: HadGEM2-ES r1	1.332: FGOALS-s2 r1	0.688: HadGEM2-CC r2	1.632: FGOALS-s2 r2
		0.864: HadGEM2-ES r2	1.308: GFDL-ESM2M r1	0.832: CMCC-CM r1	1.359: MPI-ESM-LR r2	0.938: MRI-CGCM3 r1	1.240: CSIRO-Mk3-6-0 r3	0.821: HadGEM2-ES r1	1.631: CMCC-CESM r1
		0.968: CSIRO-Mk3-6-0 r8	1.279: CSIRO-Mk3-6-0 r5	0.895: MPI-ESM-MR r1	1.350: FGOALS-s2 r3	0.966: HadGEM2-ES r3	1.233: CSIRO-Mk3-6-0 r2	0.825: HadGEM2-CC r3	1.433: FGOALS-s2 r3
	b	0.941: CSIRO-Mk3-6-0 r10	1.124: HadGEM2-ES r1	0.934: MPI-ESM-LR r2	1.078: IPSL-CM5A-LR r4	0.966: CSIRO-Mk3-6-0 r2	1.062: HadGEM2-ES r1	0.943: CMCC-CESM r1	1.143: HadGEM2-CC r2
		0.948: CanESM2 r3	1.065: HadGEM2-ES r2	0.942: CSIRO-Mk3-6-0 r3	1.066: MPI-ESM-MR r1	0.971: CSIRO-Mk3-6-0 r9	1.040: HadGEM2-ES r3	0.953: CSIRO-Mk3-6-0 r7	1.141: HadGEM2-CC r3
		0.952: CSIRO-Mk3-6-0 r5	1.033: IPSL-CM5A-LR r3	0.946: CSIRO-Mk3-6-0 r10	1.056: HadGEM2-ES r1	0.972: CSIRO-Mk3-6-0 r3	1.038: HadGEM2-ES r2	0.959: CSIRO-Mk3-6-0 r8	1.110: HadGEM2-ES r1
Summer half year	P_{30}	0.658: HadGEM2-ES r2	1.220: MIROC-ESM-CHEM r1	0.477: CSIRO-Mk3-6-0 r9	1.476: IPSL-CM5B-LR r1	0.500: CSIRO-Mk3-6-0 r3	1.224: MIROC-ESM-CHEM r1	0.346: HadGEM2-ES r3	1.100: CNRM-CM5 r1
		0.663: CSIRO-Mk3-6-0 r9	1.187: CNRM-CM5 r1	0.515: CSIRO-Mk3-6-0 r8	1.192: MIROC-ESM-CHEM r1	0.521: CSIRO-Mk3-6-0 r5	1.080: MIROC-ESM r1	0.354: HadGEM2-CC r2	1.090: MIROC-ESM-CHEM r1
		0.682: CSIRO-Mk3-6-0 r5	1.131: MIROC-ESM r1	0.520: HadGEM2-ES r3	1.115: CNRM-CM5 r1	0.526: CSIRO-Mk3-6-0 r8	0.844: CCSM4 r6	0.366: HadGEM2-ES r4	1.027: MIROC-ESM r1
	P_{60}	0.786: CSIRO-Mk3-6-0 r7	1.198: MIROC-ESM-CHEM r1	0.656: CSIRO-Mk3-6-0 r9	1.292: IPSL-CM5B-LR r1	0.682: CSIRO-Mk3-6-0 r3	1.221: MIROC-ESM-CHEM r1	0.529: HadGEM2-ES r3	1.181: MIROC-ESM r1
		0.800: HadGEM2-ES r2	1.192: MIROC-ESM r1	0.689: CSIRO-Mk3-6-0 r1	1.186: MIROC-ESM r1	0.699: CSIRO-Mk3-6-0 r6	1.157: MIROC-ESM r1	0.536: HadGEM2-CC r2	1.176: MIROC-ESM-CHEM r1
		0.813: HadGEM2-ES r3	1.124: CNRM-CM5 r1	0.698: HadGEM2-ES r3	1.177: MIROC-ESM-CHEM r1	0.705: HadGEM2-ES r2	0.970: MIROC5 r1	0.555: HadGEM2-ES r4	1.106: CNRM-CM5 r1
	P_{90}	0.862: HadGEM2-ES r3	1.222: MIROC-ESM r1	0.811: inmcm4 r1	1.234: MIROC-ESM r1	0.859: CSIRO-Mk3-6-0 r3	1.214: MIROC-ESM r1	0.748: HadGEM2-ES r3	1.298: MIROC-ESM r1
		0.875: CSIRO-Mk3-6-0 r7	1.175: MIROC-ESM-CHEM r1	0.851: CSIRO-Mk3-6-0 r9	1.196: IPSL-CM5B-LR r1	0.861: HadGEM2-ES r2	1.211: MIROC-ESM-CHEM r1	0.773: HadGEM2-ES r4	1.241: MIROC-ESM-CHEM r1
		0.926: CSIRO-Mk3-6-0 r1	1.132: MIROC5 r1	0.852: CSIRO-Mk3-6-0 r1	1.175: MIROC-ESM-CHEM r1	0.862: CSIRO-Mk3-6-0 r1	1.108: MIROC5 r1	0.775: HadGEM2-CC r2	1.183: MIROC5 r2
	E	0.974: HadGEM2-ES r3	1.249: CSIRO-Mk3-6-0 r8	0.895: inmcm4 r1	1.289: MIROC-ESM-CHEM r1	0.994: bcc-csm1-1-m r1	1.305: MIROC5 r1	0.935: inmcm4 r1	1.456: MIROC5 r1
		0.974: MRI-CGCM3 r1	1.242: CSIRO-Mk3-6-0 r9	0.984: MPI-ESM-LR r3	1.250: MIROC-ESM r1	1.016: bcc-csm1-1 r1	1.281: MIROC-ESM r1	0.999: CSIRO-Mk3-6-0 r7	1.397: MIROC-ESM r1
		0.985: MPI-ESM-LR r3	1.210: HadGEM2-ES r2	0.994: MPI-ESM-MR r3	1.246: MIROC5 r1	1.026: GFDL-ESM2M r1	1.262: GFDL-CM3 r1	1.014: bcc-csm1-1-m r1	1.368: IPSL-CM5A-LR r4
	α	0.520: HadGEM2-ES r2	1.265: CNRM-CM5 r1	0.375: CSIRO-Mk3-6-0 r9	1.683: IPSL-CM5B-LR r1	0.381: CSIRO-Mk3-6-0 r8	1.195: MIROC-ESM-CHEM r1	0.227: HadGEM2-ES r3	1.081: CNRM-CM5 r1
		0.534: CSIRO-Mk3-6-0 r9	1.244: MIROC-ESM-CHEM r1	0.376: HadGEM2-ES r3	1.198: MIROC-ESM-CHEM r1	0.386: CSIRO-Mk3-6-0 r3	0.980: MIROC-ESM r1	0.229: CMCC-CM r1	0.943: MIROC-ESM-CHEM r1
		0.546: CSIRO-Mk3-6-0 r5	1.179: MIROC5 r2	0.391: CSIRO-Mk3-6-0 r8	1.187: CNRM-CM5 r1	0.391: CSIRO-Mk3-6-0 r5	0.749: CCSM4 r6	0.238: HadGEM2-ES r4	0.870: IPSL-CM5B-LR r1
	b	0.958: CNRM-CM5 r1	1.234: CSIRO-Mk3-6-0 r9	0.897: IPSL-CM5B-LR r1	1.373: CSIRO-Mk3-6-0 r9	1.004: MIROC-ESM-CHEM r1	1.364: CSIRO-Mk3-6-0 r5	1.011: CNRM-CM5 r1	1.674: HadGEM2-ES r2
		0.979: IPSL-CM5A-LR r4	1.233: CSIRO-Mk3-6-0 r5	0.963: CNRM-CM5 r1	1.351: CSIRO-Mk3-6-0 r8	1.067: MIROC-ESM r1	1.348: HadGEM2-ES r4	1.055: MRI-CGCM3 r1	1.617: HadGEM2-CC r1
		0.981: MIROC5 r2	1.215: HadGEM2-ES r2	0.994: MIROC-ESM-CHEM r1	1.335: CSIRO-Mk3-6-0 r1	1.077: CCSM4 r6	1.346: CSIRO-Mk3-6-0 r8	1.085: MIROC-ESM-CHEM r1	1.600: HadGEM2-ES r3

Table 3: The three lowest and highest model runs per season and RCP in terms of quantile change factors and transformation coefficients. The table shows the basin mean results for the Rhine in the far future only. Note that the parameters and values descibe the same data as Figure 17, which originates from appendix A.

	Highest 20							Lowest 20							
	model	run	rcp	P60	P30	P90	E	model	run	rcp	P60	P30	P90	E	
Summer	FGOALS-s 2	r3i1p 1	85	1.246	1.398	1.166	1.115	HadGEM2-E S	r4i1p 1	85	0.745	0.581	0.898	1 122	Near Future
	MIROC 5	r2i1p 1	26	1.210	1.203	1.216	1.196	HadGEM2-E S	r3i1p 1	60	0.760	0.604	0.905	1.085	
	MIROC 5	r2i1p 1	85	1.197	1.205	1.191	1.181	HadGEM2-E S	r2i1p 1	45	0.779	0.618	0.924	1.076	
	MIROC 5	r2i1p 1	45	1.194	1.198	1.187	1.123	HadGEM2-E S	r3i1p 1	85	0.806	0.670	0.921	1.025	
	MIROC-ES M	r1i1p 1	26	1.182	1.176	1.178	1.094	HadGEM2-E S	r4i1p 1	45	0.814	0.693	0.925	1.056	
	CNRM-CM 5	r1i1p 1	85	1.181	1.232	1.152	1.150	CSIRO-Mk3-6- 0	r1i1p 1	26	0.820	0.691	0.937	1.075	
	MIROC-ES M	r1i1p 1	85	1.180	1.173	1.184	1.139	bcc-csm1-1- m	r1i1p 1	85	0.823	0.695	0.931	1.042	
	MIROC-ES M	r1i1p 1	60	1.180	1.192	1.169	1.083	bcc-csm1-1- m	r1i1p 1	26	0.824	0.689	0.938	1.070	
	MIROC 5	r1i1p 1	60	1.176	1.225	1.145	1.149	bcc-csm1-1- m	r1i1p 1	60	0.824	0.707	0.926	1.104	
	MIROC-ESM-CHE M	r1i1p 1	85	1.158	1.178	1.143	1.109	HadGEM2-E S	r3i1p 1	26	0.824	0.682	0.947	1.077	
	IPSL-CM5B-L R	r1i1p 1	85	1.153	1.222	1.115	1.157	HadGEM2-E S	r2i1p 1	85	0.831	0.705	0.949	1.121	
	CMCC-CES M	r1i1p 1	85	1.148	1.187	1.131	1.172	bcc-csm1-1- m	r1i1p 1	45	0.842	0.716	0.950	1.104	
	CNRM-CM 5	r1i1p 1	45	1.147	1.172	1.129	1.099	HadGEM2-E S	r3i1p 1	45	0.843	0.727	0.943	1.095	
	MIROC-ESM-CHE M	r1i1p 1	60	1.145	1.166	1.134	1.132	HadGEM2-E S	r2i1p 1	60	0.846	0.742	0.935	1.057	
	MIROC-ESM-CHE M	r1i1p 1	45	1.145	1.154	1.143	1.174	HadGEM2-E S	r4i1p 1	60	0.854	0.731	0.969	1.117	
	MIROC 5	r1i1p 1	85	1.143	1.097	1.180	1.231	CSIRO-Mk3-6- 0	r10i1p 1	45	0.866	0.793	0.932	1.060	
	MIROC-ES M	r1i1p 1	45	1.129	1.085	1.161	1.189	CSIRO-Mk3-6- 0	r4i1p 1	26	0.869	0.773	0.954	1.104	
	MIROC 5	r1i1p 1	45	1.127	1.127	1.133	1.150	HadGEM2-C C	r2i1p 1	85	0.869	0.748	0.975	1.108	
	MIROC-ESM-CHE M	r1i1p 1	26	1.116	1.095	1.137	1.214	CSIRO-Mk3-6- 0	r4i1p 1	45	0.884	0.795	0.961	1.079	
	MIROC 5	r3i1p 1	85	1.094	1.027	1.142	1.155	CSIRO-Mk3-6-0	r7i1p 1	45	0.884	0.794	0.958	1.058	
Winter	model	run	rcp	P60	P30	P90	E	model	run	rcp	P60	P30	P90	E	
	EC-EART H	r6i1p 1	85	1.212	1.349	1.132	1.091	CMCC-CM S	r1i1p 1	85	0.928	0.821	1.005	1.090	
	MIROC 5	r2i1p 1	26	1.198	1.294	1.151	1.120	HadGEM2-E S	r4i1p 1	60	0.952	0.842	1.035	1.100	
	FGOALS-s 2	r1i1p 1	60	1.179	1.182	1.180	1.178	MIROC 5	r3i1p 1	26	0.971	0.910	1.015	1.080	
	MIROC 5	r2i1p 1	85	1.171	1.256	1.123	1.059	inmcm 4	r1i1p 1	45	0.981	0.958	0.994	0.998	
	MPI-ESM-L R	r2i1p 1	85	1.170	1.294	1.084	0.854	MPI-ESM-M R	r3i1p 1	45	0.983	0.927	1.024	1.103	
	CMCC-C M	r1i1p 1	85	1.164	1.241	1.113	1.034	HadGEM2-E S	r3i1p 1	26	0.984	0.929	1.026	1.005	
	EC-EART H	r8i1p 1	85	1.156	1.234	1.101	1.015	HadGEM2-E S	r1i1p 1	26	0.985	0.920	1.036	1.180	
	CMCC-CES M	r1i1p 1	85	1.150	1.157	1.140	1.081	GFDL-ESM2 G	r1i1p 1	26	0.986	0.960	1.005	1.070	
	FGOALS-s 2	r1i1p 1	85	1.147	1.114	1.155	1.075	IPSL-CM5A-L R	r4i1p 1	85	0.986	0.903	1.046	1.118	
	CNRM-CM 5	r1i1p 1	85	1.145	1.221	1.104	1.083	HadGEM2-C C	r1i1p 1	45	0.995	0.959	1.018	1.030	
	MIROC 5	r1i1p 1	60	1.142	1.178	1.124	1.101	GFDL-ESM2 G	r1i1p 1	45	0.996	0.985	1.003	1.052	
	MIROC 5	r1i1p 1	85	1.139	1.187	1.106	1.045	CMCC-C M	r1i1p 1	45	0.997	0.952	1.027	1.055	
	GFDL-ESM2 M	r1i1p 1	85	1.136	1.192	1.093	0.992	MPI-ESM-L R	r1i1p 1	85	0.997	0.954	1.031	1.071	
	CNRM-CM 5	r1i1p 1	26	1.136	1.186	1.102	1.032	IPSL-CM5A-L R	r4i1p 1	45	0.999	0.938	1.051	1.251	
	HadGEM2-E S	r2i1p 1	85	1.135	1.226	1.076	0.987	MPI-ESM-M R	r1i1p 1	85	1.000	0.978	1.019	1.092	
	MIROC-ES M	r1i1p 1	26	1.132	1.134	1.130	1.100	GFDL-ESM2 G	r1i1p 1	85	1.002	0.981	1.019	1.114	
	FGOALS-s 2	r2i1p 1	85	1.130	1.109	1.137	1.075	HadGEM2-E S	r2i1p 1	45	1.007	0.922	1.063	1.046	
	MPI-ESM-L R	r2i1p 1	26	1.129	1.202	1.072	0.872	MRI-CGCM 3	r1i1p 1	45	1.009	0.979	1.032	1.058	
	MIROC 5	r1i1p 1	45	1.129	1.183	1.094	1.060	HadGEM2-E S	r4i1p 1	85	1.012	0.971	1.038	1.056	
	EC-EARTH	r7i1p 1	85	1.126	1.095	1.145	1.160	GISS-E2- R	r6i1p 1	45	1.013	0.985	1.029	0.995	
Summer	model	run	rcp	P60	P30	P90	E	model	run	rcp	P60	P30	P90	E	Far Future
	IPSL-CM5B-L R	r1i1p 1	45	1.316	1.512	1.212	1.174	HadGEM2-C C	r2i1p 1	85	0.563	0.393	0.791	1.191	
	MIROC-ESM-CHE M	r1i1p 1	26	1.218	1.231	1.204	1.134	HadGEM2-E S	r4i1p 1	85	0.572	0.390	0.794	1.138	
	MIROC-ES M	r1i1p 1	26	1.212	1.228	1.198	1.112	HadGEM2-E S	r3i1p 1	85	0.590	0.421	0.797	1.101	
	MIROC-ES M	r1i1p 1	60	1.211	1.181	1.233	1.234	HadGEM2-E S	r2i1p 1	85	0.605	0.460	0.813	1.142	
	MIROC-ES M	r1i1p 1	85	1.208	1.098	1.297	1.443	CSIRO-Mk3-6- 0	r4i1p 1	85	0.615	0.442	0.821	1.254	
	MIROC-ES M	r1i1p 1	45	1.197	1.144	1.233	1.217	CSIRO-Mk3-6- 0	r9i1p 1	85	0.635	0.458	0.849	1.225	
	CNRM-CM 5	r1i1p 1	85	1.191	1.176	1.207	1.283	CSIRO-Mk3-6- 0	r1i1p 1	85	0.641	0.463	0.844	1.153	
	MIROC-ESM-CHE M	r1i1p 1	60	1.182	1.143	1.211	1.231	ACCESS1- 0	r1i1p 1	85	0.650	0.478	0.871	1.210	
	FGOALS-s 2	r3i1p 1	45	1.178	1.244	1.157	1.071	HadGEM2-C C	r1i1p 1	85	0.651	0.481	0.873	1.267	
	MIROC-ESM-CHE M	r1i1p 1	85	1.177	1.096	1.244	1.377	CSIRO-Mk3-6- 0	r6i1p 1	85	0.665	0.493	0.865	1.225	
	MIROC 5	r2i1p 1	85	1.169	1.088	1.235	1.327	CSIRO-Mk3-6- 0	r7i1p 1	85	0.669	0.526	0.828	1.088	
	MIROC 5	r2i1p 1	26	1.163	1.170	1.158	1.156	bcc-csm1-1- m	r1i1p 1	85	0.670	0.516	0.837	1.159	
	IPSL-CM5B-L R	r1i1p 1	85	1.162	1.158	1.178	1.278	HadGEM2-C C	r3i1p 1	85	0.675	0.540	0.858	1.227	
	MIROC-ESM-CHE M	r1i1p 1	45	1.158	1.156	1.173	1.321	CSIRO-Mk3-6- 0	r8i1p 1	85	0.677	0.522	0.877	1.264	
	MIROC 5	r1i1p 1	45	1.155	1.123	1.180	1.206	HadGEM2-E S	r1i1p 1	85	0.686	0.531	0.886	1.257	
	CNRM-CM 5	r1i1p 1	26	1.149	1.205	1.113	1.097	CanESM 2	r2i1p 1	85	0.687	0.507	0.873	1.168	
	MIROC 5	r1i1p 1	26	1.141	1.081	1.189	1.245	inmcm 4	r1i1p 1	85	0.690	0.586	0.783	0.949	
	MIROC 5	r2i1p 1	45	1.133	1.127	1.137	1.140	CanESM 2	r1i1p 1	85	0.692	0.521	0.875	1.252	
	IPSL-CM5A-L R	r1i1p 1	26	1.133	1.152	1.122	1.127	CSIRO-Mk3-6- 0	r3i1p 1	85	0.695	0.513	0.891	1.247	
	CNRM-CM 5	r1i1p 1	45	1.127	1.179	1.094	1.098	CMCC-C M	r1i1p 1	85	0.702	0.490	0.919	1.170	
Winter	model	run	rcp	P60	P30	P90	E	model	run	rcp	P60	P30	P90	E	
	FGOALS-s 2	r2i1p 1	85	1.389	1.412	1.355	1.163	IPSL-CM5A-L R	r4i1p 1	45	0.964	0.883	1.031	1.192	
	CMCC-CES M	r1i1p 1	85	1.367	1.429	1.315	1.191	GFDL-ESM2 G	r1i1p 1	26	0.983	0.957	1.001	1.074	
	FGOALS-s 2	r1i1p 1	85	1.310	1.285	1.319	1.257	HadGEM2-E S	r1i1p 1	26	0.991	0.899	1.060	1.137	
	FGOALS-s 2	r3i1p 1	85	1.305	1.273	1.326	1.366	GFDL-ESM2 G	r1i1p 1	45	0.999	0.961	1.029	1.138	
	CanESM 2	r2i1p 1	85	1.259	1.286	1.242	1.247	GISS-E2- R	r6i1p 1	45	1.004	0.984	1.014	1.031	
	MIROC 5	r1i1p 1	85	1.254	1.283	1.229	1.155	inmcm 4	r1i1p 1	45	1.011	1.006	1.014	1.042	
	FGOALS-s 2	r1i1p 1	60	1.247	1.248	1.240	1.179	MPI-ESM-M R	r1i1p 1	85	1.019	0.929	1.084	1.205	
	FGOALS-s 2	r1i1p 1	45	1.243	1.297	1.207	1.127	IPSL-CM5A-L R	r4i1p 1	26	1.023	1.021	1.032	1.114	
	CanESM 2	r1i1p 1	85	1.235	1.247	1.222	1.206	HadGEM2-E S	r1i1p 1	60	1.024	0.981	1.059	1.131	
	EC-EART H	r6i1p 1	85	1.232	1.331	1.172	1.111	HadGEM2-C C	r2i1p 1	85	1.029	0.962	1.096	1.355	
	CNRM-CM 5	r1i1p 1	85	1.231	1.255	1.215	1.143	ACCESS1- 3	r1i1p 1	45	1.031	1.053	1.027	1.143	
	EC-EART H	r8i1p 1	85	1.227	1.279	1.186	1.118	CMCC-C M	r1i1p 1	45	1.034	0.988	1.067	1.040	
	MIROC 5	r2i1p 1	85	1.227	1.244	1.216	1.185	bcc-csm1- 1	r1i1p 1	26	1.035	1.026	1.034	0.968	
	MPI-ESM-L R	r2i1p 1	85	1.224	1.293	1.164	0.976	MPI-ESM-M R	r1i1p 1	45	1.037	0.980	1.078	1.149	
	EC-EART H	r7i1p 1	85	1.213	1.198	1.227	1.212	inmcm 4	r1i1p 1	85	1.038	1.006	1.059	1.092	
	MIROC-ES M	r1i1p 1	45	1.213	1.227	1.197	1.121	CanESM 2	r1i1p 1	26	1.040	1.021	1.049	1.026	
	CanESM 2	r5i1p 1	85	1.212	1.232	1.200	1.253	CanESM 2	r5i1p 1	45	1.041	1.012	1.069	1.220	
	EC-EART H	r2i1p 1	85	1.200	1.267	1.155	1.112	CSIRO-Mk3-6- 0	r3i1p 1	26	1.041	1.072	1.025	1.050	
	IPSL-CM5A-M R	r1i1p 1	85	1.196	1.189	1.201	1.164	CanESM 2	r5i1p 1	26	1.046	0.997	1.084	1.203	
	CSIRO-Mk3-6- 0	r8i1p 1	85	1.196	1.173	1.210	1.269	CanESM 2	r3i1p 1	45	1.046	1.028	1.060	1.109	

Table 4: The 20 model runs with the lowest and highest changes for P_{60} and their changes in P_{30}, P_{90} and excess. The table shows the basin mean of the relative changes for the Rhine only.

3.7. Model runs with the largest changes

There is some variability in the extreme model runs over the parameters and RCPs, but a handful of models and runs represents the gross of the extremes (Table 3 and 4). For the winter period, all runs of the FGOALS-s2 model are predominantly present as the highest changes that are found. Difference with the second highest change is often in the order of 10%, which is reasonably large considering that the differences between the second and third largest runs are generally within 5%. The lowest changes are not so much represented by a single model. Nevertheless, the HadGEM2-ES and MRI-CGCM3 models are dominantly present.

The summer period lows are mostly represented by runs of the CSIRO-Mk3-6-0 and HadGEM2-ES models. The extreme large positive changes are often due to MIROC-ESM and MIROC-ESM-CHEM. Noteworthy is the very large positive change in the RCP 4.5 P_{30} caused by run 1 of the IPSL-CM5B-LR model. It is approximately 20% larger than the second largest change, i.e. respectively 1.476 and 1.192.

Table 4 presents the twenty model runs with the lowest and highest changes in P_{60} for the Rhine basin. It shows that there can be quite a difference between the relative amounts of change between the three quantiles over all model runs. For instance, the run with the largest change in P_{60} does not necessarily have the largest change in P_{90}. Also noteworthy is the pattern that there is quite a variety of RCPs present in the 20 extreme runs. Except for the far future lowest changes in summer and the highest changes in winter, where RCP 8.5 dominates.

3.8. Return levels and return periods of 10-day precipitation sums

Winter (Oct-Mar)

The return periods for 10-day basin-average winter precipitation, for which the return probabilities are determined by using a Gumbel distribution (appendix in Ruiter, 2012), show that most model runs have increased return levels for all return periods compared to the reference period (Fig. 18). For the near future there is little difference between the 4 RCPs, which is noticeable as well from Figure 19 that shows the relative differences of the RCP means with the reference precipitation. The values for the 10-day precipitation sum with a return period of 50 years range from about 150 to 200 mm for the Meuse and 110 to 140 mm for the Rhine.

In the far future the different RCPs deviate from each other more strongly, a pattern also observable from Figure 17. The relative change of the RCP means (Fig. 19) shows there is a relatively linear change compared to the reference precipitation, i.e. the general trend regarding relative change of the RCP ensemble means is similar for all return periods visible by the horizontal lines. The range of 10-day precipitation return levels found in the far future for the 50 year return precipitation is about 150 to 250 mm for the Meuse and 110 to 155 mm for the Rhine. Remarkably, the relative change of the EC-EARTH mean is larger than the RCP 8.5 mean for the near future, while it is similar in the far future.

Summer (Apr-Sep)

The 10-day precipitation returns levels are considerably lower in summer than in winter (Figs. 18 and 20). Near future 50-year return levels range from about 85 to 125 mm for the Meuse and 90 to 120 mm for the Rhine, far future levels range from respectively 80 to 135 mm and 90 to 125 mm. In the near and far future the summer precipitation amounts deviate from the reference precipitation both positively and negatively, with a mean tendency toward positive change of about 5% (Fig. 21). A difference with the winter return levels of the 10-day precipitation sums is that the relative change seems non-linear.

Precipitation related to lower return periods has a lower relative change than precipitation related to higher return periods, noticeable from Figure 21 by the tilted RCP ensemble means.

Again the EC-EARTH runs show a deviation with the bulk of the RCP 8.5 runs. Especially in the far future, the general trend in the EC-EARTH mean (Fig. 21) is more similar to RCP 2.6 than RCP 8.5. The 50-year return value, however, is comparable with RCP 8.5. Another difference in RCP means is present for the far future 50 year return level of the Meuse. In contrast to the Rhine, lower forcings tend to cause higher return levels of the 10-day precipitation sums.

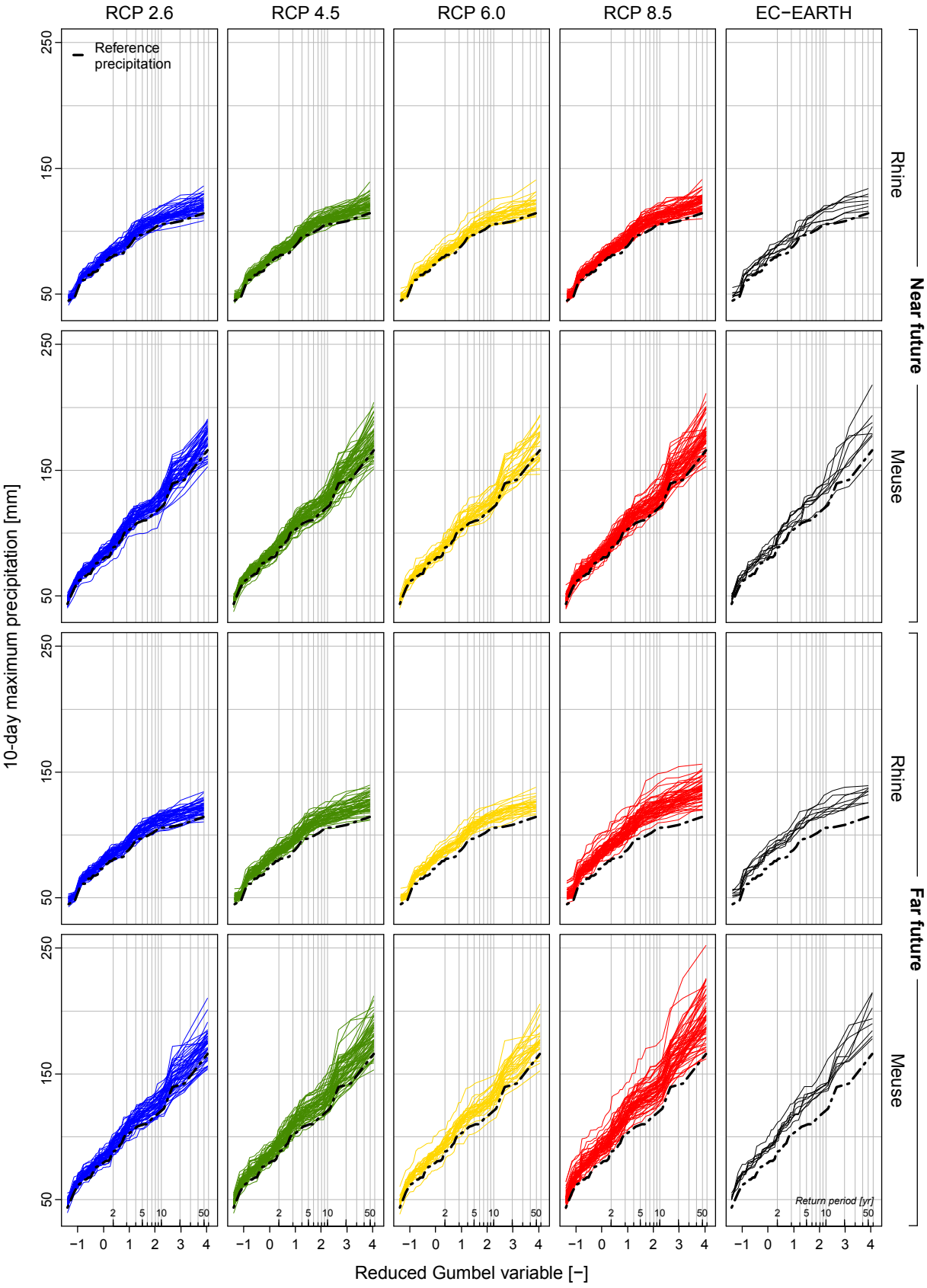

Figure 18: Return levels and periods of the 10-day maximum precipitation in winter (Oct-Mar) for the two basins in the near and far future. The model runs based on different RCPs as well as EC-EARTH runs are shown seperately. The 10-day precipiation sums are calculated using basin-average precipitation, as high basin-average precipitation is causal for high river discharges.

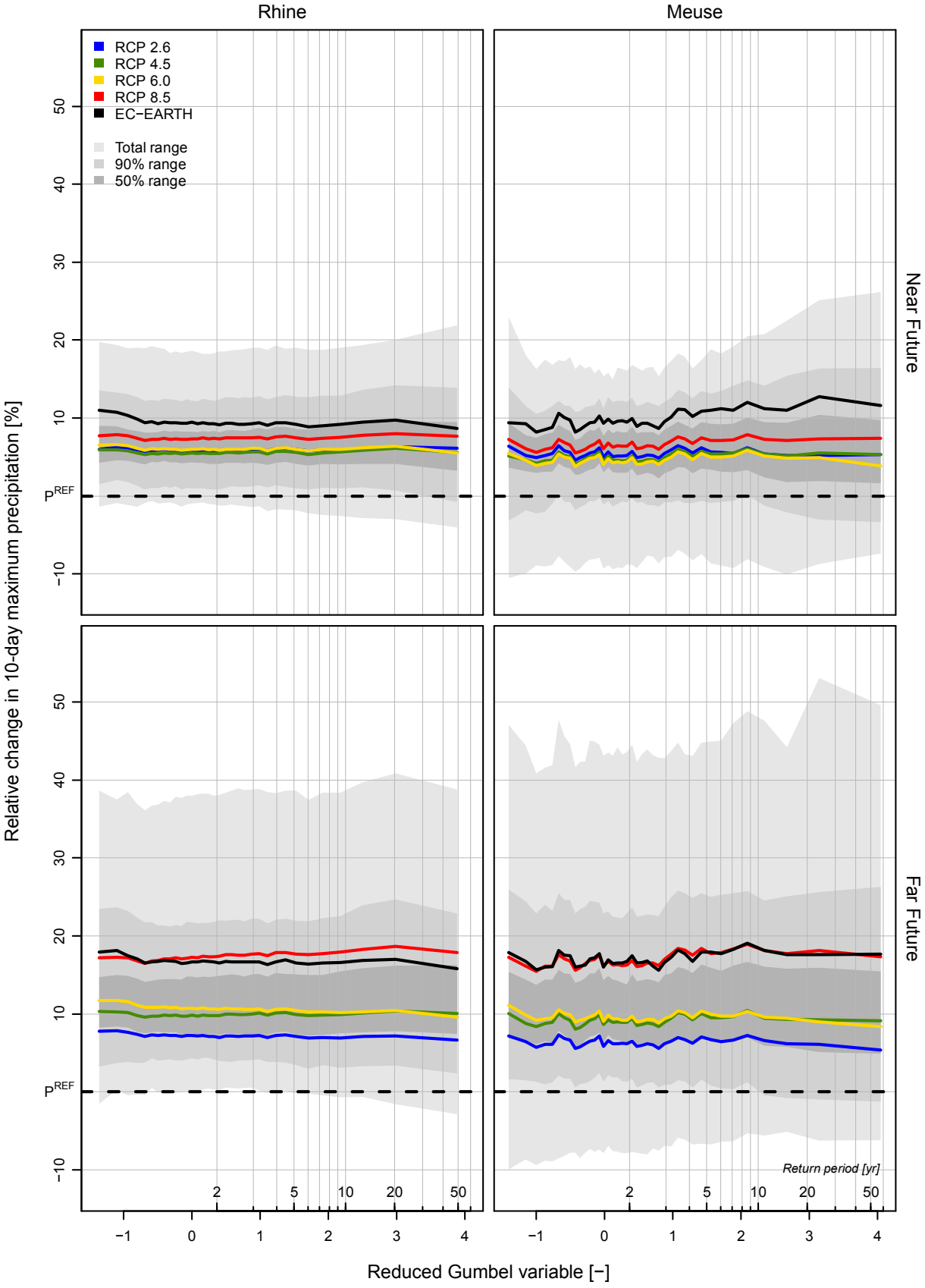

Figure 19: Changes in the return levels of the 10-day maximum precipitation sums in winter relative to the reference precipitation per RCP ensemble. The two basins, the near and far future and RCPs are plotted separately. Note that for plotting clarity these plots are based on averaged 10-day maximum precipitation sums of the separate sub-basins instead of the precipitation sums of the basin-wide average precipitation, which is the case in Figure 20. The grey shading is based on the distribution of the 10-day maximum precipitation sums in winter for the entire CMIP5 ensemble.

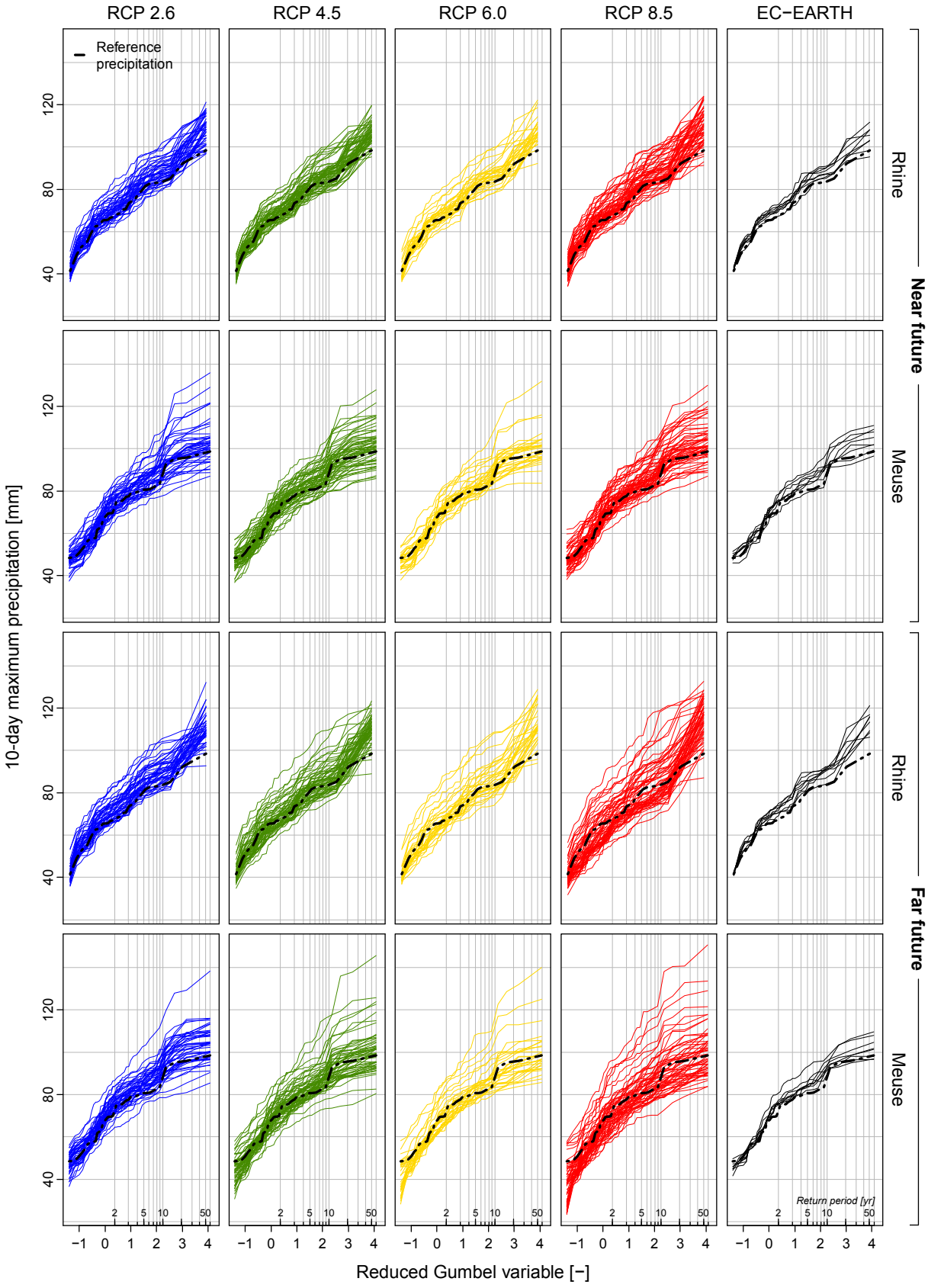

Figure 20: Return levels and periods of the 10-day maximum precipitation in summer (Apr-Sep) for the two basins in the near and far future. The model runs based on different RCPs as well as EC-EARTH runs are shown seperately. The 10-day precipiation sums are calculated using basin-average precipitation, as high basin-average precipitation is causal for high river discharges.

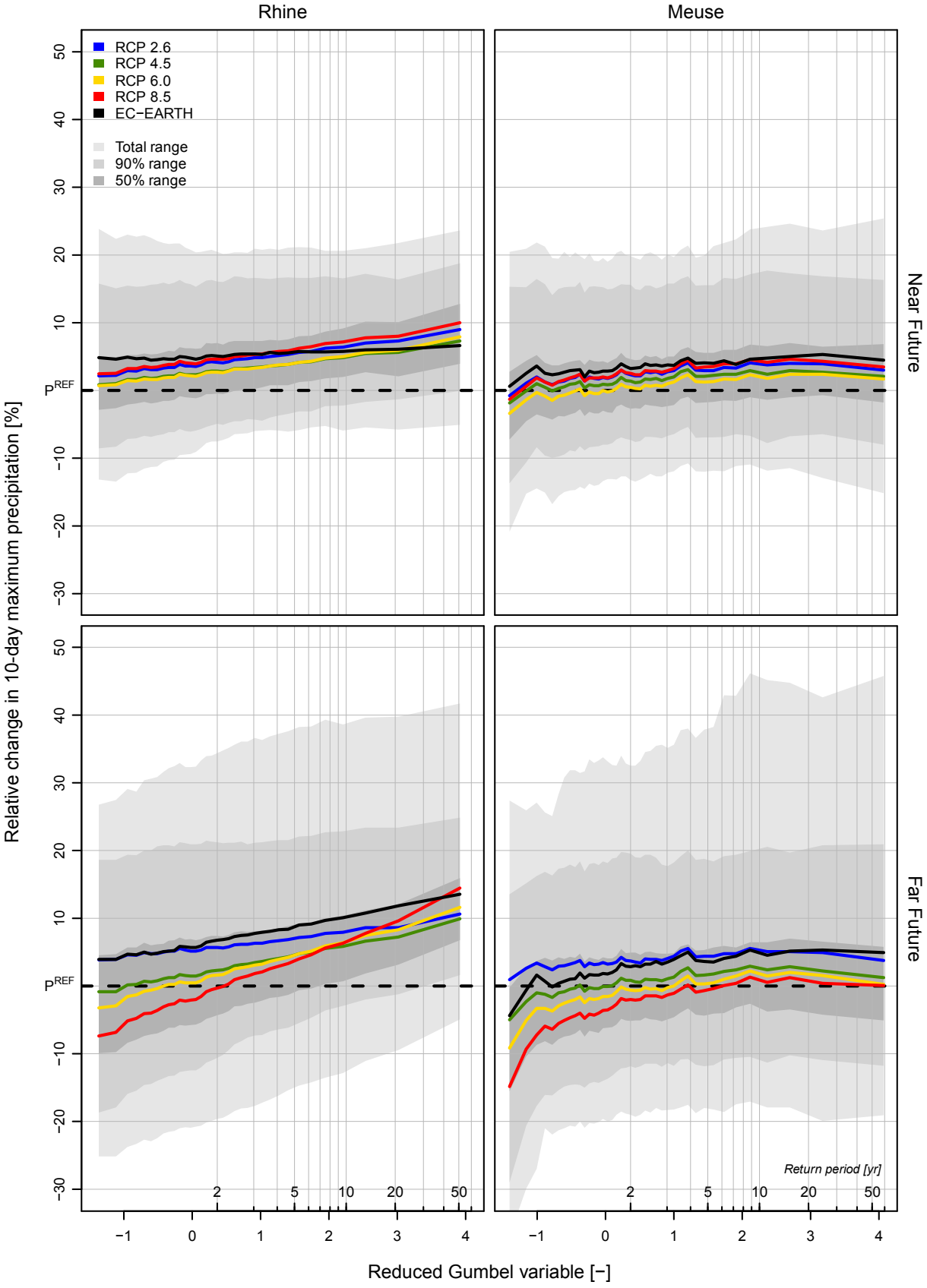

Figure 21: Changes in the return levels of the 10-day maximum precipitation sums in summer relative to the reference precipitation per RCP ensemble. The two basins, the near and far future and RCPs are plotted separately. Note that for plotting clarity these plots are based on averaged 10-day maximum precipitation sums of the separate sub-basins instead of the precipitation sums of the basin-wide average precipitation, which is the case in Figure 20. The grey shading is based on the distribution of the 10-day maximum precipitation sums in summer for the entire CMIP5 ensemble.

4. DISCUSSION AND CONCLUSIONS

4.1. Achievements of the research

In this study improvements are made regarding the possible application of the ADC method to a larger focus area in order to serve other researchers that are interested in the method. Using a different spatial smoothing technique and by using the E-OBS dataset transformation coefficients could be determined for most of Europe. The number of GCM runs that are taken into account is considerably increased from 38 to 199. In addition the near future (2021-2051) is added as a future forcing period besides the far future (2071-2100) period. So in total 398 different climate change signals are derived and made available for time series transformation. The complete dataset with transformation coefficients is ready to be used by other researchers to transform their own historical datasets to data representative for the future periods. User friendly R-scripts are developed for this purpose. The determined coefficients are successfully applied to historical datasets of the Rhine and the Meuse basins to obtain transformed daily data representative of the future that will be used by Deltares and RWS-Waterdienst.

4.2. Upscaling the parameter calculation

Using the E-OBS dataset for the bias correction that is needed in the ADC method yields advantages with regard to the focus area for which ADC parameters can be determined. There is a side effect to using this dataset, however, as its historical time series are not completely equal to those of the historical datasets to which the ADC method is, or will typically be, applied. This results in not fully accurate bias corrections during the parameter calculation of the ADC method. Further research must determine the absolute effects, though they are estimated to be relatively small. Large systematic errors in one of the datasets though, are thought to able to cause significant differences in the result. These are however only expected to occur when there are large differences between the climatologies of E-OBS and the historical dataset to which the ADC transformation is applied or when there are systematic errors in the latter. It is more likely that such errors are small compared to the errors that would occur when no bias-correction would be applied to account for systematic differences between E-OBS and GCM control runs, but this was not thoroughly tested.

The moving window smoothing technique used to reduce spatial noise of the *b* parameter has been assessed and proven to work. It is however possible that further improvements to the window algorithm may result in more accurate transformation results. For example, currently diagonally neighbouring cells have the same weight during the smoothing process as directly neighbouring cells although their distance to the centre cell is larger. Also the effect of small differences in the surface area of the latitude longitude based common grid cells could be taken into account.

4.3. Non-linearity of precipitation changes and the ADC method

The use of ADC method is based on the idea that future precipitation changes non-linearly, i.e. the shape of the precipitation distribution changes. This study shows that the non-linear change is indeed present. However, for the data and study area used in this research, this non-linearity is primarily present for the summer precipitation where the relative changes in P_{30}, P_{60} and P_{90} are considerably different (Fig. 16 and 17). The mean relative changes in the precipitation quantiles of winter precipitation are not so different. Especially for the moderate RCPs 4.5 and 6.0 the precipitation transformations resulted to be relatively linear. The extreme RCPs show more non-linearity in the ensemble mean changes, although not as clear as for the quantiles of summer precipitation. Important to note is that individual runs may show considerably more non-linearity in the winter than the ensemble mean.

As the focus of the ADC method is to aid hydrological modelling of extreme discharge events that occur during the high discharge winter season, the rather linear changes in the winter period question the method's added value to a certain extent. I should be noted that when the ADC method performs a linear transformation this does not affect the results in any way when compared to the classical delta method's linear transformation, thereby no negative effects occurs from its use. This, combined with fact that it was initially unknown if non-linear precipitation changes in the high discharge season would occur, although they were anticipated, results in the conclusion that the choice for the ADC method is justified. Other study areas than the Rhine or the Meuse may encounter more distinct non-linear precipitation changes in the high discharge season and therefore it remains highly advisable to use the ADC method.

4.4. Increase in 10-day precipitation return levels

Important for extreme discharge modelling are the return levels and return periods of extreme multi-day precipitation events. The 10-day maximum precipitation levels in winter increase for about 95% of all GCM runs in both the near and far future (Fig. 19). Thus, the CMIP5 ensemble indicates a high probability of an increased number of extreme discharge events and increased severity of these events. As a result, flooding frequency and severity are both expected to rise. Coupling with hydrological models is however required to quantify these effects.

The ensemble mean return levels per RCP for the summer period (Fig. 21) show a slight increase in 10-day maximum precipitation with approx. 5-10%. This does however not directly mean that there will be an increased possibility of summer floods. Namely, the increase in temperature in the future will likely be accompanied by an increase of evapo(transpi)ration. Again coupling with hydrological models is needed to determine the overall effects on flooding frequency and severity.

When a comparison is made between the relative changes in the return levels of the 10-day precipitation sums in the winter (Fig. 19) and those in the quantiles and excesses of precipitation (Fig. 17), it can be noted that the linear relative changes in return levels of the 10-day precipitation sums per RCP closely resemble the average changes in the excess. This gives rise to the idea that the 10-day maximum precipitation is mainly controlled by the change in excess precipitation during winter. For the summer precipitation this is not the case. Here the relative changes in the return levels of the 10-day precipitation sums, besides being non-linear which is visible by the tilted lines, are smaller than the relative increases in excess. The latter is likely related to the large decreases in the bulk of the precipitation distribution as denoted by the decreases in P_{30}, P_{60} and P_{90} (Fig. 17). One should however be careful with such comparisons, as the changes the excesses are based on consecutive 5-day sums that cannot be translated directly to changes in seasonal maximum 10-day sums.

4.5. Quantification of the differences between Rhine and Meuse results

There are relatively little differences between the relative changes in the precipitation quantiles of the Rhine and the Meuse basins, as can be noted from Figures 12 and 13. The slight differences that do exist are difficult to quantify, due to the large difference between the size of the Rhine and Meuse basins. Namely, the Rhine basin is divided into 134 sub-basins while the Meuse consists of 15 sub-basins. Statistical comparison of the results from such different sample sizes is generally difficult.

The relatively large difference between the return levels of the 10-day precipitation sums for the Rhine and the Meuse basins is due to the difference in size of the two basins (Figs. 18 and 20); the larger the basin the smaller the extreme 10-day precipitation as basin-wide precipitation averages are very likely to be lower. The differences of the ensemble mean 10-day return levels with those of the reference precipitation shown in Figures 19 and 21 can be compared because these denote relative changes. Note

however that the Rhine and the Meuse rivers are of a considerably different scale and the noticeable differences are therefore not surprising. In further research it is possibly more interesting to compare the results for the Meuse basin with similarly large Rhine tributaries, such as the Moselle, Neckar and Main. Comparison of results for the Moselle is especially interesting, as it is in close vicinity of the Meuse and the upper sections of both rivers encounter relatively similar geologic, geographic and climatologic conditions.

4.6. Differences between RCPs

The results of this study show that the different RCPs have noticeably different effects. That is, when means or medians of each RCP are considered. When focusing on their entire distributions there is a large overlap between the values of the different RCPs (Fig. 17). This is the case for both seasons, although overlapping is especially present in the winter period where the interquartile ranges of the various RCPs can overlap by about 65% for each quantile. Further statistical analyses must show whether the different forcings truly result in systematically different changes in the precipitation characteristics of the winter period.

The large overlapping in the winter does have an advantage in terms of extreme discharge modelling. As different future climate paths yield comparable extreme precipitation amounts and thereby comparable extreme discharges, the probability that those discharges will occur in the future becomes higher and the likely range of extreme discharges smaller. This will provide more certainty in the determination of a new design discharge.

4.7. Accuracy of P_{30} transformation

A determination of the expected increase in the number and severity of summer droughts in the near and far future via the ADC method is scientifically valuable for ecological, agricultural and geographical studies. To be able to determine these properly, the transformation of low quantiles must be accurate. As seen in the results of this study as well as in Ruiter's (Ruiter, 2012), the transformed P_{30} is considerably less accurate than P_{60} and P_{90} for individual model runs. Namely, the reproduction of GCM climate signal of P_{30} in the transformed precipitation can deviate up to about 25% (Figs. 12 and 13), which is about 4 times more than P_{60} and P_{90} that have maximum deviations of approx. 3 to 7%.

This pattern most likely caused by the fact that P_{30} is not taken into account directly in the calculation of the ADC method's transformation coefficients. To improve the relative inaccuracy present for individual model runs, a new revised version of the ADC method could be developed in future research that performs separate transformations for the part of the precipitation above and below P_{60}, e.g. using respectively P_{30} and P_{90}.

4.8. Extreme or erroneous model runs

There are a few model runs of which the results deviate strongly from other runs (section 0). For the MIROC model it is known from earlier versions described in literature that they produce relatively wet summer months in the Northern Hemisphere (Van Den Hurk et al., 2006; Van Ulden & Van Oldenborgh, 2006), which is not exceptional for this model.

The extreme values of IPSL-CM5B-LR r1i1p1 for RCP 4.5 are questionable however. The change in (extreme) summer precipitation for this model run is so large compared to the other CMIP5 GCMs that it raises the question if there is a systematic error in this model. No evidence for such an error could however be found in published literature.

The high extremes of the FGOALS-s2 model in the winter precipitation for all RCPs are questionable as well. Although its runs are not extremely different from the other models as in the case of IPSL-CM5B-LR r1i1p1, the change in (extreme) winter precipitation is systematically larger than in any of the other models. This might be related to other odd characteristics found for this model, e.g. a peculiar change of the global mean temperature over time that may be related to a too large CH_4 forcing (pers. comm. Van Oldenborgh, KNMI).

It is clear that more research is needed to make definite statements about the status of these model runs. For now it is advised to acknowledge these potential problems and to carefully reconsider their suitability for hydrological modelling purposes.

REFERENCES

Alley, R., T. Berntsen & N. Bindoff. (2007), Climate Change 2007-The Physical Science Basis. Working group I contribution to the fourth assessment report of the IPCC.

Bergström, S. & V. Singh. (1995), The HBV model. Computer models of watershed hydrology. Water Resources Publications, pp.443-476.

Bouwer, L.M., P. Bubeck & J.C. Aerts. (2010), Changes in future flood risk due to climate and development in a Dutch polder area. Global Environmental Change 20(3), pp.463-471.

Buishand, T.A. & R. Leander. (2011), Rainfall generator for the Meuse basin: Extension of the base period with the years1999-2008. KNMI publication (196-V).

Burrough, P. A., McDonnell, R., Burrough, P. A. & McDonnell, R. (1998). Principles of geographical information systemsOxford university press Oxford.

Eberle, M., H. Buiteveld, J. Beersma et al. (2002). Estimation of extreme floods in the river rhine basin by combining precipitation-runoff modelling and a rainfall generator. Paper presented at the Proceedings International Conference on Flood Estimation, Berne, Switzerland, pp.6-8.

Haylock, M., N. Hofstra, A.K. Tank et al. (2008), A European daily high-resolution gridded data set of surface temperature and precipitation for 1950–2006. Journal of Geophysical Research 113(D20), pp.D20119.

Hazeleger, W., C. Severijns, T. Semmler et al. (2010), EC-earth: a seamless earth-system prediction approach in action. Bulletin of the American Meteorological Society 91(10), pp.1357-1363.

IIASA. (2013). RCP Database [online]. Retrieved January, 2013. Available on the world wide web: <https://tntcat.iiasa.ac.at:8743/RcpDb/>.

Kew, S., F. Selten, G. Lenderink et al. (2011), Robust assessment of future changes in extreme precipitation over the Rhine basin using a GCM. Hydrology and Earth System Sciences 15(4), pp.1157-1166.

Leander, R. (2009), Simulation of precipitation and discharge extremes of the river Meuse in current and future climate. Utrecht University dissertation.

Max Planck Institute for Meteorology. (2012), Climate Data Operators. Hamburg, Germany.

Nakićenović, N., J. Alcamo, G. Davis et al. (2000), IPCC special report on emissions scenarios (SRES).

Perrin, C., C. Görgen, E. Sauquet et al. (2010). The RheinBlick2050 and Imagine2030 projects: A perspective on the hydrological impacts of climate change in two river basins in europe. Paper presented at the Euraqua Symposium, Koblenz, Germany.

R Development Core Team. (2008), R: A language and environment for statistical computing. R Foundation for Statistical Computing, Vienna, Austria.

Ruiter A. (2012). Delta-change approach for CMIP5 GCMs, Trainee Report, KNMI, pp 30.

Taylor, K.E., R.J. Stouffer & G.A. Meehl. (2012), An overview of CMIP5 and the experiment design. Bulletin of the American Meteorological Society 93(4), pp.485.

van de Ven, G. & M. Lowlands. (2004), History of Water Management and Land Reclamation in The Netherlands. Stichting Matrijs, Utrecht.

Van Den Hurk, B., Klein Tank, A., Lenderink, G., Van Ulden, A., Van Oldenborgh, G., Katsman, C. et al. (2006). KNMI climate change scenarios 2006 for the NetherlandsKNMI De Bilt.

Van Pelt, S., J. Beersma, T. Buishand et al. (2012), Future changes in extreme precipitation in the Rhine basin based on global and regional climate model simulations. Hydrol. Earth Syst. Sci. 16, pp.4517-4530.

Van Stokkom, H.T., A.J. Smits & R.S. Leuven. (2005), Flood Defense in The Netherlands. Water International 30(1), pp.76-87.

Van Ulden, A. & G. Van Oldenborgh. (2006), Large-scale atmospheric circulation biases and changes in global climate model simulations and their importance for climate change in Central Europe. Atmospheric Chemistry and Physics 6(4), pp.863-881.

Wit, M. D. & Buishand, A. (2007). Generator of rainfall and discharge extremes (GRADE) for the Rhine and Meuse basins. Lelystad: RWS RIZA.

APPENDICES

Rhine basin - Near Future (2021-2050)

Model info				Winter						Summer					
Index	GCM	Run	RCP	P30	P60	P90	E	a	b	P30	P60	P90	E	a	b
1.1	ACCESS1-0	r1i1p1	45	1,075	1,048	1,035	1,085	1,080	0,989	0,824	0,901	0,969	1,059	0,729	1,120
1.1	ACCESS1-0	r1i1p1	85	1,090	1,091	1,090	1,121	1,098	1,004	0,942	1,017	1,091	1,165	0,905	1,107
2.1	ACCESS1-3	r1i1p1	45	1,088	1,021	0,982	0,982	1,138	0,959	0,823	0,914	0,999	1,159	0,761	1,111
2.1	ACCESS1-3	r1i1p1	85	1,132	1,067	1,039	1,119	1,199	0,962	0,744	0,902	1,045	1,260	0,634	1,183
3.1	bcc-csm1-1	r1i1p1	26	1,045	1,051	1,054	1,030	1,029	1,007	0,949	0,986	1,011	1,000	0,835	1,073
3.1	bcc-csm1-1	r1i1p1	45	1,003	1,036	1,051	1,000	0,974	1,023	1,046	1,024	1,018	1,024	1,026	1,023
3.1	bcc-csm1-1	r1i1p1	60	1,118	1,096	1,073	0,954	1,122	0,990	0,939	0,992	1,034	1,080	0,819	1,081
3.1	bcc-csm1-1	r1i1p1	85	1,120	1,090	1,064	1,015	1,139	0,982	0,902	0,950	0,990	1,065	0,777	1,077
4.1	bcc-csm1-1-m	r1i1p1	26	1,007	1,051	1,076	1,061	0,946	1,042	0,689	0,824	0,938	1,070	0,525	1,185
4.1	bcc-csm1-1-m	r1i1p1	45	1,053	1,062	1,063	1,022	1,063	1,006	0,716	0,842	0,950	1,104	0,581	1,164
4.1	bcc-csm1-1-m	r1i1p1	60	1,013	1,025	1,030	1,027	0,998	1,014	0,707	0,824	0,926	1,104	0,570	1,165
4.1	bcc-csm1-1-m	r1i1p1	85	1,015	1,050	1,071	1,093	0,977	1,030	0,695	0,823	0,931	1,042	0,574	1,164
5.1	BNU-ESM	r1i1p1	26	1,081	1,064	1,052	1,048	1,091	0,988	0,945	0,989	1,023	1,055	0,850	1,059
5.1	BNU-ESM	r1i1p1	45	1,058	1,058	1,060	1,102	1,026	1,008	0,933	0,978	1,016	1,106	0,817	1,063
5.1	BNU-ESM	r1i1p1	85	1,055	1,071	1,080	1,093	1,038	1,011	1,005	1,018	1,039	1,163	0,920	1,038
6.1	CanESM2	r1i1p1	26	1,080	1,103	1,111	1,040	1,061	1,020	0,896	0,958	1,009	1,096	0,834	1,056
6.2	CanESM2	r2i1p1	26	1,072	1,066	1,064	1,094	1,071	1,004	0,939	0,983	1,017	1,063	0,849	1,055
6.3	CanESM2	r3i1p1	26	1,054	1,070	1,080	1,126	1,067	1,007	1,086	1,073	1,071	1,112	1,132	0,992
6.4	CanESM2	r4i1p1	26	1,034	1,042	1,047	1,070	1,080	0,994	0,841	0,888	0,932	1,050	0,805	1,049
6.5	CanESM2	r5i1p1	26	0,943	1,022	1,071	1,089	0,920	1,052	0,910	1,010	1,088	1,160	0,805	1,093
6.1	CanESM2	r1i1p1	45	0,981	1,041	1,072	1,037	0,970	1,038	0,878	0,951	1,012	1,152	0,812	1,075
6.2	CanESM2	r2i1p1	45	1,116	1,082	1,057	1,028	1,082	0,995	0,926	1,007	1,066	1,090	0,821	1,083
6.3	CanESM2	r3i1p1	45	1,005	1,027	1,037	1,043	1,024	1,011	0,980	0,998	1,019	1,069	1,002	1,025
6.4	CanESM2	r4i1p1	45	1,004	1,031	1,050	1,146	1,030	1,010	0,850	0,934	1,007	1,184	0,795	1,074
6.5	CanESM2	r5i1p1	45	0,965	1,020	1,060	1,157	1,008	1,027	0,818	0,920	1,002	1,073	0,720	1,113
6.1	CanESM2	r1i1p1	85	1,071	1,099	1,111	1,065	1,092	1,021	0,850	0,959	1,044	1,108	0,718	1,119
6.2	CanESM2	r2i1p1	85	1,161	1,125	1,102	1,148	1,159	0,988	0,879	0,966	1,039	1,155	0,780	1,086
6.3	CanESM2	r3i1p1	85	0,965	1,024	1,068	1,215	0,958	1,037	0,975	1,005	1,037	1,133	0,943	1,040
6.4	CanESM2	r4i1p1	85	1,116	1,102	1,096	1,171	1,191	0,983	0,952	0,957	0,975	1,120	0,954	1,016
6.5	CanESM2	r5i1p1	85	0,996	1,039	1,068	1,101	1,006	1,033	0,880	0,977	1,057	1,189	0,774	1,099
7.1	CCSM4	r1i1p1	26	1,049	1,028	1,011	1,024	1,068	0,988	0,906	0,959	0,999	1,034	0,812	1,065
7.2	CCSM4	r2i1p1	26	1,066	1,063	1,056	1,000	1,085	0,995	0,858	0,936	0,991	1,000	0,789	1,073
7.6	CCSM4	r6i1p1	26	1,073	1,048	1,021	0,916	1,092	0,988	0,886	0,958	1,021	1,193	0,787	1,081
7.1	CCSM4	r1i1p1	45	1,093	1,041	1,005	0,957	1,120	0,973	0,900	0,952	0,992	1,072	0,835	1,056
7.2	CCSM4	r2i1p1	45	1,081	1,078	1,072	1,064	1,069	1,002	0,893	0,944	0,980	0,974	0,820	1,059
7.6	CCSM4	r6i1p1	45	1,022	1,037	1,043	1,017	1,031	1,008	0,823	0,906	0,975	1,120	0,711	1,098
7.1	CCSM4	r1i1p1	60	1,067	1,033	1,008	0,989	1,086	0,985	0,839	0,911	0,967	1,064	0,740	1,086
7.2	CCSM4	r2i1p1	60	1,036	1,048	1,054	1,031	1,006	1,015	0,978	1,011	1,035	1,053	0,932	1,033
7.6	CCSM4	r6i1p1	60	1,059	1,060	1,058	0,991	1,042	1,008	0,964	1,000	1,028	1,090	0,913	1,037
7.1	CCSM4	r1i1p1	85	1,047	1,059	1,064	1,045	1,031	1,008	0,946	0,981	1,011	1,088	0,894	1,040
7.2	CCSM4	r2i1p1	85	0,992	1,034	1,064	1,104	0,978	1,026	0,852	0,946	1,022	1,114	0,759	1,092
7.6	CCSM4	r6i1p1	85	1,052	1,035	1,020	0,979	1,070	0,991	0,874	0,940	0,991	1,064	0,780	1,072
8.1	CMCC-CESM	r1i1p1	85	1,157	1,150	1,140	1,081	1,252	0,987	1,187	1,148	1,131	1,172	1,238	0,983
9.1	CMCC-CM	r1i1p1	45	0,952	0,997	1,027	1,055	0,933	1,032	0,948	0,989	1,021	1,028	0,862	1,055
9.1	CMCC-CM	r1i1p1	85	1,241	1,164	1,113	1,034	1,311	0,958	0,930	1,002	1,050	1,023	0,810	1,083
10.1	CMCC-CMS	r1i1p1	45	0,976	1,022	1,048	1,017	0,934	1,036	0,924	0,941	0,951	0,942	0,856	1,038
10.1	CMCC-CMS	r1i1p1	85	0,821	0,928	1,005	1,090	0,758	1,089	0,860	0,899	0,933	0,999	0,759	1,072
11.1	CNRM-CM5	r1i1p1	26	1,186	1,136	1,102	1,032	1,212	0,974	1,103	1,085	1,078	1,095	1,157	0,979
11.1	CNRM-CM5	r1i1p1	45	1,093	1,084	1,075	1,025	1,088	1,001	1,172	1,147	1,129	1,099	1,158	0,989
11.1	CNRM-CM5	r1i1p1	85	1,221	1,145	1,104	1,083	1,266	0,964	1,232	1,181	1,152	1,150	1,366	0,947
12.10	CSIRO-Mk3-6-0	r10i1p1	26	1,062	1,058	1,056	1,106	1,040	1,004	0,941	0,997	1,048	1,206	0,900	1,060
12.1	CSIRO-Mk3-6-0	r1i1p1	26	1,066	1,064	1,054	1,019	1,058	1,001	0,691	0,820	0,937	1,075	0,565	1,187
12.2	CSIRO-Mk3-6-0	r2i1p1	26	1,061	1,062	1,063	1,065	1,016	1,016	1,001	1,030	1,056	1,101	0,953	1,034
12.3	CSIRO-Mk3-6-0	r3i1p1	26	1,112	1,076	1,054	1,045	1,102	0,988	0,863	0,947	1,016	1,119	0,755	1,102
12.4	CSIRO-Mk3-6-0	r4i1p1	26	0,996	1,030	1,054	1,161	0,986	1,026	0,773	0,869	0,954	1,104	0,657	1,138
12.5	CSIRO-Mk3-6-0	r5i1p1	26	1,119	1,079	1,046	0,972	1,125	0,979	0,846	0,918	0,975	1,016	0,733	1,101
12.6	CSIRO-Mk3-6-0	r6i1p1	26	1,116	1,106	1,097	1,062	1,107	0,997	0,807	0,913	1,000	1,126	0,690	1,124
12.7	CSIRO-Mk3-6-0	r7i1p1	26	1,017	1,023	1,021	0,986	1,000	1,010	0,829	0,926	1,006	1,121	0,696	1,118
12.8	CSIRO-Mk3-6-0	r8i1p1	26	0,976	1,019	1,047	1,098	0,926	1,041	0,782	0,891	0,979	1,085	0,638	1,142
12.9	CSIRO-Mk3-6-0	r9i1p1	26	1,064	1,078	1,091	1,174	1,044	1,012	0,779	0,907	1,024	1,224	0,674	1,162
12.10	CSIRO-Mk3-6-0	r10i1p1	45	1,058	1,048	1,039	1,055	1,095	0,990	0,793	0,866	0,932	1,060	0,710	1,118
12.1	CSIRO-Mk3-6-0	r1i1p1	45	1,005	1,073	1,104	1,005	0,934	1,054	0,838	0,941	1,017	1,010	0,722	1,114
12.2	CSIRO-Mk3-6-0	r2i1p1	45	1,113	1,082	1,069	1,074	1,121	0,992	0,964	1,013	1,047	1,074	0,854	1,069
12.3	CSIRO-Mk3-6-0	r3i1p1	45	1,036	1,048	1,052	1,055	1,036	1,005	0,865	0,933	0,987	1,038	0,792	1,074
12.4	CSIRO-Mk3-6-0	r4i1p1	45	1,084	1,092	1,088	1,075	1,050	1,012	0,795	0,884	0,961	1,079	0,658	1,130
12.5	CSIRO-Mk3-6-0	r5i1p1	45	1,168	1,098	1,052	0,983	1,213	0,961	0,803	0,888	0,956	1,017	0,666	1,127
12.6	CSIRO-Mk3-6-0	r6i1p1	45	1,074	1,074	1,068	0,994	1,093	1,000	0,803	0,907	0,996	1,117	0,698	1,143
12.7	CSIRO-Mk3-6-0	r7i1p1	45	1,035	1,044	1,046	1,020	0,992	1,020	0,794	0,884	0,958	1,058	0,705	1,101
12.8	CSIRO-Mk3-6-0	r8i1p1	45	1,098	1,086	1,078	1,093	1,052	1,007	0,828	0,926	1,002	1,075	0,691	1,121
12.9	CSIRO-Mk3-6-0	r9i1p1	45	1,042	1,049	1,050	1,039	1,004	1,015	0,775	0,901	1,011	1,168	0,621	1,165
12.10	CSIRO-Mk3-6-0	r10i1p1	60	1,034	1,051	1,060	1,085	1,004	1,015	0,865	0,950	1,019	1,113	0,750	1,097
12.1	CSIRO-Mk3-6-0	r1i1p1	60	1,096	1,094	1,078	0,940	1,066	1,005	0,809	0,913	0,995	1,081	0,699	1,115
12.2	CSIRO-Mk3-6-0	r2i1p1	60	1,057	1,051	1,044	1,020	1,057	0,999	0,947	1,017	1,073	1,131	0,823	1,081
12.3	CSIRO-Mk3-6-0	r3i1p1	60	1,052	1,035	1,021	0,991	1,042	0,998	0,837	0,911	0,978	1,149	0,740	1,089
12.4	CSIRO-Mk3-6-0	r4i1p1	60	1,006	1,025	1,040	1,145	0,967	1,025	0,942	0,983	1,020	1,112	0,878	1,054
12.5	CSIRO-Mk3-6-0	r5i1p1	60	1,175	1,091	1,042	1,047	1,209	0,958	0,877	0,933	0,975	1,000	0,785	1,075
12.6	CSIRO-Mk3-6-0	r6i1p1	60	1,027	1,044	1,054	1,086	1,051	1,008	0,810	0,906	0,988	1,120	0,685	1,126
12.7	CSIRO-Mk3-6-0	r7i1p1	60	1,099	1,080	1,064	1,038	1,115	0,989	0,865	0,935	0,990	1,041	0,767	1,088
12.8	CSIRO-Mk3-6-0	r8i1p1	60	1,084	1,080	1,073	1,058	1,062	1,005	0,812	0,910	0,990	1,092	0,667	1,133
12.9	CSIRO-Mk3-6-0	r9i1p1	60	1,089	1,067	1,051	1,047	1,085	0,991	0,819	0,908	0,986	1,122	0,739	1,109
12.10	CSIRO-Mk3-6-0	r10i1p1	85	1,044	1,049	1,049	1,081	1,003	1,013	0,784	0,886	0,977	1,139	0,647	1,148
12.1	CSIRO-Mk3-6-0	r1i1p1	85	1,121	1,122	1,115	1,058	1,095	1,006	0,825	0,950	1,048	1,116	0,653	1,154
12.2	CSIRO-Mk3-6-0	r2i1p1	85	1,147	1,104	1,079	1,068	1,147	0,985	0,868	0,957	1,029	1,105	0,747	1,117

	12.3	CSIRO-Mk3-6-0	r3i1p1	85	1,132	1,104	1,082	1,029	1,136	0,990	0,802	0,893	0,974	1,123	0,712	1,114
	12.4	CSIRO-Mk3-6-0	r4i1p1	85	1,051	1,072	1,086	1,157	1,027	1,015	0,866	0,967	1,051	1,210	0,751	1,103
	12.5	CSIRO-Mk3-6-0	r5i1p1	85	1,178	1,109	1,061	1,008	1,215	0,962	0,853	0,913	0,962	1,020	0,717	1,105
	12.6	CSIRO-Mk3-6-0	r6i1p1	85	1,103	1,105	1,107	1,115	1,089	1,006	0,881	0,958	1,022	1,139	0,759	1,101
	12.7	CSIRO-Mk3-6-0	r7i1p1	85	1,036	1,045	1,047	1,039	1,018	1,009	0,789	0,893	0,981	1,110	0,649	1,134
	12.8	CSIRO-Mk3-6-0	r8i1p1	85	1,094	1,098	1,092	1,028	1,089	1,006	0,808	0,923	1,020	1,125	0,678	1,139
	12.9	CSIRO-Mk3-6-0	r9i1p1	85	1,087	1,064	1,047	1,027	1,078	0,995	0,802	0,900	0,994	1,162	0,724	1,145
	13.1	FGOALS-s2	r1i1p1	26	1,101	1,116	1,125	1,124	1,095	1,011	1,025	1,072	1,112	1,171	0,959	1,049
	13.1	FGOALS-s2	r1i1p1	45	1,105	1,111	1,118	1,080	1,086	1,018	1,011	1,046	1,079	1,124	0,943	1,049
	13.2	FGOALS-s2	r2i1p1	45	1,141	1,126	1,103	0,994	1,125	1,000	1,023	1,054	1,078	1,081	0,918	1,058
	13.3	FGOALS-s2	r3i1p1	45	1,160	1,125	1,106	1,112	1,189	0,979	1,116	1,086	1,073	1,103	1,126	0,993
	13.1	FGOALS-s2	r1i1p1	60	1,182	1,179	1,180	1,178	1,166	1,009	0,854	0,977	1,075	1,204	0,680	1,145
	13.1	FGOALS-s2	r1i1p1	85	1,114	1,147	1,155	1,075	1,104	1,023	1,066	1,076	1,099	1,137	1,091	1,038
	13.2	FGOALS-s2	r2i1p1	85	1,109	1,130	1,137	1,075	1,146	1,007	0,925	0,977	1,020	1,045	0,917	1,057
	13.3	FGOALS-s2	r3i1p1	85	1,142	1,124	1,109	1,060	1,139	0,996	1,398	1,246	1,166	1,115	1,857	0,900
	14.1	GFDL-CM3	r1i1p1	26	1,085	1,089	1,085	1,040	1,077	1,003	0,881	0,979	1,061	1,212	0,778	1,101
	14.1	GFDL-CM3	r1i1p1	60	1,075	1,063	1,055	1,047	1,058	0,996	0,954	1,014	1,059	1,098	0,931	1,044
	14.1	GFDL-CM3	r1i1p1	85	1,198	1,124	1,068	0,962	1,206	0,968	0,942	1,006	1,061	1,139	0,863	1,070
	15.1	GFDL-ESM2G	r1i1p1	26	0,960	0,986	1,005	1,070	0,954	1,019	0,874	0,951	1,021	1,254	0,750	1,091
	15.1	GFDL-ESM2G	r1i1p1	45	0,985	0,996	1,003	1,052	0,951	1,020	0,946	0,983	1,019	1,152	0,881	1,041
	15.1	GFDL-ESM2G	r1i1p1	60	0,993	1,019	1,035	1,089	0,986	1,016	0,888	0,956	1,013	1,111	0,792	1,077
	15.1	GFDL-ESM2G	r1i1p1	85	0,981	1,002	1,019	1,114	0,975	1,025	0,856	0,955	1,045	1,290	0,715	1,112
	16.1	GFDL-ESM2M	r1i1p1	26	1,044	1,066	1,069	0,950	1,037	1,011	1,004	1,022	1,034	1,033	0,971	1,022
	16.1	GFDL-ESM2M	r1i1p1	45	1,078	1,085	1,077	0,985	1,067	1,004	0,952	1,005	1,045	1,088	0,903	1,048
	16.1	GFDL-ESM2M	r1i1p1	60	1,094	1,089	1,072	0,912	1,088	0,997	0,932	0,981	1,012	0,989	0,883	1,047
	16.1	GFDL-ESM2M	r1i1p1	85	1,192	1,136	1,093	0,992	1,236	0,963	0,921	0,977	1,016	1,019	0,830	1,067
	17.6	GISS-E2-R	r6i1p1	45	0,985	1,013	1,029	0,995	0,969	1,019	0,981	1,016	1,042	1,064	0,944	1,031
	18.1	HadGEM2-CC	r1i1p1	45	0,959	0,995	1,018	1,030	0,932	1,031	0,901	0,975	1,040	1,127	0,784	1,110
	18.1	HadGEM2-CC	r1i1p1	85	0,966	1,027	1,071	1,165	0,968	1,039	0,920	0,986	1,043	1,155	0,828	1,088
	18.2	HadGEM2-CC	r2i1p1	85	1,033	1,030	1,030	1,045	1,042	0,999	0,748	0,869	0,975	1,108	0,648	1,154
	18.3	HadGEM2-CC	r3i1p1	85	1,010	1,040	1,064	1,172	1,038	1,018	0,851	0,947	1,020	1,071	0,769	1,104
	19.1	HadGEM2-ES	r1i1p1	26	0,920	0,985	1,036	1,180	0,890	1,051	0,799	0,908	1,015	1,140	0,718	1,163
	19.2	HadGEM2-ES	r2i1p1	26	1,021	1,064	1,087	1,010	0,992	1,030	0,768	0,885	0,981	1,068	0,629	1,161
	19.3	HadGEM2-ES	r3i1p1	26	0,929	0,984	1,026	1,005	0,892	1,052	0,682	0,824	0,947	1,077	0,563	1,188
	19.4	HadGEM2-ES	r4i1p1	26	1,055	1,040	1,035	1,025	1,038	0,999	0,868	0,953	1,021	1,111	0,762	1,093
	19.1	HadGEM2-ES	r1i1p1	45	1,131	1,093	1,065	1,038	1,209	0,975	0,907	0,949	1,007	1,128	0,917	1,098
	19.2	HadGEM2-ES	r2i1p1	45	0,922	1,007	1,063	1,046	0,915	1,051	0,618	0,779	0,924	1,076	0,464	1,238
	19.3	HadGEM2-ES	r3i1p1	45	0,995	1,026	1,050	0,982	0,945	1,035	0,727	0,843	0,943	1,095	0,577	1,163
	19.4	HadGEM2-ES	r4i1p1	45	1,079	1,072	1,064	0,993	1,085	1,014	0,693	0,814	0,925	1,056	0,569	1,187
	19.1	HadGEM2-ES	r1i1p1	60	0,973	1,022	1,060	1,109	0,997	1,036	0,843	0,930	1,000	1,083	0,764	1,097
	19.2	HadGEM2-ES	r2i1p1	60	1,011	1,038	1,059	1,044	1,002	1,021	0,742	0,846	0,935	1,057	0,586	1,169
	19.3	HadGEM2-ES	r3i1p1	60	1,065	1,088	1,100	1,071	1,070	1,015	0,604	0,760	0,905	1,085	0,456	1,240
	19.4	HadGEM2-ES	r4i1p1	60	0,842	0,952	1,035	1,100	0,761	1,098	0,731	0,854	0,969	1,117	0,613	1,184
	19.1	HadGEM2-ES	r1i1p1	85	1,104	1,098	1,092	1,113	1,147	1,000	0,856	0,928	1,005	1,152	0,823	1,133
	19.2	HadGEM2-ES	r2i1p1	85	1,226	1,135	1,076	0,987	1,286	0,952	0,705	0,831	0,949	1,121	0,544	1,212
	19.3	HadGEM2-ES	r3i1p1	85	1,120	1,082	1,059	1,010	1,132	0,984	0,670	0,806	0,921	1,025	0,517	1,192
	19.4	HadGEM2-ES	r4i1p1	85	0,971	1,012	1,038	1,056	0,917	1,050	0,581	0,745	0,898	1,122	0,425	1,250
	20.1	inmcm4	r1i1p1	45	0,958	0,981	0,994	0,998	0,919	1,025	0,865	0,909	0,948	1,033	0,814	1,056
	20.1	inmcm4	r1i1p1	85	1,086	1,050	1,030	1,051	1,074	0,990	0,895	0,927	0,962	1,093	0,821	1,050
	21.1	IPSL-CM5A-LR	r1i1p1	26	1,097	1,058	1,035	1,038	1,091	0,985	1,015	1,037	1,055	1,076	1,012	1,016
	21.2	IPSL-CM5A-LR	r2i1p1	26	1,151	1,107	1,091	1,068	1,165	0,985	0,972	1,016	1,048	1,043	0,914	1,052
	21.3	IPSL-CM5A-LR	r3i1p1	26	1,006	1,042	1,069	1,135	0,998	1,021	1,077	1,090	1,107	1,200	1,093	1,007
	21.4	IPSL-CM5A-LR	r4i1p1	26	1,002	1,017	1,026	1,039	0,978	1,016	1,022	1,038	1,057	1,153	0,934	1,036
	21.1	IPSL-CM5A-LR	r1i1p1	45	1,132	1,070	1,038	1,050	1,111	0,978	1,043	1,064	1,085	1,191	1,038	1,016
	21.2	IPSL-CM5A-LR	r2i1p1	45	1,107	1,080	1,070	1,050	1,077	1,003	0,949	0,992	1,028	1,101	0,844	1,060
	21.3	IPSL-CM5A-LR	r3i1p1	45	1,019	1,039	1,065	1,179	0,976	1,025	0,986	1,057	1,111	1,201	0,865	1,074
	21.4	IPSL-CM5A-LR	r4i1p1	45	0,938	0,999	1,051	1,251	0,885	1,048	0,994	1,011	1,028	1,080	0,943	1,028
	21.1	IPSL-CM5A-LR	r1i1p1	60	1,108	1,075	1,061	1,098	1,157	0,975	1,048	1,043	1,041	1,057	1,077	0,995
	21.1	IPSL-CM5A-LR	r1i1p1	85	1,121	1,070	1,044	1,097	1,135	0,974	1,075	1,094	1,114	1,183	1,036	1,022
	21.2	IPSL-CM5A-LR	r2i1p1	85	1,088	1,070	1,063	1,140	1,108	0,988	1,001	1,025	1,042	1,063	0,940	1,034
	21.3	IPSL-CM5A-LR	r3i1p1	85	1,007	1,033	1,054	1,153	0,991	1,021	1,044	1,061	1,080	1,181	1,015	1,023
	21.4	IPSL-CM5A-LR	r4i1p1	85	0,903	0,986	1,046	1,118	0,831	1,069	0,937	0,995	1,044	1,112	0,812	1,079
	22.1	IPSL-CM5A-MR	r1i1p1	26	1,033	1,046	1,053	1,081	0,999	1,013	1,107	1,064	1,036	0,968	1,150	0,976
	22.1	IPSL-CM5A-MR	r1i1p1	45	1,085	1,084	1,080	1,074	1,041	1,005	0,864	0,936	0,990	1,029	0,739	1,092
	22.1	IPSL-CM5A-MR	r1i1p1	60	1,103	1,046	1,009	0,955	1,126	0,966	0,989	0,985	0,982	0,953	0,992	1,000
	22.1	IPSL-CM5A-MR	r1i1p1	85	1,115	1,068	1,034	0,992	1,104	0,986	0,888	0,938	0,976	0,988	0,795	1,069
	23.1	IPSL-CM5B-LR	r1i1p1	45	1,065	1,045	1,040	1,073	1,077	0,991	1,078	1,083	1,096	1,171	1,086	1,002
	23.1	IPSL-CM5B-LR	r1i1p1	85	1,083	1,048	1,030	1,091	1,086	0,986	1,222	1,153	1,115	1,157	1,287	0,952
	24.1	MIROC-ESM	r1i1p1	26	1,134	1,132	1,130	1,100	1,143	0,997	1,176	1,182	1,178	1,094	1,165	1,007
	24.1	MIROC-ESM	r1i1p1	45	1,113	1,115	1,114	1,092	1,105	1,000	1,085	1,129	1,161	1,189	0,986	1,050
	24.1	MIROC-ESM	r1i1p1	60	1,147	1,121	1,099	1,001	1,138	0,989	1,192	1,180	1,169	1,083	1,235	0,994
	24.1	MIROC-ESM	r1i1p1	85	1,132	1,108	1,090	1,038	1,166	0,981	1,173	1,180	1,184	1,139	1,117	1,022
	25.1	MIROC-ESM-CHEM	r1i1p1	26	1,119	1,094	1,076	1,048	1,102	0,992	1,095	1,116	1,137	1,214	1,033	1,028
	25.1	MIROC-ESM-CHEM	r1i1p1	45	1,116	1,076	1,050	1,053	1,092	0,988	1,154	1,145	1,143	1,174	1,083	1,019
	25.1	MIROC-ESM-CHEM	r1i1p1	60	1,144	1,093	1,059	1,021	1,165	0,972	1,166	1,145	1,134	1,132	1,152	0,998
	25.1	MIROC-ESM-CHEM	r1i1p1	85	1,154	1,112	1,074	0,949	1,139	0,988	1,178	1,158	1,143	1,109	1,160	0,999
	26.1	MIROC5	r1i1p1	26	1,104	1,086	1,074	1,032	1,065	1,003	1,011	1,064	1,107	1,190	0,959	1,054
	26.2	MIROC5	r2i1p1	26	1,294	1,198	1,151	1,120	1,327	0,957	1,203	1,210	1,216	1,196	1,222	0,999
	26.3	MIROC5	r3i1p1	26	0,910	0,971	1,015	1,080	0,907	1,044	1,022	1,077	1,114	1,080	1,013	1,040
	26.1	MIROC5	r1i1p1	45	1,183	1,129	1,094	1,060	1,169	0,982	1,127	1,127	1,133	1,150	1,102	1,015
	26.2	MIROC5	r2i1p1	45	1,130	1,102	1,092	1,029	1,137	0,997	1,198	1,194	1,187	1,123	1,162	1,004
	26.3	MIROC5	r3i1p1	45	1,091	1,030	0,997	0,975	1,112	0,978	0,986	1,045	1,082	1,041	0,907	1,062
	26.1	MIROC5	r1i1p1	60	1,178	1,142	1,124	1,101	1,185	0,985	1,225	1,176	1,145	1,149	1,305	0,965
	26.1	MIROC5	r1i1p1	85	1,187	1,139	1,106	1,045	1,197	0,979	1,097	1,143	1,180	1,231	1,084	1,036
	26.2	MIROC5	r2i1p1	85	1,256	1,171	1,123	1,059	1,244	0,966	1,205	1,197	1,191	1,181	1,175	1,002
	26.3	MIROC5	r3i1p1	85	1,195	1,097	1,043	1,033	1,236	0,958	1,027	1,094	1,142	1,155	0,943	1,068
	27.1	MPI-ESM-LR	r1i1p1	26	1,162	1,089	1,040	0,938	1,183	0,969	1,016	1,020	1,026	1,072	0,985	1,021
	27.2	MPI-ESM-LR	r2i1p1	26	1,202	1,129	1,072	0,872	1,242	0,960	0,919	0,964	0,998	1,035	0,832	1,055
	27.3	MPI-ESM-LR	r3i1p1	26	1,135	1,060	1,018	1,077	1,146	0,965	0,943	0,971	0,996	1,051	0,832	1,059

	27.1	MPI-ESM-LR	r1i1p1	45	1,126	1,086	1,061	1,051	1,163	0,974	0,956	0,980	1,005	1,105	0,889	1,048
	27.2	MPI-ESM-LR	r2i1p1	45	1,154	1,075	1,026	0,883	1,227	0,956	0,923	0,960	0,984	0,958	0,868	1,041
	27.3	MPI-ESM-LR	r3i1p1	45	1,208	1,097	1,027	1,012	1,259	0,943	0,925	0,950	0,971	1,022	0,873	1,034
	27.1	MPI-ESM-LR	r1i1p1	85	0,954	0,997	1,031	1,071	0,917	1,036	0,944	0,955	0,972	1,101	0,904	1,026
	27.2	MPI-ESM-LR	r2i1p1	85	1,294	1,170	1,084	0,854	1,346	0,941	0,865	0,932	0,982	1,007	0,764	1,079
	27.3	MPI-ESM-LR	r3i1p1	85	1,070	1,032	1,007	1,018	1,079	0,984	0,918	0,953	0,984	1,062	0,831	1,053
	28.1	MPI-ESM-MR	r1i1p1	26	1,091	1,054	1,037	1,079	1,094	0,986	0,900	0,952	0,993	1,036	0,796	1,069
	28.1	MPI-ESM-MR	r1i1p1	45	1,130	1,073	1,040	1,037	1,154	0,973	0,892	0,937	0,973	1,042	0,810	1,058
	28.2	MPI-ESM-MR	r2i1p1	45	1,008	1,031	1,045	1,103	1,002	1,020	0,850	0,918	0,973	1,068	0,740	1,088
	28.3	MPI-ESM-MR	r3i1p1	45	0,927	0,983	1,024	1,103	0,909	1,043	0,916	0,971	1,016	1,066	0,855	1,056
	28.1	MPI-ESM-MR	r1i1p1	85	0,978	1,000	1,019	1,092	0,957	1,021	0,866	0,943	1,001	1,044	0,739	1,091
	29.1	MRI-CGCM3	r1i1p1	26	1,082	1,065	1,054	1,010	1,105	0,989	1,086	1,078	1,072	1,052	1,091	1,001
	29.1	MRI-CGCM3	r1i1p1	45	0,979	1,009	1,032	1,058	0,975	1,023	0,992	1,026	1,052	1,056	0,928	1,043
	29.1	MRI-CGCM3	r1i1p1	60	1,174	1,118	1,084	1,052	1,219	0,967	1,005	1,041	1,071	1,114	1,013	1,021
	29.1	MRI-CGCM3	r1i1p1	85	1,191	1,121	1,083	1,073	1,191	0,972	1,052	1,066	1,072	1,034	1,002	1,024
	30.1	NorESM1-M	r1i1p1	26	0,995	1,033	1,060	1,129	0,967	1,026	0,911	0,979	1,032	1,108	0,820	1,072
	30.1	NorESM1-M	r1i1p1	45	1,092	1,074	1,056	1,013	1,100	0,988	0,875	0,969	1,042	1,110	0,764	1,096
	30.1	NorESM1-M	r1i1p1	60	1,040	1,037	1,034	1,052	1,045	0,997	0,897	0,972	1,035	1,153	0,811	1,076
	30.1	NorESM1-M	r1i1p1	85	1,024	1,057	1,080	1,097	0,986	1,026	0,872	0,967	1,045	1,164	0,762	1,098
	EC.1	EC-EARTH	r1i1p1	85	1,165	1,096	1,047	0,973	1,235	0,958	1,003	1,023	1,045	1,112	0,948	1,040
	EC.2	EC-EARTH	r2i1p1	85	1,173	1,102	1,061	1,042	1,213	0,964	0,967	1,022	1,066	1,125	0,915	1,055
	EC.3	EC-EARTH	r3i1p1	85	1,142	1,103	1,068	0,961	1,200	0,972	0,964	1,019	1,056	1,046	0,885	1,056
	EC.4	EC-EARTH	r4i1p1	85	1,043	1,076	1,107	1,099	1,035	1,027	0,956	0,983	1,004	1,024	0,918	1,033
	EC.5	EC-EARTH	r5i1p1	85	1,051	1,081	1,097	1,064	1,059	1,016	0,964	1,010	1,045	1,069	0,903	1,042
	EC.6	EC-EARTH	r6i1p1	85	1,349	1,212	1,132	1,091	1,457	0,927	1,036	1,049	1,061	1,092	1,010	1,016
	EC.7	EC-EARTH	r7i1p1	85	1,095	1,126	1,145	1,160	1,100	1,009	1,053	1,075	1,088	1,067	1,052	1,012
	EC.8	EC-EARTH	r8i1p1	85	1,234	1,156	1,101	1,015	1,303	0,955	1,122	1,077	1,046	1,019	1,192	0,965

Summary statistics

		Winter						Summer					
		P30	P60	P90	E	a	b	P30	P60	P90	E	a	b
Overall	Mean	1,075	1,068	1,063	1,054	1,075	1,002	0,923	0,980	1,029	1,099	0,851	1,074
	Coefficient of variation	0,076	0,043	0,031	0,058	0,097	0,027	0,143	0,093	0,060	0,056	0,221	0,054
	Minimum	0,821	0,928	0,982	0,854	0,758	0,927	0,581	0,745	0,898	0,942	0,425	0,900
	1th Quartile	1,020	1,037	1,040	1,019	1,004	0,985	0,845	0,925	0,987	1,059	0,739	1,037
	Median	1,080	1,067	1,060	1,052	1,077	1,003	0,916	0,971	1,020	1,101	0,821	1,069
	3rd Quartile	1,121	1,097	1,081	1,092	1,138	1,019	1,001	1,024	1,058	1,139	0,943	1,108
	Maximum	1,349	1,212	1,180	1,251	1,457	1,098	1,398	1,246	1,216	1,290	1,857	1,250
RCP 2.6	Mean	1,063	1,062	1,061	1,054	1,057	1,005	0,928	0,985	1,033	1,103	0,857	1,071
	Coefficient of variation	0,071	0,041	0,030	0,061	0,086	0,024	0,135	0,088	0,058	0,061	0,202	0,052
	Minimum	0,910	0,971	1,005	0,872	0,890	0,957	0,682	0,820	0,932	0,968	0,525	0,976
	1th Quartile	1,018	1,041	1,038	1,024	0,998	0,988	0,849	0,929	0,998	1,053	0,751	1,035
	Median	1,065	1,063	1,055	1,055	1,066	1,004	0,915	0,979	1,022	1,095	0,832	1,060
	3rd Quartile	1,103	1,084	1,076	1,093	1,100	1,018	1,016	1,038	1,060	1,150	0,968	1,101
	Maximum	1,294	1,198	1,151	1,180	1,327	1,052	1,203	1,210	1,216	1,254	1,222	1,188
RCP 4.5	Mean	1,059	1,056	1,054	1,045	1,055	1,005	0,917	0,973	1,020	1,087	0,838	1,075
	Coefficient of variation	0,066	0,036	0,028	0,055	0,084	0,025	0,131	0,087	0,059	0,053	0,182	0,047
	Minimum	0,922	0,981	0,982	0,883	0,885	0,943	0,618	0,779	0,924	0,942	0,464	0,989
	1th Quartile	1,004	1,030	1,038	1,012	0,976	0,989	0,828	0,918	0,975	1,056	0,729	1,041
	Median	1,075	1,058	1,052	1,043	1,067	1,005	0,916	0,960	1,012	1,080	0,835	1,062
	3rd Quartile	1,113	1,084	1,070	1,074	1,111	1,020	0,986	1,016	1,047	1,123	0,918	1,110
	Maximum	1,208	1,129	1,118	1,251	1,259	1,054	1,198	1,194	1,187	1,201	1,162	1,238
RCP 6.0	Mean	1,071	1,065	1,061	1,043	1,069	1,001	0,903	0,965	1,018	1,091	0,827	1,081
	Coefficient of variation	0,067	0,041	0,032	0,058	0,084	0,026	0,152	0,097	0,060	0,047	0,235	0,058
	Minimum	0,842	0,952	1,008	0,912	0,761	0,958	0,604	0,760	0,905	0,953	0,456	0,965
	1th Quartile	1,035	1,037	1,041	1,006	1,015	0,989	0,824	0,911	0,983	1,068	0,709	1,039
	Median	1,071	1,062	1,059	1,047	1,064	0,999	0,883	0,964	1,013	1,095	0,789	1,081
	3rd Quartile	1,107	1,091	1,073	1,086	1,125	1,015	0,962	1,008	1,040	1,119	0,927	1,114
	Maximum	1,182	1,179	1,180	1,178	1,219	1,098	1,225	1,180	1,169	1,204	1,305	1,240
RCP 8.5	Mean	1,096	1,082	1,073	1,067	1,105	0,997	0,933	0,988	1,037	1,112	0,866	1,074
	Coefficient of variation	0,085	0,047	0,032	0,059	0,109	0,030	0,156	0,098	0,063	0,056	0,255	0,058
	Minimum	0,821	0,928	1,005	0,854	0,758	0,927	0,581	0,745	0,898	0,988	0,425	0,900
	1th Quartile	1,043	1,048	1,047	1,033	1,031	0,979	0,856	0,938	0,990	1,065	0,747	1,036
	Median	1,103	1,090	1,071	1,071	1,100	0,995	0,920	0,967	1,039	1,115	0,823	1,072
	3rd Quartile	1,154	1,121	1,096	1,101	1,191	1,018	1,003	1,023	1,061	1,155	0,943	1,107
	Maximum	1,349	1,212	1,155	1,215	1,457	1,089	1,398	1,246	1,191	1,290	1,857	1,250

Meuse basin - Near Future (2021-2050)

Model info				Winter						Summer					
Index	GCM	Run	RCP	P30	P60	P90	E	a	b	P30	P60	P90	E	a	b
1.1	ACCESS1-0	r1i1p1	45	1,123	1,093	1,074	1,142	1,147	0,975	0,772	0,830	0,900	1,082	0,721	1,101
1.1	ACCESS1-0	r1i1p1	85	1,134	1,124	1,118	1,109	1,123	1,003	0,935	0,970	1,024	1,132	0,942	1,086
2.1	ACCESS1-3	r1i1p1	45	1,018	1,005	0,997	1,045	1,042	0,990	0,654	0,822	0,975	1,139	0,534	1,222
2.1	ACCESS1-3	r1i1p1	85	1,073	1,043	1,031	1,243	1,120	0,986	0,610	0,810	0,992	1,223	0,461	1,272
3.1	bcc-csm1-1	r1i1p1	26	1,062	1,062	1,056	1,009	1,076	0,993	0,949	0,978	0,997	0,962	0,862	1,048
3.1	bcc-csm1-1	r1i1p1	45	1,017	1,033	1,045	1,030	0,996	1,013	1,105	1,046	1,018	0,967	1,126	1,001
3.1	bcc-csm1-1	r1i1p1	60	1,100	1,082	1,059	0,927	1,114	0,987	0,996	1,002	1,014	0,985	0,967	1,026
3.1	bcc-csm1-1	r1i1p1	85	1,125	1,078	1,038	0,959	1,174	0,965	0,919	0,952	0,981	0,999	0,844	1,051
4.1	bcc-csm1-1-m	r1i1p1	26	1,040	1,075	1,096	1,022	0,983	1,033	0,722	0,828	0,916	1,052	0,592	1,132
4.1	bcc-csm1-1-m	r1i1p1	45	1,029	1,046	1,055	1,020	1,010	1,019	0,679	0,829	0,954	1,061	0,539	1,184
4.1	bcc-csm1-1-m	r1i1p1	60	1,016	1,039	1,049	1,018	0,998	1,018	0,697	0,829	0,944	1,071	0,550	1,192
4.1	bcc-csm1-1-m	r1i1p1	85	1,061	1,073	1,079	1,089	1,041	1,010	0,637	0,797	0,928	1,002	0,495	1,210
5.1	BNU-ESM	r1i1p1	26	1,095	1,075	1,061	1,089	1,131	0,980	0,939	0,966	0,988	1,022	0,855	1,055
5.1	BNU-ESM	r1i1p1	45	1,073	1,057	1,052	1,151	1,073	0,993	0,974	0,977	0,987	1,044	0,933	1,019
5.1	BNU-ESM	r1i1p1	85	1,076	1,092	1,106	1,158	1,062	1,010	0,985	0,995	1,011	1,103	0,947	1,027
6.1	CanESM2	r1i1p1	26	1,093	1,091	1,085	1,005	1,078	1,013	0,852	0,954	1,036	1,133	0,725	1,106
6.2	CanESM2	r2i1p1	26	1,006	1,043	1,076	1,194	1,000	1,021	0,848	0,939	1,015	1,119	0,731	1,103
6.3	CanESM2	r3i1p1	26	1,075	1,089	1,103	1,113	1,062	1,013	1,030	1,018	1,022	1,020	1,032	1,015
6.4	CanESM2	r4i1p1	26	1,031	1,037	1,046	1,094	1,071	0,997	0,767	0,858	0,939	1,102	0,658	1,117
6.5	CanESM2	r5i1p1	26	0,928	1,003	1,063	1,093	0,839	1,077	0,863	1,018	1,140	1,203	0,723	1,139
6.1	CanESM2	r1i1p1	45	1,075	1,050	1,029	0,984	1,079	0,992	0,897	0,968	1,029	1,125	0,795	1,087
6.2	CanESM2	r2i1p1	45	1,064	1,064	1,061	1,032	1,079	0,991	0,904	0,998	1,076	1,146	0,800	1,098
6.3	CanESM2	r3i1p1	45	1,064	1,065	1,062	1,035	1,067	0,998	0,944	0,972	1,012	1,040	0,950	1,049
6.4	CanESM2	r4i1p1	45	1,040	1,066	1,084	1,124	1,044	1,016	0,793	0,904	1,000	1,146	0,703	1,112
6.5	CanESM2	r5i1p1	45	0,993	1,024	1,058	1,207	1,018	1,024	0,783	0,916	1,030	1,142	0,627	1,159
6.1	CanESM2	r1i1p1	85	1,107	1,090	1,072	1,042	1,129	0,998	0,876	0,967	1,038	1,077	0,749	1,102
6.2	CanESM2	r2i1p1	85	1,156	1,124	1,108	1,136	1,173	0,986	0,840	0,978	1,093	1,200	0,715	1,130
6.3	CanESM2	r3i1p1	85	1,048	1,068	1,091	1,227	1,033	1,015	0,982	0,989	1,017	1,110	0,979	1,039
6.4	CanESM2	r4i1p1	85	1,123	1,101	1,097	1,260	1,174	0,984	0,904	0,936	0,977	1,092	0,851	1,051
6.5	CanESM2	r5i1p1	85	0,999	1,031	1,063	1,142	0,978	1,041	0,869	0,987	1,083	1,129	0,755	1,111
7.1	CCSM4	r1i1p1	26	1,024	1,009	1,001	1,011	1,032	0,996	0,792	0,903	0,989	1,032	0,677	1,125
7.2	CCSM4	r2i1p1	26	1,030	1,026	1,020	1,019	1,060	0,996	0,861	0,937	0,998	1,077	0,781	1,072
7.6	CCSM4	r6i1p1	26	1,098	1,051	1,012	0,906	1,136	0,976	0,902	0,937	0,975	1,113	0,843	1,044
7.1	CCSM4	r1i1p1	45	1,100	1,018	0,959	0,894	1,207	0,939	0,801	0,887	0,961	1,067	0,710	1,100
7.2	CCSM4	r2i1p1	45	1,088	1,052	1,028	1,100	1,114	0,981	0,827	0,904	0,958	1,003	0,744	1,077
7.6	CCSM4	r6i1p1	45	1,038	1,050	1,050	0,981	1,032	1,010	0,788	0,887	0,976	1,148	0,674	1,119
7.1	CCSM4	r1i1p1	60	1,034	0,996	0,968	0,948	1,101	0,978	0,778	0,868	0,944	1,052	0,643	1,124
7.2	CCSM4	r2i1p1	60	1,030	1,025	1,018	1,005	1,040	0,999	0,922	0,972	1,006	1,036	0,868	1,053
7.6	CCSM4	r6i1p1	60	1,046	1,051	1,052	1,032	1,053	1,006	0,953	0,976	1,006	1,107	0,939	1,024
7.1	CCSM4	r1i1p1	85	0,978	1,019	1,042	0,992	0,961	1,029	0,802	0,893	0,972	1,103	0,709	1,105
7.2	CCSM4	r2i1p1	85	0,990	1,007	1,024	1,161	0,983	1,014	0,817	0,921	1,001	1,126	0,711	1,103
7.6	CCSM4	r6i1p1	85	1,053	1,031	1,009	0,922	1,090	0,986	0,820	0,900	0,963	1,078	0,751	1,073
8.1	CMCC-CESM	r1i1p1	85	1,240	1,182	1,141	1,074	1,322	0,962	1,278	1,173	1,135	1,244	1,416	0,947
9.1	CMCC-CM	r1i1p1	45	0,896	0,935	0,974	1,069	0,859	1,042	0,813	0,916	0,994	1,023	0,711	1,105
9.1	CMCC-CM	r1i1p1	85	1,099	1,059	1,028	1,014	1,192	0,967	0,823	0,953	1,049	1,034	0,714	1,125
10.1	CMCC-CMS	r1i1p1	45	0,992	1,030	1,065	1,095	0,924	1,042	0,969	0,986	0,995	0,951	0,889	1,034
10.1	CMCC-CMS	r1i1p1	85	0,831	0,923	1,012	1,171	0,723	1,099	0,848	0,898	0,950	1,056	0,756	1,074
11.1	CNRM-CM5	r1i1p1	26	1,173	1,124	1,081	0,979	1,255	0,959	1,012	1,033	1,050	1,069	1,032	1,007
11.1	CNRM-CM5	r1i1p1	45	1,076	1,046	1,020	0,977	1,126	0,979	1,113	1,118	1,119	1,099	1,082	1,012
11.1	CNRM-CM5	r1i1p1	85	1,210	1,126	1,076	1,086	1,290	0,949	1,207	1,166	1,151	1,222	1,278	0,963
12.10	CSIRO-Mk3-6-0	r10i1p1	26	1,037	1,025	1,021	1,098	1,020	0,999	0,839	0,932	1,014	1,126	0,739	1,113
12.1	CSIRO-Mk3-6-0	r1i1p1	26	1,124	1,077	1,049	1,047	1,150	0,970	0,631	0,773	0,906	1,082	0,510	1,222
12.2	CSIRO-Mk3-6-0	r2i1p1	26	1,050	1,045	1,040	1,050	1,050	1,005	0,973	1,013	1,051	1,124	0,913	1,043
12.3	CSIRO-Mk3-6-0	r3i1p1	26	1,152	1,099	1,059	1,021	1,185	0,968	0,829	0,937	1,022	1,125	0,719	1,114
12.4	CSIRO-Mk3-6-0	r4i1p1	26	1,002	1,017	1,032	1,110	0,986	1,023	0,754	0,826	0,898	1,062	0,681	1,123
12.5	CSIRO-Mk3-6-0	r5i1p1	26	1,129	1,081	1,039	0,944	1,186	0,963	0,734	0,863	0,977	1,062	0,609	1,185
12.6	CSIRO-Mk3-6-0	r6i1p1	26	1,137	1,114	1,099	1,049	1,138	0,990	0,717	0,832	0,929	1,074	0,620	1,146
12.7	CSIRO-Mk3-6-0	r7i1p1	26	1,028	1,029	1,030	1,005	1,032	1,003	0,756	0,891	1,000	1,101	0,621	1,157
12.8	CSIRO-Mk3-6-0	r8i1p1	26	1,050	1,038	1,034	1,074	1,048	0,996	0,708	0,826	0,929	1,075	0,589	1,165
12.9	CSIRO-Mk3-6-0	r9i1p1	26	1,110	1,106	1,106	1,154	1,113	0,999	0,709	0,862	1,005	1,235	0,616	1,182
12.10	CSIRO-Mk3-6-0	r10i1p1	45	1,083	1,035	1,007	1,042	1,144	0,964	0,695	0,783	0,868	1,005	0,639	1,146
12.1	CSIRO-Mk3-6-0	r1i1p1	45	1,027	1,071	1,107	1,035	0,951	1,050	0,775	0,889	0,980	1,060	0,658	1,133
12.2	CSIRO-Mk3-6-0	r2i1p1	45	1,089	1,070	1,057	1,070	1,131	0,985	0,890	0,961	1,025	1,113	0,797	1,086
12.3	CSIRO-Mk3-6-0	r3i1p1	45	1,052	1,058	1,068	1,122	1,017	1,012	0,848	0,938	1,008	1,109	0,758	1,088
12.4	CSIRO-Mk3-6-0	r4i1p1	45	1,119	1,104	1,090	1,062	1,125	0,991	0,782	0,867	0,948	1,068	0,684	1,124
12.5	CSIRO-Mk3-6-0	r5i1p1	45	1,157	1,095	1,045	0,986	1,252	0,954	0,731	0,858	0,975	1,040	0,627	1,177
12.6	CSIRO-Mk3-6-0	r6i1p1	45	1,025	1,032	1,036	0,970	1,032	1,010	0,718	0,835	0,942	1,089	0,640	1,171
12.7	CSIRO-Mk3-6-0	r7i1p1	45	1,043	1,030	1,022	1,000	1,072	0,989	0,729	0,836	0,929	1,003	0,646	1,128
12.8	CSIRO-Mk3-6-0	r8i1p1	45	1,166	1,102	1,057	1,067	1,233	0,955	0,778	0,889	0,986	1,107	0,683	1,136
12.9	CSIRO-Mk3-6-0	r9i1p1	45	1,039	1,035	1,035	1,063	1,029	1,007	0,702	0,865	1,013	1,207	0,551	1,206
12.10	CSIRO-Mk3-6-0	r10i1p1	60	1,043	1,047	1,050	1,018	1,019	1,010	0,797	0,897	0,975	1,048	0,716	1,105
12.1	CSIRO-Mk3-6-0	r1i1p1	60	1,120	1,086	1,057	0,941	1,118	0,987	0,776	0,866	0,955	1,122	0,677	1,124
12.2	CSIRO-Mk3-6-0	r2i1p1	60	1,029	1,022	1,017	1,038	1,039	0,999	0,893	0,974	1,051	1,148	0,822	1,087
12.3	CSIRO-Mk3-6-0	r3i1p1	60	1,091	1,040	1,002	0,959	1,126	0,970	0,766	0,866	0,956	1,107	0,671	1,117
12.4	CSIRO-Mk3-6-0	r4i1p1	60	1,014	1,039	1,059	1,135	0,997	1,023	0,901	0,953	1,003	1,086	0,859	1,060
12.5	CSIRO-Mk3-6-0	r5i1p1	60	1,210	1,086	1,005	0,976	1,352	0,917	0,818	0,904	0,981	1,007	0,735	1,115
12.6	CSIRO-Mk3-6-0	r6i1p1	60	1,008	1,033	1,055	1,107	0,976	1,027	0,766	0,860	0,950	1,091	0,667	1,137
12.7	CSIRO-Mk3-6-0	r7i1p1	60	1,043	1,044	1,042	1,003	1,098	0,993	0,808	0,887	0,946	0,989	0,711	1,103
12.8	CSIRO-Mk3-6-0	r8i1p1	60	1,128	1,078	1,038	0,940	1,137	0,977	0,829	0,916	0,989	1,061	0,706	1,113
12.9	CSIRO-Mk3-6-0	r9i1p1	60	1,129	1,068	1,026	1,037	1,198	0,954	0,708	0,825	0,936	1,157	0,640	1,144
12.10	CSIRO-Mk3-6-0	r10i1p1	85	1,132	1,081	1,047	1,000	1,121	0,979	0,738	0,857	0,955	1,044	0,617	1,150
12.1	CSIRO-Mk3-6-0	r1i1p1	85	1,135	1,106	1,088	1,057	1,149	0,983	0,747	0,863	0,971	1,133	0,606	1,168
12.2	CSIRO-Mk3-6-0	r2i1p1	85	1,111	1,078	1,054	1,071	1,138	0,978	0,814	0,917	1,006	1,108	0,710	1,121

	12.3	CSIRO-Mk3-6-0	r3i1p1	85	1,206	1,149	1,101	1,005	1,256	0,964	0,697	0,831	0,950	1,113	0,599	1,164
	12.4	CSIRO-Mk3-6-0	r4i1p1	85	1,050	1,066	1,079	1,142	1,057	1,009	0,822	0,921	1,007	1,170	0,739	1,103
	12.5	CSIRO-Mk3-6-0	r5i1p1	85	1,139	1,069	1,018	1,004	1,242	0,952	0,750	0,840	0,928	1,000	0,636	1,152
	12.6	CSIRO-Mk3-6-0	r6i1p1	85	1,114	1,102	1,095	1,085	1,124	0,995	0,809	0,921	1,017	1,116	0,697	1,141
	12.7	CSIRO-Mk3-6-0	r7i1p1	85	0,985	1,003	1,021	1,104	0,976	1,015	0,737	0,856	0,957	1,085	0,609	1,154
	12.8	CSIRO-Mk3-6-0	r8i1p1	85	1,099	1,094	1,087	1,051	1,093	0,997	0,735	0,890	1,027	1,138	0,622	1,187
	12.9	CSIRO-Mk3-6-0	r9i1p1	85	1,058	1,030	1,008	0,967	1,084	0,983	0,695	0,815	0,929	1,128	0,614	1,175
	13.1	FGOALS-s2	r1i1p1	26	1,072	1,089	1,094	1,050	1,094	1,006	0,919	1,024	1,119	1,167	0,845	1,103
	13.1	FGOALS-s2	r1i1p1	45	1,090	1,103	1,107	0,998	1,066	1,024	1,031	1,080	1,116	1,140	0,954	1,052
	13.2	FGOALS-s2	r2i1p1	45	1,098	1,081	1,061	0,963	1,094	0,995	0,966	1,041	1,103	1,084	0,843	1,094
	13.3	FGOALS-s2	r3i1p1	45	1,159	1,130	1,109	1,129	1,243	0,970	1,021	1,039	1,062	1,071	0,962	1,037
	13.1	FGOALS-s2	r1i1p1	60	1,232	1,200	1,173	1,079	1,252	0,988	0,771	0,939	1,080	1,182	0,633	1,188
	13.1	FGOALS-s2	r1i1p1	85	1,185	1,166	1,145	1,060	1,169	1,005	1,050	1,099	1,149	1,184	1,023	1,059
	13.2	FGOALS-s2	r2i1p1	85	1,079	1,083	1,086	1,030	1,100	1,010	0,766	0,893	1,019	1,083	0,679	1,182
	13.3	FGOALS-s2	r3i1p1	85	1,181	1,155	1,137	1,146	1,189	0,987	1,293	1,191	1,151	1,151	1,447	0,953
	14.1	GFDL-CM3	r1i1p1	26	1,070	1,081	1,088	1,087	1,049	1,008	0,764	0,891	1,005	1,130	0,635	1,161
	14.1	GFDL-CM3	r1i1p1	60	1,061	1,038	1,027	1,101	1,083	0,980	0,842	0,951	1,036	1,092	0,721	1,112
	14.1	GFDL-CM3	r1i1p1	85	1,237	1,131	1,053	0,966	1,355	0,928	0,875	0,980	1,071	1,155	0,755	1,121
	15.1	GFDL-ESM2G	r1i1p1	26	0,980	1,007	1,027	1,082	0,954	1,025	0,800	0,903	0,993	1,241	0,693	1,109
	15.1	GFDL-ESM2G	r1i1p1	45	1,007	1,015	1,016	1,002	0,986	1,015	0,909	0,959	1,002	1,134	0,839	1,052
	15.1	GFDL-ESM2G	r1i1p1	60	1,013	1,027	1,038	1,092	1,002	1,016	0,833	0,903	0,963	1,097	0,737	1,085
	15.1	GFDL-ESM2G	r1i1p1	85	1,031	1,029	1,030	1,063	1,052	1,006	0,784	0,892	0,988	1,169	0,677	1,118
	16.1	GFDL-ESM2M	r1i1p1	26	1,074	1,081	1,076	0,935	1,050	1,010	1,008	1,018	1,021	0,993	1,000	1,012
	16.1	GFDL-ESM2M	r1i1p1	45	1,162	1,111	1,070	0,945	1,181	0,976	0,941	0,979	1,012	1,068	0,885	1,047
	16.1	GFDL-ESM2M	r1i1p1	60	1,121	1,101	1,076	0,910	1,126	0,990	0,886	0,929	0,961	0,967	0,836	1,049
	16.1	GFDL-ESM2M	r1i1p1	85	1,235	1,161	1,102	0,990	1,322	0,947	0,876	0,934	0,988	1,077	0,802	1,073
	17.6	GISS-E2-R	r6i1p1	45	0,960	0,986	1,010	0,975	0,921	1,031	0,929	0,981	1,021	1,086	0,878	1,045
	18.1	HadGEM2-CC	r1i1p1	45	0,911	0,955	0,986	0,941	0,856	1,044	0,821	0,908	0,998	1,153	0,740	1,131
	18.1	HadGEM2-CC	r1i1p1	85	0,931	0,998	1,055	1,078	0,860	1,077	0,910	0,973	1,041	1,133	0,808	1,104
	18.2	HadGEM2-CC	r2i1p1	85	0,962	0,992	1,020	1,123	0,965	1,022	0,671	0,831	0,968	1,079	0,557	1,190
	18.3	HadGEM2-CC	r3i1p1	85	1,002	1,027	1,054	1,202	0,998	1,020	0,740	0,883	1,004	1,058	0,639	1,164
	19.1	HadGEM2-ES	r1i1p1	26	0,866	0,967	1,055	1,102	0,743	1,113	0,850	0,918	1,003	1,101	0,826	1,150
	19.2	HadGEM2-ES	r2i1p1	26	1,025	1,080	1,123	1,067	0,952	1,051	0,755	0,870	0,965	1,042	0,601	1,160
	19.3	HadGEM2-ES	r3i1p1	26	0,822	0,923	1,016	1,000	0,726	1,112	0,581	0,749	0,893	0,965	0,464	1,237
	19.4	HadGEM2-ES	r4i1p1	26	1,012	1,010	1,025	1,083	0,998	1,008	0,918	0,974	1,027	1,120	0,839	1,067
	19.1	HadGEM2-ES	r1i1p1	45	1,073	1,057	1,049	1,064	1,105	0,994	0,944	0,963	1,018	1,130	1,015	1,085
	19.2	HadGEM2-ES	r2i1p1	45	0,953	1,014	1,065	1,072	0,884	1,057	0,582	0,740	0,877	1,015	0,436	1,235
	19.3	HadGEM2-ES	r3i1p1	45	0,966	1,020	1,072	1,081	0,900	1,048	0,639	0,802	0,936	1,009	0,477	1,220
	19.4	HadGEM2-ES	r4i1p1	45	1,058	1,057	1,056	1,028	1,062	1,010	0,649	0,766	0,873	0,996	0,572	1,186
	19.1	HadGEM2-ES	r1i1p1	60	0,963	1,019	1,075	1,153	0,915	1,063	0,826	0,932	1,022	1,099	0,756	1,106
	19.2	HadGEM2-ES	r2i1p1	60	0,948	1,019	1,078	1,078	0,857	1,075	0,713	0,806	0,895	1,071	0,576	1,157
	19.3	HadGEM2-ES	r3i1p1	60	0,948	1,011	1,068	1,148	0,920	1,050	0,511	0,691	0,856	1,024	0,371	1,291
	19.4	HadGEM2-ES	r4i1p1	60	0,805	0,912	1,013	1,202	0,695	1,115	0,720	0,834	0,945	1,069	0,661	1,181
	19.1	HadGEM2-ES	r1i1p1	85	1,038	1,058	1,082	1,141	1,002	1,033	0,938	0,942	0,968	1,078	0,947	1,064
	19.2	HadGEM2-ES	r2i1p1	85	1,137	1,100	1,072	1,034	1,167	0,979	0,658	0,803	0,938	1,119	0,510	1,220
	19.3	HadGEM2-ES	r3i1p1	85	1,028	1,031	1,035	1,040	1,057	0,996	0,564	0,721	0,860	1,005	0,428	1,247
	19.4	HadGEM2-ES	r4i1p1	85	0,930	0,965	0,993	1,061	0,884	1,048	0,530	0,730	0,908	1,109	0,378	1,276
	20.1	inmcm4	r1i1p1	45	1,010	0,995	0,992	1,062	0,994	0,993	0,875	0,902	0,920	0,894	0,844	1,032
	20.1	inmcm4	r1i1p1	85	1,116	1,068	1,037	1,053	1,121	0,977	0,876	0,932	0,972	0,995	0,784	1,066
	21.1	IPSL-CM5A-LR	r1i1p1	26	1,071	1,059	1,047	1,071	1,074	0,993	0,936	1,006	1,052	1,074	0,906	1,048
	21.2	IPSL-CM5A-LR	r2i1p1	26	1,139	1,114	1,091	0,982	1,165	0,984	0,978	1,026	1,061	1,073	0,901	1,051
	21.3	IPSL-CM5A-LR	r3i1p1	26	0,966	1,029	1,086	1,172	0,902	1,053	0,970	1,017	1,064	1,173	0,956	1,034
	21.4	IPSL-CM5A-LR	r4i1p1	26	1,028	1,044	1,053	1,034	1,003	1,012	1,029	1,045	1,068	1,173	0,966	1,034
	21.1	IPSL-CM5A-LR	r1i1p1	45	1,077	1,054	1,043	1,107	1,068	0,991	0,974	1,038	1,087	1,123	0,924	1,052
	21.2	IPSL-CM5A-LR	r2i1p1	45	1,151	1,097	1,059	0,978	1,198	0,965	0,938	0,979	1,010	1,085	0,850	1,055
	21.3	IPSL-CM5A-LR	r3i1p1	45	1,033	1,062	1,090	1,195	0,983	1,028	0,941	1,018	1,082	1,175	0,840	1,082
	21.4	IPSL-CM5A-LR	r4i1p1	45	0,961	1,034	1,093	1,150	0,869	1,061	0,943	0,974	1,004	1,081	0,904	1,035
	21.1	IPSL-CM5A-LR	r1i1p1	60	1,042	1,058	1,070	1,168	1,030	1,011	0,944	0,995	1,027	1,051	0,919	1,040
	21.1	IPSL-CM5A-LR	r1i1p1	85	1,086	1,070	1,060	1,090	1,083	0,990	1,070	1,094	1,110	1,159	1,048	1,023
	21.2	IPSL-CM5A-LR	r2i1p1	85	1,107	1,067	1,035	1,011	1,172	0,962	0,934	0,983	1,020	1,053	0,874	1,056
	21.3	IPSL-CM5A-LR	r3i1p1	85	1,009	1,021	1,045	1,191	0,987	1,018	1,048	1,022	1,022	1,183	1,080	0,988
	21.4	IPSL-CM5A-LR	r4i1p1	85	0,953	1,019	1,071	1,108	0,847	1,064	0,904	0,968	1,022	1,133	0,808	1,075
	22.1	IPSL-CM5A-MR	r1i1p1	26	1,052	1,057	1,067	1,103	1,023	1,011	1,056	1,050	1,052	1,068	1,051	1,004
	22.1	IPSL-CM5A-MR	r1i1p1	45	1,083	1,087	1,090	1,068	1,060	1,007	0,831	0,926	1,004	1,067	0,718	1,109
	22.1	IPSL-CM5A-MR	r1i1p1	60	1,086	1,059	1,032	0,950	1,103	0,982	0,958	0,979	1,001	1,055	0,908	1,030
	22.1	IPSL-CM5A-MR	r1i1p1	85	1,099	1,063	1,035	1,014	1,108	0,987	0,784	0,856	0,926	1,083	0,693	1,098
	23.1	IPSL-CM5B-LR	r1i1p1	45	0,974	1,023	1,068	1,181	0,925	1,041	0,959	1,013	1,060	1,170	0,939	1,030
	23.1	IPSL-CM5B-LR	r1i1p1	85	1,032	1,013	1,010	1,085	1,029	0,996	1,109	1,072	1,053	1,074	1,130	0,977
	24.1	MIROC-ESM	r1i1p1	26	1,078	1,098	1,111	1,077	1,065	1,013	1,133	1,163	1,182	1,175	1,089	1,026
	24.1	MIROC-ESM	r1i1p1	45	1,072	1,091	1,102	1,067	1,068	1,008	1,049	1,107	1,149	1,174	0,974	1,052
	24.1	MIROC-ESM	r1i1p1	60	1,156	1,117	1,081	0,970	1,186	0,972	1,165	1,187	1,196	1,152	1,115	1,023
	24.1	MIROC-ESM	r1i1p1	85	1,084	1,081	1,074	1,031	1,098	0,998	1,135	1,166	1,178	1,121	1,090	1,026
	25.1	MIROC-ESM-CHEM	r1i1p1	26	1,110	1,080	1,061	1,043	1,085	0,990	1,098	1,108	1,121	1,172	1,051	1,019
	25.1	MIROC-ESM-CHEM	r1i1p1	45	1,084	1,049	1,028	1,100	1,100	0,978	1,169	1,150	1,133	1,134	1,163	0,991
	25.1	MIROC-ESM-CHEM	r1i1p1	60	1,069	1,033	1,010	1,033	1,119	0,969	1,150	1,126	1,109	1,093	1,183	0,988
	25.1	MIROC-ESM-CHEM	r1i1p1	85	1,113	1,084	1,050	0,903	1,106	0,986	1,165	1,155	1,142	1,083	1,156	0,996
	26.1	MIROC5	r1i1p1	26	1,065	1,041	1,025	1,022	1,071	0,990	0,865	0,962	1,043	1,138	0,756	1,115
	26.2	MIROC5	r2i1p1	26	1,229	1,150	1,103	1,121	1,304	0,951	1,140	1,161	1,190	1,190	1,163	1,011
	26.3	MIROC5	r3i1p1	26	0,928	0,960	0,988	1,028	0,851	1,041	0,981	1,042	1,089	1,063	0,929	1,052
	26.1	MIROC5	r1i1p1	45	1,079	1,064	1,052	1,006	1,095	0,993	1,074	1,079	1,090	1,130	1,043	1,024
	26.2	MIROC5	r2i1p1	45	1,108	1,077	1,072	1,092	1,108	1,003	1,222	1,202	1,191	1,159	1,223	0,992
	26.3	MIROC5	r3i1p1	45	1,044	1,011	0,983	0,941	1,071	0,977	0,907	1,015	1,100	1,089	0,769	1,112
	26.1	MIROC5	r1i1p1	60	1,142	1,096	1,070	1,046	1,181	0,977	1,122	1,108	1,110	1,157	1,124	0,998
	26.1	MIROC5	r1i1p1	85	1,079	1,065	1,054	1,056	1,120	0,991	0,997	1,068	1,126	1,240	0,956	1,059
	26.2	MIROC5	r2i1p1	85	1,206	1,135	1,084	1,066	1,264	0,952	1,127	1,141	1,153	1,209	1,083	1,020
	26.3	MIROC5	r3i1p1	85	1,202	1,102	1,027	0,973	1,253	0,941	0,953	1,034	1,098	1,171	0,823	1,090
	27.1	MPI-ESM-LR	r1i1p1	26	1,104	1,050	1,006	0,955	1,190	0,963	1,036	1,032	1,038	1,043	1,034	1,015
	27.2	MPI-ESM-LR	r2i1p1	26	1,153	1,102	1,053	0,904	1,220	0,957	0,894	0,960	1,006	0,968	0,809	1,067
	27.3	MPI-ESM-LR	r3i1p1	26	1,066	1,005	0,976	1,092	1,132	0,957	0,919	0,934	0,947	0,959	0,862	1,031

	27.1	MPI-ESM-LR	r1i1p1	45	1,086	1,048	1,021	1,051	1,140	0,973	0,967	0,990	1,018	1,084	0,937	1,035
	27.2	MPI-ESM-LR	r2i1p1	45	1,063	1,038	1,025	0,914	1,108	0,983	0,875	0,941	0,984	0,951	0,792	1,076
	27.3	MPI-ESM-LR	r3i1p1	45	1,145	1,059	1,005	1,035	1,236	0,944	0,847	0,891	0,922	0,988	0,781	1,058
	27.1	MPI-ESM-LR	r1i1p1	85	0,885	0,945	1,008	1,119	0,800	1,071	0,923	0,950	0,983	1,076	0,898	1,040
	27.2	MPI-ESM-LR	r2i1p1	85	1,251	1,151	1,079	0,896	1,340	0,941	0,812	0,893	0,955	0,983	0,723	1,088
	27.3	MPI-ESM-LR	r3i1p1	85	1,045	0,978	0,951	0,992	1,063	0,981	0,892	0,897	0,911	0,996	0,848	1,029
	28.1	MPI-ESM-MR	r1i1p1	26	1,109	1,092	1,080	1,061	1,136	0,981	0,952	1,016	1,063	1,047	0,846	1,073
	28.1	MPI-ESM-MR	r1i1p1	45	1,177	1,100	1,045	1,027	1,264	0,943	0,930	0,979	1,019	1,062	0,856	1,055
	28.2	MPI-ESM-MR	r2i1p1	45	0,938	0,975	1,014	1,216	0,899	1,044	0,848	0,909	0,964	1,081	0,765	1,078
	28.3	MPI-ESM-MR	r3i1p1	45	0,889	0,954	1,013	1,148	0,840	1,062	0,858	0,921	0,980	1,094	0,783	1,074
	28.1	MPI-ESM-MR	r1i1p1	85	1,040	1,050	1,067	1,133	1,024	1,010	0,856	0,957	1,032	1,029	0,731	1,110
	29.1	MRI-CGCM3	r1i1p1	26	0,896	0,901	0,911	0,946	0,910	1,003	0,983	0,967	0,970	1,015	1,011	0,996
	29.1	MRI-CGCM3	r1i1p1	45	0,887	0,894	0,908	1,032	0,896	1,007	0,926	0,940	0,959	1,039	0,899	1,026
	29.1	MRI-CGCM3	r1i1p1	60	0,992	0,962	0,944	1,021	1,046	0,972	0,892	0,947	0,997	1,139	0,849	1,052
	29.1	MRI-CGCM3	r1i1p1	85	1,007	0,951	0,920	1,039	1,085	0,955	0,925	0,939	0,954	1,020	0,908	1,019
	30.1	NorESM1-M	r1i1p1	26	1,004	1,038	1,064	1,074	0,971	1,030	0,812	0,902	0,975	1,085	0,717	1,104
	30.1	NorESM1-M	r1i1p1	45	1,041	1,049	1,047	0,975	1,057	1,003	0,780	0,916	1,023	1,078	0,647	1,147
	30.1	NorESM1-M	r1i1p1	60	0,998	1,020	1,038	1,019	0,979	1,021	0,830	0,916	0,988	1,139	0,754	1,088
	30.1	NorESM1-M	r1i1p1	85	0,976	1,030	1,075	1,118	0,908	1,051	0,772	0,904	1,014	1,135	0,654	1,145
	EC.1	EC-EARTH	r1i1p1	85	1,170	1,108	1,064	0,996	1,238	0,961	1,006	1,042	1,082	1,099	0,950	1,058
	EC.2	EC-EARTH	r2i1p1	85	1,145	1,104	1,073	1,029	1,178	0,975	0,871	0,962	1,039	1,184	0,785	1,094
	EC.3	EC-EARTH	r3i1p1	85	1,183	1,098	1,040	0,984	1,280	0,945	0,936	0,994	1,039	1,090	0,853	1,063
	EC.4	EC-EARTH	r4i1p1	85	0,975	1,029	1,083	1,199	0,909	1,051	0,852	0,916	0,964	1,013	0,779	1,074
	EC.5	EC-EARTH	r5i1p1	85	1,024	1,067	1,106	1,139	0,983	1,035	0,890	0,954	1,010	1,130	0,831	1,061
	EC.6	EC-EARTH	r6i1p1	85	1,226	1,142	1,085	1,094	1,325	0,941	0,964	1,001	1,031	1,056	0,901	1,039
	EC.7	EC-EARTH	r7i1p1	85	1,007	1,082	1,145	1,181	0,919	1,060	0,921	0,981	1,024	1,016	0,904	1,048
	EC.8	EC-EARTH	r8i1p1	85	1,190	1,163	1,136	1,020	1,199	0,987	1,133	1,075	1,045	1,020	1,190	0,967

Summary statistics

		Winter						Summer					
		P30	P60	P90	E	a	b	P30	P60	P90	E	a	b
Overall	Mean	1,062	1,055	1,051	1,054	1,068	1,000	0,875	0,946	1,010	1,090	0,802	1,092
	Coefficient of variation	0,078	0,049	0,039	0,071	0,115	0,035	0,163	0,103	0,068	0,059	0,232	0,060
	Minimum	0,805	0,894	0,908	0,894	0,695	0,917	0,511	0,691	0,856	0,894	0,371	0,947
	1th Quartile	1,015	1,027	1,027	1,005	0,998	0,979	0,778	0,890	0,964	1,052	0,677	1,045
	Median	1,064	1,057	1,054	1,051	1,071	0,996	0,871	0,939	1,005	1,086	0,781	1,087
	3rd Quartile	1,114	1,088	1,077	1,101	1,137	1,016	0,953	0,997	1,042	1,133	0,911	1,131
	Maximum	1,251	1,200	1,173	1,260	1,355	1,115	1,293	1,202	1,196	1,244	1,447	1,291
RCP 2.6	Mean	1,052	1,052	1,053	1,047	1,050	1,005	0,882	0,954	1,016	1,090	0,806	1,089
	Coefficient of variation	0,075	0,048	0,039	0,062	0,113	0,035	0,148	0,096	0,067	0,064	0,210	0,057
	Minimum	0,822	0,901	0,911	0,904	0,726	0,951	0,581	0,749	0,893	0,959	0,464	0,996
	1th Quartile	1,024	1,027	1,028	1,010	0,999	0,986	0,773	0,894	0,976	1,048	0,678	1,036
	Median	1,064	1,054	1,056	1,050	1,061	1,001	0,880	0,957	1,010	1,080	0,818	1,088
	3rd Quartile	1,103	1,087	1,084	1,091	1,132	1,013	0,977	1,018	1,052	1,129	0,925	1,130
	Maximum	1,229	1,150	1,123	1,194	1,304	1,113	1,140	1,163	1,190	1,241	1,163	1,237
RCP 4.5	Mean	1,050	1,045	1,044	1,050	1,054	1,002	0,874	0,944	1,007	1,079	0,798	1,091
	Coefficient of variation	0,067	0,043	0,037	0,070	0,102	0,030	0,155	0,100	0,068	0,059	0,211	0,055
	Minimum	0,887	0,894	0,908	0,894	0,840	0,939	0,582	0,740	0,868	0,894	0,436	0,991
	1th Quartile	1,017	1,024	1,021	0,998	0,994	0,981	0,782	0,889	0,964	1,040	0,683	1,047
	Median	1,063	1,050	1,050	1,045	1,067	0,998	0,875	0,940	1,004	1,084	0,792	1,085
	3rd Quartile	1,088	1,070	1,068	1,095	1,114	1,019	0,944	0,990	1,029	1,130	0,904	1,128
	Maximum	1,177	1,130	1,109	1,216	1,264	1,062	1,222	1,202	1,191	1,207	1,223	1,235
RCP 6.0	Mean	1,054	1,047	1,043	1,035	1,062	1,001	0,852	0,928	0,995	1,082	0,777	1,097
	Coefficient of variation	0,080	0,048	0,039	0,075	0,117	0,039	0,163	0,106	0,068	0,051	0,227	0,060
	Minimum	0,805	0,912	0,944	0,910	0,695	0,917	0,511	0,691	0,856	0,967	0,371	0,988
	1th Quartile	1,013	1,023	1,020	0,972	0,999	0,977	0,772	0,867	0,951	1,051	0,668	1,050
	Median	1,043	1,040	1,046	1,027	1,068	0,992	0,830	0,923	0,989	1,089	0,736	1,104
	3rd Quartile	1,115	1,076	1,066	1,089	1,124	1,018	0,917	0,974	1,020	1,118	0,866	1,124
	Maximum	1,232	1,200	1,173	1,202	1,352	1,115	1,165	1,187	1,196	1,182	1,183	1,291
RCP 8.5	Mean	1,082	1,067	1,060	1,072	1,095	0,996	0,878	0,950	1,016	1,103	0,807	1,094
	Coefficient of variation	0,085	0,052	0,040	0,075	0,124	0,037	0,179	0,109	0,069	0,059	0,263	0,066
	Minimum	0,831	0,923	0,920	0,896	0,723	0,928	0,530	0,721	0,860	0,983	0,378	0,947
	1th Quartile	1,024	1,030	1,035	1,014	1,002	0,975	0,784	0,893	0,968	1,058	0,679	1,051
	Median	1,084	1,069	1,063	1,066	1,100	0,991	0,875	0,942	1,011	1,103	0,779	1,088
	3rd Quartile	1,137	1,102	1,085	1,133	1,174	1,015	0,938	0,989	1,041	1,135	0,908	1,141
	Maximum	1,251	1,182	1,145	1,260	1,355	1,099	1,293	1,191	1,178	1,244	1,447	1,276

Rhine basin - Far Future (2071-2100)

Model info				Winter						Summer					
Index	GCM	Run	RCP	P30	P60	P90	E	a	b	P30	P60	P90	E	a	b
1.1	ACCESS1-0	r1i1p1	45	1,105	1,111	1,116	1,205	1,121	1,005	0,708	0,837	0,964	1,179	0,558	1,227
1.1	ACCESS1-0	r1i1p1	85	1,040	1,059	1,078	1,169	1,005	1,045	0,478	0,650	0,871	1,210	0,319	1,508
2.1	ACCESS1-3	r1i1p1	45	1,053	1,031	1,027	1,143	1,059	0,998	0,805	0,916	1,014	1,157	0,694	1,143
2.1	ACCESS1-3	r1i1p1	85	1,066	1,078	1,091	1,143	1,041	1,025	0,538	0,755	0,999	1,414	0,366	1,395
3.1	bcc-csm1-1	r1i1p1	26	1,026	1,035	1,034	0,968	1,010	1,010	1,092	1,089	1,085	1,046	1,071	1,008
3.1	bcc-csm1-1	r1i1p1	45	0,988	1,061	1,103	1,087	0,936	1,050	1,005	1,031	1,052	1,062	0,961	1,042
3.1	bcc-csm1-1	r1i1p1	60	1,150	1,126	1,100	1,001	1,158	0,985	0,792	0,890	0,968	1,077	0,614	1,150
3.1	bcc-csm1-1	r1i1p1	85	1,057	1,103	1,130	1,150	0,985	1,045	0,640	0,789	0,926	1,035	0,446	1,260
4.1	bcc-csm1-1-m	r1i1p1	26	1,034	1,077	1,104	1,110	1,018	1,026	0,760	0,866	0,958	1,077	0,660	1,138
4.1	bcc-csm1-1-m	r1i1p1	45	1,077	1,096	1,107	1,142	1,058	1,017	0,720	0,826	0,921	1,122	0,607	1,140
4.1	bcc-csm1-1-m	r1i1p1	60	1,122	1,115	1,109	1,136	1,120	1,001	0,603	0,741	0,870	1,059	0,455	1,251
4.1	bcc-csm1-1-m	r1i1p1	85	1,140	1,155	1,156	1,111	1,125	1,014	0,516	0,670	0,837	1,159	0,362	1,359
5.1	BNU-ESM	r1i1p1	26	1,089	1,063	1,051	1,108	1,076	0,990	0,993	1,026	1,056	1,111	0,877	1,056
5.1	BNU-ESM	r1i1p1	45	1,015	1,061	1,092	1,111	0,984	1,030	0,904	0,974	1,028	1,073	0,750	1,098
5.1	BNU-ESM	r1i1p1	85	0,998	1,071	1,114	1,113	0,898	1,065	0,852	0,955	1,039	1,145	0,669	1,134
6.1	CanESM2	r1i1p1	26	1,021	1,040	1,049	1,026	1,060	1,016	0,964	1,014	1,050	1,073	0,892	1,056
6.2	CanESM2	r2i1p1	26	1,225	1,149	1,096	1,009	1,281	0,963	1,022	1,033	1,047	1,069	1,029	1,015
6.3	CanESM2	r3i1p1	26	1,128	1,085	1,063	1,086	1,169	0,974	1,110	1,092	1,078	1,049	1,151	0,992
6.4	CanESM2	r4i1p1	26	1,143	1,101	1,073	1,050	1,239	0,964	1,016	1,025	1,041	1,124	1,069	1,002
6.5	CanESM2	r5i1p1	26	0,997	1,046	1,084	1,203	1,023	1,024	0,915	0,998	1,060	1,079	0,832	1,076
6.1	CanESM2	r1i1p1	45	1,069	1,096	1,113	1,113	1,056	1,037	0,772	0,903	1,016	1,150	0,615	1,166
6.2	CanESM2	r2i1p1	45	1,154	1,118	1,097	1,119	1,176	0,987	0,867	0,963	1,040	1,132	0,733	1,109
6.3	CanESM2	r3i1p1	45	1,028	1,046	1,060	1,109	1,062	1,008	0,902	0,952	0,999	1,111	0,846	1,074
6.4	CanESM2	r4i1p1	45	1,031	1,055	1,078	1,153	1,085	1,022	0,782	0,880	0,981	1,244	0,740	1,111
6.5	CanESM2	r5i1p1	45	1,012	1,041	1,069	1,220	1,063	1,022	0,836	0,918	0,989	1,078	0,774	1,090
6.1	CanESM2	r1i1p1	85	1,247	1,235	1,222	1,206	1,256	1,011	0,521	0,692	0,875	1,252	0,371	1,308
6.2	CanESM2	r2i1p1	85	1,286	1,259	1,242	1,247	1,310	1,008	0,507	0,687	0,873	1,168	0,339	1,338
6.3	CanESM2	r3i1p1	85	1,201	1,196	1,194	1,254	1,258	0,992	0,692	0,806	0,911	1,070	0,549	1,180
6.4	CanESM2	r4i1p1	85	1,173	1,189	1,209	1,323	1,243	1,012	0,651	0,778	0,908	1,235	0,542	1,190
6.5	CanESM2	r5i1p1	85	1,232	1,212	1,200	1,253	1,280	0,996	0,593	0,739	0,887	1,131	0,466	1,240
7.1	CCSM4	r1i1p1	26	1,110	1,065	1,039	1,091	1,103	0,980	0,974	1,016	1,046	1,078	0,894	1,048
7.2	CCSM4	r2i1p1	26	1,053	1,059	1,059	1,045	1,051	1,004	0,928	0,987	1,036	1,118	0,886	1,049
7.6	CCSM4	r6i1p1	26	1,070	1,059	1,043	0,943	1,094	0,990	0,901	0,964	1,015	1,099	0,842	1,058
7.1	CCSM4	r1i1p1	45	1,142	1,088	1,050	1,031	1,164	0,972	0,807	0,901	0,979	1,131	0,683	1,121
7.2	CCSM4	r2i1p1	45	1,036	1,078	1,101	1,125	1,014	1,025	0,867	0,961	1,034	1,082	0,753	1,097
7.6	CCSM4	r6i1p1	45	1,091	1,092	1,085	1,023	1,107	0,997	0,891	0,951	1,004	1,150	0,836	1,060
7.1	CCSM4	r1i1p1	60	1,142	1,106	1,078	1,042	1,141	0,984	0,801	0,904	0,983	1,034	0,658	1,125
7.2	CCSM4	r2i1p1	60	1,082	1,096	1,102	1,092	1,059	1,012	0,863	0,924	0,971	1,031	0,803	1,061
7.6	CCSM4	r6i1p1	60	1,031	1,062	1,079	1,068	1,010	1,021	0,865	0,945	1,010	1,124	0,733	1,095
7.1	CCSM4	r1i1p1	85	1,138	1,126	1,121	1,191	1,118	1,000	0,688	0,818	0,927	1,042	0,543	1,172
7.2	CCSM4	r2i1p1	85	1,070	1,115	1,147	1,208	1,037	1,030	0,670	0,825	0,959	1,135	0,518	1,192
7.6	CCSM4	r6i1p1	85	1,042	1,075	1,095	1,075	0,990	1,034	0,698	0,827	0,937	1,111	0,532	1,172
8.1	CMCC-CESM	r1i1p1	85	1,429	1,367	1,315	1,191	1,573	0,970	0,885	0,982	1,069	1,212	0,759	1,134
9.1	CMCC-CM	r1i1p1	45	0,988	1,034	1,067	1,040	1,001	1,033	0,738	0,860	0,965	1,081	0,557	1,195
9.1	CMCC-CM	r1i1p1	85	0,997	1,088	1,157	1,196	0,990	1,070	0,490	0,702	0,919	1,170	0,271	1,423
10.1	CMCC-CMS	r1i1p1	45	1,018	1,052	1,079	1,180	1,004	1,029	0,882	0,928	0,969	1,049	0,801	1,073
10.1	CMCC-CMS	r1i1p1	85	0,999	1,081	1,136	1,196	0,933	1,071	0,671	0,800	0,931	1,115	0,493	1,263
11.1	CNRM-CM5	r1i1p1	26	1,072	1,050	1,032	0,953	1,076	0,992	1,205	1,149	1,113	1,097	1,271	0,959
11.1	CNRM-CM5	r1i1p1	45	1,235	1,155	1,099	1,020	1,302	0,955	1,179	1,127	1,094	1,098	1,288	0,951
11.1	CNRM-CM5	r1i1p1	85	1,255	1,231	1,215	1,143	1,211	1,006	1,176	1,191	1,207	1,283	1,168	1,007
12.10	CSIRO-Mk3-6-0	r10i1p1	26	1,130	1,111	1,095	1,109	1,116	0,993	0,813	0,921	1,015	1,198	0,679	1,135
12.1	CSIRO-Mk3-6-0	r1i1p1	26	1,096	1,094	1,084	1,030	1,056	1,008	0,767	0,876	0,970	1,053	0,607	1,173
12.2	CSIRO-Mk3-6-0	r2i1p1	26	1,113	1,084	1,066	1,051	1,114	0,989	0,854	0,953	1,030	1,095	0,726	1,118
12.3	CSIRO-Mk3-6-0	r3i1p1	26	1,072	1,041	1,025	1,050	1,095	0,988	0,754	0,858	0,948	1,111	0,616	1,155
12.4	CSIRO-Mk3-6-0	r4i1p1	26	1,122	1,099	1,081	1,106	1,135	0,991	0,831	0,908	0,984	1,128	0,750	1,119
12.5	CSIRO-Mk3-6-0	r5i1p1	26	1,164	1,116	1,080	1,028	1,190	0,974	0,765	0,880	0,980	1,112	0,626	1,153
12.6	CSIRO-Mk3-6-0	r6i1p1	26	1,088	1,094	1,092	1,101	1,090	1,005	0,815	0,907	0,996	1,210	0,712	1,137
12.7	CSIRO-Mk3-6-0	r7i1p1	26	1,124	1,074	1,041	1,021	1,125	0,980	0,735	0,819	0,897	1,095	0,617	1,136
12.8	CSIRO-Mk3-6-0	r8i1p1	26	0,996	1,060	1,103	1,118	0,945	1,049	0,740	0,875	0,995	1,162	0,583	1,185
12.9	CSIRO-Mk3-6-0	r9i1p1	26	1,090	1,074	1,066	1,128	1,081	0,996	0,765	0,909	1,042	1,263	0,630	1,189
12.10	CSIRO-Mk3-6-0	r10i1p1	45	1,160	1,139	1,127	1,174	1,128	0,998	0,667	0,800	0,934	1,217	0,505	1,243
12.1	CSIRO-Mk3-6-0	r1i1p1	45	1,023	1,078	1,112	1,139	0,972	1,045	0,600	0,745	0,890	1,082	0,417	1,307
12.2	CSIRO-Mk3-6-0	r2i1p1	45	1,175	1,138	1,120	1,124	1,176	0,993	0,695	0,861	1,007	1,167	0,484	1,248
12.3	CSIRO-Mk3-6-0	r3i1p1	45	1,187	1,132	1,092	1,024	1,202	0,977	0,716	0,822	0,923	1,123	0,579	1,183
12.4	CSIRO-Mk3-6-0	r4i1p1	45	1,199	1,168	1,148	1,223	1,190	0,991	0,649	0,781	0,917	1,177	0,492	1,246
12.5	CSIRO-Mk3-6-0	r5i1p1	45	1,159	1,133	1,117	1,111	1,173	0,997	0,685	0,814	0,936	1,094	0,530	1,226
12.6	CSIRO-Mk3-6-0	r6i1p1	45	1,134	1,148	1,150	1,123	1,131	1,010	0,675	0,792	0,914	1,121	0,535	1,243
12.7	CSIRO-Mk3-6-0	r7i1p1	45	1,125	1,109	1,093	1,073	1,143	0,998	0,627	0,768	0,912	1,134	0,450	1,274
12.8	CSIRO-Mk3-6-0	r8i1p1	45	1,037	1,084	1,110	1,128	1,016	1,037	0,618	0,786	0,959	1,147	0,447	1,300
12.9	CSIRO-Mk3-6-0	r9i1p1	45	1,088	1,088	1,081	1,060	1,060	1,010	0,535	0,705	0,900	1,247	0,392	1,361
12.10	CSIRO-Mk3-6-0	r10i1p1	60	1,042	1,082	1,109	1,139	1,003	1,039	0,700	0,835	0,970	1,211	0,562	1,233
12.1	CSIRO-Mk3-6-0	r1i1p1	60	1,087	1,118	1,127	1,039	1,032	1,030	0,616	0,765	0,906	1,069	0,436	1,271
12.2	CSIRO-Mk3-6-0	r2i1p1	60	1,143	1,129	1,115	1,094	1,153	0,995	0,682	0,833	0,971	1,209	0,478	1,238
12.3	CSIRO-Mk3-6-0	r3i1p1	60	1,150	1,138	1,123	1,058	1,143	0,999	0,606	0,749	0,898	1,183	0,460	1,266
12.4	CSIRO-Mk3-6-0	r4i1p1	60	1,150	1,135	1,126	1,175	1,165	0,996	0,675	0,805	0,932	1,153	0,517	1,216
12.5	CSIRO-Mk3-6-0	r5i1p1	60	1,178	1,136	1,105	1,024	1,148	0,995	0,648	0,790	0,926	1,080	0,471	1,261
12.6	CSIRO-Mk3-6-0	r6i1p1	60	1,028	1,077	1,103	1,080	1,028	1,031	0,598	0,760	0,920	1,153	0,427	1,287
12.7	CSIRO-Mk3-6-0	r7i1p1	60	1,126	1,122	1,112	1,064	1,093	1,011	0,637	0,773	0,908	1,077	0,473	1,260
12.8	CSIRO-Mk3-6-0	r8i1p1	60	1,062	1,128	1,161	1,121	1,007	1,045	0,581	0,753	0,928	1,169	0,410	1,313
12.9	CSIRO-Mk3-6-0	r9i1p1	60	1,157	1,123	1,096	1,077	1,137	0,994	0,684	0,836	0,983	1,226	0,526	1,234
12.10	CSIRO-Mk3-6-0	r10i1p1	85	1,174	1,157	1,144	1,146	1,132	1,006	0,557	0,705	0,864	1,143	0,396	1,351
12.1	CSIRO-Mk3-6-0	r1i1p1	85	1,191	1,188	1,177	1,128	1,137	1,019	0,463	0,641	0,844	1,153	0,274	1,453
12.2	CSIRO-Mk3-6-0	r2i1p1	85	1,164	1,164	1,161	1,194	1,146	1,007	0,550	0,723	0,903	1,188	0,376	1,344

	12.3	CSIRO-Mk3-6-0	r3i1p1	85	1,113	1,129	1,132	1,092	1,086	1,022	0,513	0,695	0,891	1,247	0,324	1,382
	12.4	CSIRO-Mk3-6-0	r4i1p1	85	1,196	1,194	1,192	1,248	1,168	1,019	0,442	0,615	0,821	1,254	0,262	1,477
	12.5	CSIRO-Mk3-6-0	r5i1p1	85	1,201	1,190	1,177	1,110	1,183	1,005	0,572	0,713	0,869	1,083	0,406	1,362
	12.6	CSIRO-Mk3-6-0	r6i1p1	85	1,122	1,155	1,177	1,235	1,109	1,027	0,493	0,665	0,865	1,225	0,318	1,433
	12.7	CSIRO-Mk3-6-0	r7i1p1	85	1,198	1,160	1,133	1,107	1,159	1,002	0,526	0,669	0,828	1,088	0,363	1,368
	12.8	CSIRO-Mk3-6-0	r8i1p1	85	1,173	1,196	1,210	1,269	1,131	1,030	0,522	0,677	0,877	1,264	0,361	1,444
	12.9	CSIRO-Mk3-6-0	r9i1p1	85	1,172	1,175	1,173	1,154	1,125	1,019	0,458	0,635	0,849	1,225	0,293	1,487
	13.1	FGOALS-s2	r1i1p1	26	1,223	1,151	1,119	1,121	1,268	0,971	1,122	1,120	1,124	1,148	1,080	1,015
	13.1	FGOALS-s2	r1i1p1	45	1,297	1,243	1,207	1,127	1,269	0,994	0,706	0,887	1,042	1,181	0,488	1,238
	13.2	FGOALS-s2	r2i1p1	45	1,159	1,176	1,177	1,091	1,161	1,013	0,843	0,973	1,082	1,200	0,685	1,144
	13.3	FGOALS-s2	r3i1p1	45	1,180	1,159	1,138	1,055	1,213	0,989	1,244	1,178	1,157	1,071	1,362	1,005
	13.1	FGOALS-s2	r1i1p1	60	1,248	1,247	1,240	1,179	1,241	1,009	0,864	1,008	1,142	1,282	0,673	1,197
	13.1	FGOALS-s2	r1i1p1	85	1,285	1,310	1,319	1,257	1,222	1,039	0,737	0,935	1,114	1,229	0,474	1,291
	13.2	FGOALS-s2	r2i1p1	85	1,412	1,389	1,355	1,163	1,433	1,004	0,709	0,871	1,032	1,174	0,483	1,298
	13.3	FGOALS-s2	r3i1p1	85	1,273	1,305	1,326	1,366	1,206	1,039	0,970	1,000	1,064	1,204	0,907	1,134
	14.1	GFDL-CM3	r1i1p1	26	1,120	1,085	1,058	1,027	1,096	0,990	0,950	1,018	1,075	1,171	0,864	1,070
	14.1	GFDL-CM3	r1i1p1	60	1,091	1,125	1,139	1,108	1,022	1,035	0,790	0,950	1,091	1,264	0,604	1,195
	14.1	GFDL-CM3	r1i1p1	85	1,005	1,080	1,131	1,200	0,890	1,072	0,627	0,806	0,990	1,260	0,425	1,309
	15.1	GFDL-ESM2G	r1i1p1	26	0,957	0,983	1,001	1,074	0,967	1,014	0,957	0,993	1,028	1,143	0,883	1,042
	15.1	GFDL-ESM2G	r1i1p1	45	0,961	0,999	1,029	1,138	0,922	1,035	0,897	0,961	1,018	1,182	0,801	1,070
	15.1	GFDL-ESM2G	r1i1p1	60	1,031	1,065	1,081	1,062	0,979	1,033	0,801	0,904	0,999	1,281	0,614	1,146
	15.1	GFDL-ESM2G	r1i1p1	85	1,041	1,074	1,102	1,217	0,975	1,041	0,701	0,850	0,991	1,381	0,499	1,210
	16.1	GFDL-ESM2M	r1i1p1	26	1,208	1,165	1,123	0,972	1,232	0,974	1,000	1,040	1,071	1,099	0,956	1,040
	16.1	GFDL-ESM2M	r1i1p1	45	1,110	1,126	1,126	1,026	1,071	1,017	0,938	0,994	1,035	1,071	0,848	1,061
	16.1	GFDL-ESM2M	r1i1p1	60	1,179	1,170	1,148	1,007	1,173	0,994	0,842	0,942	1,019	1,084	0,710	1,118
	16.1	GFDL-ESM2M	r1i1p1	85	1,111	1,147	1,159	1,082	1,076	1,026	0,862	0,931	0,986	1,057	0,764	1,085
	17.6	GISS-E2-R	r6i1p1	45	0,984	1,004	1,014	1,031	0,956	1,019	0,956	1,022	1,072	1,147	0,869	1,064
	18.1	HadGEM2-CC	r1i1p1	45	1,059	1,071	1,081	1,127	1,057	1,019	0,654	0,793	0,931	1,145	0,506	1,242
	18.1	HadGEM2-CC	r1i1p1	85	1,108	1,134	1,159	1,248	1,137	1,031	0,481	0,651	0,873	1,267	0,334	1,515
	18.2	HadGEM2-CC	r2i1p1	85	0,962	1,029	1,096	1,355	0,928	1,060	0,393	0,563	0,791	1,191	0,258	1,559
	18.3	HadGEM2-CC	r3i1p1	85	1,014	1,069	1,132	1,255	1,036	1,063	0,540	0,675	0,858	1,227	0,402	1,443
	19.1	HadGEM2-ES	r1i1p1	26	0,899	0,991	1,060	1,137	0,919	1,074	0,839	0,961	1,084	1,216	0,768	1,168
	19.2	HadGEM2-ES	r2i1p1	26	1,032	1,056	1,066	0,986	1,017	1,024	0,742	0,869	0,982	1,187	0,609	1,165
	19.3	HadGEM2-ES	r3i1p1	26	1,190	1,121	1,071	0,956	1,228	0,960	0,839	0,913	0,974	1,051	0,694	1,115
	19.4	HadGEM2-ES	r4i1p1	26	1,116	1,076	1,061	1,101	1,143	0,982	0,900	0,967	1,023	1,130	0,808	1,086
	19.1	HadGEM2-ES	r1i1p1	45	1,057	1,105	1,140	1,237	1,059	1,030	0,723	0,844	0,982	1,177	0,631	1,236
	19.2	HadGEM2-ES	r2i1p1	45	1,105	1,101	1,095	1,076	1,151	0,998	0,645	0,787	0,928	1,077	0,504	1,272
	19.3	HadGEM2-ES	r3i1p1	45	1,090	1,090	1,085	1,050	1,072	1,005	0,623	0,785	0,934	1,102	0,432	1,269
	19.4	HadGEM2-ES	r4i1p1	45	1,128	1,096	1,075	1,021	1,105	0,998	0,681	0,820	0,954	1,152	0,502	1,248
	19.1	HadGEM2-ES	r1i1p1	60	0,981	1,024	1,059	1,131	1,040	1,032	0,632	0,773	0,936	1,177	0,522	1,285
	19.2	HadGEM2-ES	r2i1p1	60	1,117	1,116	1,109	1,018	1,128	1,007	0,598	0,743	0,907	1,153	0,459	1,341
	19.3	HadGEM2-ES	r3i1p1	60	1,073	1,084	1,085	1,051	1,077	1,012	0,633	0,773	0,914	1,201	0,456	1,278
	19.4	HadGEM2-ES	r4i1p1	60	1,044	1,092	1,122	1,150	0,962	1,050	0,574	0,719	0,880	1,112	0,416	1,346
	19.1	HadGEM2-ES	r1i1p1	85	1,022	1,122	1,197	1,291	0,988	1,075	0,531	0,686	0,886	1,257	0,394	1,469
	19.2	HadGEM2-ES	r2i1p1	85	1,111	1,114	1,119	1,109	1,080	1,027	0,460	0,605	0,813	1,142	0,320	1,591
	19.3	HadGEM2-ES	r3i1p1	85	1,070	1,122	1,156	1,139	1,045	1,045	0,421	0,590	0,797	1,101	0,253	1,554
	19.4	HadGEM2-ES	r4i1p1	85	1,009	1,064	1,109	1,251	0,975	1,049	0,390	0,572	0,794	1,138	0,241	1,544
	20.1	inmcm4	r1i1p1	45	1,006	1,011	1,014	1,042	0,997	1,005	0,686	0,772	0,848	1,005	0,561	1,131
	20.1	inmcm4	r1i1p1	85	1,006	1,038	1,059	1,092	0,964	1,025	0,586	0,690	0,783	0,949	0,441	1,179
	21.1	IPSL-CM5A-LR	r1i1p1	26	1,087	1,068	1,055	1,052	1,120	0,983	1,152	1,133	1,122	1,127	1,216	0,978
	21.2	IPSL-CM5A-LR	r2i1p1	26	1,057	1,069	1,078	1,107	1,043	1,009	1,023	1,045	1,054	0,993	0,969	1,027
	21.3	IPSL-CM5A-LR	r3i1p1	26	1,015	1,055	1,083	1,146	0,980	1,028	1,075	1,098	1,117	1,165	1,042	1,027
	21.4	IPSL-CM5A-LR	r4i1p1	26	1,021	1,023	1,032	1,114	1,013	1,007	1,133	1,121	1,117	1,114	1,067	1,018
	21.1	IPSL-CM5A-LR	r1i1p1	45	1,096	1,070	1,056	1,084	1,083	0,990	1,019	1,029	1,038	1,055	1,001	1,010
	21.2	IPSL-CM5A-LR	r2i1p1	45	1,102	1,080	1,066	1,040	1,115	0,992	0,961	0,987	1,010	1,082	0,881	1,044
	21.3	IPSL-CM5A-LR	r3i1p1	45	1,041	1,047	1,054	1,118	1,027	1,008	1,004	1,056	1,099	1,182	0,894	1,062
	21.4	IPSL-CM5A-LR	r4i1p1	45	0,883	0,964	1,031	1,192	0,828	1,069	0,805	0,926	1,031	1,197	0,624	1,159
	21.1	IPSL-CM5A-LR	r1i1p1	60	1,083	1,067	1,054	1,054	1,087	0,992	0,969	1,022	1,064	1,126	0,886	1,059
	21.1	IPSL-CM5A-LR	r1i1p1	85	1,052	1,082	1,107	1,198	0,975	1,039	0,765	0,900	1,018	1,231	0,580	1,181
	21.2	IPSL-CM5A-LR	r2i1p1	85	1,107	1,137	1,157	1,206	1,065	1,025	0,803	0,902	0,994	1,274	0,633	1,137
	21.3	IPSL-CM5A-LR	r3i1p1	85	1,126	1,133	1,138	1,209	1,145	1,003	0,869	0,978	1,079	1,350	0,679	1,153
	21.4	IPSL-CM5A-LR	r4i1p1	85	1,011	1,065	1,113	1,319	0,956	1,048	0,841	0,946	1,047	1,383	0,644	1,149
	22.1	IPSL-CM5A-MR	r1i1p1	26	1,102	1,087	1,080	1,022	1,091	0,996	0,972	0,985	0,995	0,991	0,945	1,020
	22.1	IPSL-CM5A-MR	r1i1p1	45	1,044	1,057	1,063	1,058	1,022	1,016	0,918	0,961	0,989	0,965	0,810	1,065
	22.1	IPSL-CM5A-MR	r1i1p1	60	1,140	1,129	1,122	1,066	1,103	1,002	0,780	0,893	0,980	1,038	0,609	1,153
	22.1	IPSL-CM5A-MR	r1i1p1	85	1,189	1,196	1,201	1,164	1,152	1,006	0,574	0,714	0,851	1,027	0,386	1,297
	23.1	IPSL-CM5B-LR	r1i1p1	45	1,146	1,122	1,117	1,131	1,129	0,997	1,512	1,316	1,212	1,174	1,785	0,889
	23.1	IPSL-CM5B-LR	r1i1p1	85	1,175	1,174	1,180	1,279	1,113	1,019	1,158	1,162	1,178	1,278	1,063	1,025
	24.1	MIROC-ESM	r1i1p1	26	1,207	1,147	1,114	1,070	1,231	0,971	1,228	1,212	1,198	1,112	1,272	0,990
	24.1	MIROC-ESM	r1i1p1	45	1,227	1,213	1,197	1,121	1,246	0,987	1,144	1,197	1,233	1,217	1,035	1,058
	24.1	MIROC-ESM	r1i1p1	60	1,149	1,154	1,158	1,182	1,114	1,012	1,181	1,211	1,233	1,234	1,115	1,034
	24.1	MIROC-ESM	r1i1p1	85	1,143	1,171	1,187	1,199	1,086	1,028	1,098	1,208	1,297	1,443	0,886	1,109
	25.1	MIROC-ESM-CHEM	r1i1p1	26	1,198	1,141	1,096	0,984	1,239	0,967	1,231	1,218	1,204	1,134	1,216	1,003
	25.1	MIROC-ESM-CHEM	r1i1p1	45	1,154	1,115	1,084	1,017	1,129	0,991	1,156	1,158	1,173	1,321	1,089	1,022
	25.1	MIROC-ESM-CHEM	r1i1p1	60	1,130	1,135	1,132	1,104	1,091	1,010	1,143	1,182	1,211	1,231	1,005	1,059
	25.1	MIROC-ESM-CHEM	r1i1p1	85	1,124	1,113	1,111	1,196	1,068	1,014	1,096	1,177	1,244	1,377	0,890	1,105
	26.1	MIROC5	r1i1p1	26	1,189	1,155	1,128	1,051	1,178	0,988	1,081	1,141	1,189	1,245	0,986	1,062
	26.2	MIROC5	r2i1p1	26	1,170	1,140	1,126	1,093	1,180	0,992	1,170	1,163	1,158	1,156	1,203	0,990
	26.3	MIROC5	r3i1p1	26	1,156	1,099	1,069	1,054	1,182	0,983	0,929	1,010	1,073	1,116	0,845	1,081
	26.1	MIROC5	r1i1p1	45	1,129	1,128	1,128	1,111	1,103	1,011	1,123	1,155	1,180	1,206	1,086	1,031
	26.2	MIROC5	r2i1p1	45	1,211	1,157	1,129	1,111	1,182	0,990	1,127	1,133	1,137	1,140	1,079	1,015
	26.3	MIROC5	r3i1p1	45	1,099	1,077	1,073	1,145	1,088	1,001	0,984	1,077	1,146	1,175	0,836	1,100
	26.1	MIROC5	r1i1p1	60	1,128	1,109	1,092	1,044	1,115	0,997	1,033	1,111	1,174	1,320	0,944	1,071
	26.1	MIROC5	r1i1p1	85	1,283	1,254	1,229	1,155	1,278	0,990	0,905	1,078	1,226	1,382	0,724	1,164
	26.2	MIROC5	r2i1p1	85	1,244	1,227	1,216	1,185	1,207	1,001	1,088	1,169	1,235	1,327	0,916	1,096
	26.3	MIROC5	r3i1p1	85	1,032	1,050	1,063	1,105	1,041	1,014	0,809	0,964	1,095	1,280	0,614	1,179
	27.1	MPI-ESM-LR	r1i1p1	26	1,055	1,056	1,049	0,938	1,055	1,002	0,990	0,986	0,985	1,016	1,002	1,001
	27.2	MPI-ESM-LR	r2i1p1	26	1,139	1,094	1,054	0,920	1,218	0,972	0,861	0,932	0,994	1,098	0,773	1,085
	27.3	MPI-ESM-LR	r3i1p1	26	1,089	1,062	1,051	1,163	1,096	0,993	0,986	0,999	1,011	1,025	0,958	1,019

	27.1	MPI-ESM-LR	r1i1p1	45	1,036	1,054	1,065	1,074	1,023	1,018	0,807	0,888	0,957	1,074	0,712	1,115
	27.2	MPI-ESM-LR	r2i1p1	45	1,314	1,184	1,097	0,910	1,434	0,932	0,852	0,912	0,960	1,011	0,749	1,088
	27.3	MPI-ESM-LR	r3i1p1	45	1,271	1,152	1,079	1,013	1,271	0,955	0,921	0,946	0,968	0,980	0,803	1,063
	27.1	MPI-ESM-LR	r1i1p1	85	1,053	1,075	1,085	1,095	1,054	1,020	0,677	0,792	0,905	1,150	0,531	1,219
	27.2	MPI-ESM-LR	r2i1p1	85	1,293	1,224	1,164	0,976	1,384	0,971	0,721	0,845	0,967	1,150	0,571	1,207
	27.3	MPI-ESM-LR	r3i1p1	85	1,129	1,105	1,092	1,111	1,099	1,018	0,610	0,771	0,925	1,076	0,422	1,296
	28.1	MPI-ESM-MR	r1i1p1	26	1,119	1,087	1,071	1,107	1,184	0,974	0,930	0,978	1,013	1,056	0,845	1,056
	28.1	MPI-ESM-MR	r1i1p1	45	0,980	1,037	1,078	1,149	0,942	1,046	0,754	0,870	0,966	1,104	0,600	1,147
	28.2	MPI-ESM-MR	r2i1p1	45	1,147	1,106	1,076	0,996	1,177	0,982	0,778	0,894	0,992	1,159	0,614	1,157
	28.3	MPI-ESM-MR	r3i1p1	45	1,069	1,069	1,068	1,107	1,091	1,003	0,820	0,912	0,985	1,054	0,684	1,121
	28.1	MPI-ESM-MR	r1i1p1	85	0,929	1,019	1,084	1,205	0,846	1,079	0,574	0,748	0,914	1,194	0,354	1,302
	29.1	MRI-CGCM3	r1i1p1	26	1,110	1,098	1,088	1,027	1,133	0,989	0,989	1,030	1,058	1,053	0,929	1,044
	29.1	MRI-CGCM3	r1i1p1	45	1,158	1,093	1,059	1,080	1,187	0,968	0,967	1,028	1,073	1,091	0,875	1,062
	29.1	MRI-CGCM3	r1i1p1	60	1,077	1,056	1,040	1,009	1,090	0,989	0,900	0,989	1,059	1,109	0,765	1,101
	29.1	MRI-CGCM3	r1i1p1	85	1,227	1,177	1,148	1,151	1,279	0,972	1,054	1,092	1,123	1,165	0,993	1,043
	30.1	NorESM1-M	r1i1p1	26	1,062	1,051	1,038	0,974	1,075	0,994	1,003	1,054	1,097	1,175	0,927	1,052
	30.1	NorESM1-M	r1i1p1	45	1,090	1,088	1,080	1,020	1,093	0,999	0,794	0,925	1,034	1,177	0,635	1,151
	30.1	NorESM1-M	r1i1p1	60	1,109	1,107	1,097	1,030	1,115	1,000	0,841	0,953	1,044	1,167	0,687	1,129
	30.1	NorESM1-M	r1i1p1	85	1,139	1,148	1,152	1,131	1,096	1,012	0,815	0,965	1,087	1,219	0,620	1,175
	EC.1	EC-EARTH	r1i1p1	85	1,226	1,182	1,146	1,082	1,266	0,981	0,884	0,968	1,046	1,181	0,778	1,123
	EC.2	EC-EARTH	r2i1p1	85	1,267	1,200	1,155	1,112	1,342	0,962	0,875	0,990	1,088	1,218	0,741	1,141
	EC.3	EC-EARTH	r3i1p1	85	1,222	1,175	1,143	1,112	1,333	0,977	0,868	0,984	1,079	1,148	0,737	1,136
	EC.4	EC-EARTH	r4i1p1	85	1,168	1,181	1,188	1,185	1,191	1,012	0,868	0,964	1,046	1,162	0,722	1,137
	EC.5	EC-EARTH	r5i1p1	85	1,034	1,092	1,127	1,123	1,072	1,030	0,874	0,962	1,031	1,087	0,752	1,110
	EC.6	EC-EARTH	r6i1p1	85	1,331	1,232	1,172	1,111	1,513	0,945	0,863	0,973	1,063	1,172	0,740	1,125
	EC.7	EC-EARTH	r7i1p1	85	1,198	1,213	1,227	1,212	1,227	1,008	0,816	0,952	1,071	1,270	0,642	1,169
	EC.8	EC-EARTH	r8i1p1	85	1,279	1,227	1,186	1,118	1,285	0,984	0,881	0,975	1,053	1,147	0,748	1,129

Summary statistics

		Winter						Summer					
		P30	P60	P90	E	a	b	P30	P60	P90	E	a	b
Overall	Mean	1,115	1,114	1,113	1,112	1,111	1,008	0,809	0,908	1,003	1,151	0,689	1,171
	Coefficient of variation	0,080	0,059	0,052	0,074	0,101	0,026	0,251	0,166	0,101	0,075	0,373	0,115
	Minimum	0,883	0,964	1,001	0,910	0,828	0,932	0,390	0,563	0,783	0,949	0,241	0,889
	1th Quartile	1,048	1,070	1,076	1,052	1,041	0,992	0,661	0,792	0,928	1,086	0,490	1,065
	Median	1,111	1,105	1,103	1,111	1,103	1,007	0,807	0,913	0,995	1,147	0,660	1,143
	3rd Quartile	1,169	1,149	1,142	1,155	1,173	1,025	0,944	0,996	1,064	1,203	0,856	1,247
	Maximum	1,429	1,389	1,355	1,366	1,573	1,079	1,512	1,316	1,297	1,443	1,785	1,591
RCP 2.6	Mean	1,097	1,081	1,070	1,055	1,109	0,994	0,953	1,003	1,048	1,112	0,889	1,068
	Coefficient of variation	0,065	0,037	0,027	0,062	0,079	0,023	0,148	0,097	0,063	0,055	0,218	0,058
	Minimum	0,899	0,983	1,001	0,920	0,919	0,960	0,735	0,819	0,897	0,991	0,583	0,959
	1th Quartile	1,056	1,057	1,051	1,021	1,055	0,980	0,839	0,924	0,995	1,074	0,732	1,018
	Median	1,099	1,077	1,068	1,052	1,096	0,991	0,961	0,999	1,044	1,112	0,885	1,056
	3rd Quartile	1,137	1,099	1,087	1,107	1,180	1,007	1,023	1,052	1,083	1,147	1,022	1,119
	Maximum	1,225	1,165	1,128	1,203	1,281	1,074	1,231	1,218	1,204	1,263	1,272	1,189
RCP 4.5	Mean	1,099	1,095	1,093	1,096	1,098	1,006	0,845	0,930	1,009	1,128	0,737	1,135
	Coefficient of variation	0,078	0,048	0,036	0,058	0,094	0,024	0,220	0,138	0,083	0,060	0,349	0,086
	Minimum	0,883	0,964	1,014	0,910	0,828	0,932	0,535	0,705	0,848	0,965	0,392	0,889
	1th Quartile	1,036	1,061	1,068	1,042	1,027	0,992	0,706	0,826	0,957	1,081	0,557	1,063
	Median	1,096	1,092	1,085	1,111	1,091	1,005	0,807	0,916	0,992	1,132	0,694	1,121
	3rd Quartile	1,154	1,128	1,116	1,131	1,164	1,019	0,938	0,987	1,040	1,177	0,846	1,227
	Maximum	1,314	1,243	1,207	1,237	1,434	1,069	1,512	1,316	1,233	1,321	1,785	1,361
RCP 6.0	Mean	1,108	1,112	1,111	1,080	1,091	1,010	0,764	0,883	0,993	1,154	0,616	1,192
	Coefficient of variation	0,051	0,037	0,034	0,049	0,060	0,018	0,215	0,149	0,097	0,070	0,303	0,077
	Minimum	0,981	1,024	1,040	1,001	0,962	0,984	0,574	0,719	0,870	1,031	0,410	1,034
	1th Quartile	1,074	1,086	1,093	1,043	1,034	0,995	0,632	0,773	0,922	1,081	0,463	1,120
	Median	1,120	1,117	1,109	1,067	1,098	1,008	0,740	0,863	0,971	1,153	0,583	1,207
	3rd Quartile	1,148	1,129	1,125	1,118	1,140	1,028	0,858	0,949	1,038	1,211	0,704	1,265
	Maximum	1,248	1,247	1,240	1,182	1,241	1,050	1,181	1,211	1,233	1,320	1,115	1,346
RCP 8.5	Mean	1,142	1,153	1,162	1,180	1,129	1,020	0,697	0,831	0,970	1,198	0,537	1,267
	Coefficient of variation	0,094	0,067	0,052	0,063	0,129	0,028	0,290	0,203	0,129	0,083	0,406	0,118
	Minimum	0,929	1,019	1,059	0,976	0,846	0,945	0,390	0,563	0,783	0,949	0,241	1,007
	1th Quartile	1,052	1,088	1,121	1,113	1,037	1,006	0,526	0,690	0,873	1,142	0,363	1,141
	Median	1,139	1,155	1,156	1,185	1,118	1,019	0,671	0,806	0,931	1,191	0,493	1,219
	3rd Quartile	1,201	1,196	1,192	1,217	1,211	1,039	0,862	0,964	1,063	1,257	0,679	1,368
	Maximum	1,429	1,389	1,355	1,366	1,573	1,079	1,176	1,208	1,297	1,443	1,168	1,591

Meuse basin - Far Future (2071-2100)

Model info				Winter						Summer					
Index	GCM	Run	RCP	P30	P60	P90	E	a	b	P30	P60	P90	E	a	b
1.1	ACCESS1-0	r1i1p1	45	1,144	1,116	1,107	1,248	1,132	0,998	0,621	0,768	0,906	1,132	0,490	1,245
1.1	ACCESS1-0	r1i1p1	85	0,963	1,034	1,098	1,169	0,892	1,075	0,403	0,572	0,784	1,151	0,302	1,525
2.1	ACCESS1-3	r1i1p1	45	1,016	1,015	1,024	1,176	1,027	1,009	0,663	0,808	0,936	1,075	0,552	1,202
2.1	ACCESS1-3	r1i1p1	85	1,098	1,107	1,119	1,233	1,108	1,023	0,444	0,670	0,927	1,302	0,296	1,472
3.1	bcc-csm1-1	r1i1p1	26	1,017	1,023	1,023	0,963	0,983	1,014	1,079	1,062	1,049	1,028	1,099	0,987
3.1	bcc-csm1-1	r1i1p1	45	1,022	1,058	1,078	1,020	0,955	1,035	1,032	1,030	1,032	1,022	0,991	1,021
3.1	bcc-csm1-1	r1i1p1	60	1,106	1,097	1,083	1,002	1,099	0,998	0,759	0,880	0,975	1,016	0,582	1,165
3.1	bcc-csm1-1	r1i1p1	85	1,052	1,097	1,129	1,148	0,971	1,047	0,635	0,794	0,934	1,030	0,480	1,236
4.1	bcc-csm1-1-m	r1i1p1	26	1,035	1,068	1,093	1,146	1,004	1,027	0,757	0,862	0,955	1,060	0,653	1,129
4.1	bcc-csm1-1-m	r1i1p1	45	1,087	1,105	1,116	1,121	1,068	1,013	0,694	0,817	0,921	1,089	0,587	1,141
4.1	bcc-csm1-1-m	r1i1p1	60	1,082	1,118	1,140	1,118	1,047	1,028	0,620	0,757	0,869	0,994	0,496	1,211
4.1	bcc-csm1-1-m	r1i1p1	85	1,154	1,157	1,150	1,070	1,152	0,998	0,528	0,683	0,829	1,014	0,393	1,312
5.1	BNU-ESM	r1i1p1	26	1,092	1,072	1,065	1,189	1,109	0,985	1,002	1,021	1,041	1,092	0,902	1,051
5.1	BNU-ESM	r1i1p1	45	1,045	1,080	1,108	1,168	1,013	1,025	0,959	0,970	0,985	1,046	0,859	1,053
5.1	BNU-ESM	r1i1p1	85	1,062	1,104	1,132	1,105	0,994	1,039	0,796	0,907	1,001	1,177	0,655	1,134
6.1	CanESM2	r1i1p1	26	1,106	1,068	1,046	1,063	1,149	0,984	1,022	1,040	1,057	1,082	0,953	1,035
6.2	CanESM2	r2i1p1	26	1,167	1,127	1,100	1,109	1,250	0,970	1,035	1,049	1,071	1,079	1,056	1,020
6.3	CanESM2	r3i1p1	26	1,171	1,107	1,059	1,018	1,260	0,948	1,064	1,050	1,050	1,031	1,056	1,008
6.4	CanESM2	r4i1p1	26	1,147	1,121	1,099	1,027	1,227	0,972	0,954	0,987	1,024	1,144	0,921	1,046
6.5	CanESM2	r5i1p1	26	1,034	1,065	1,092	1,214	1,018	1,025	0,905	1,025	1,120	1,147	0,774	1,119
6.1	CanESM2	r1i1p1	45	1,115	1,096	1,085	1,083	1,140	1,002	0,739	0,888	1,024	1,145	0,575	1,202
6.2	CanESM2	r2i1p1	45	1,069	1,088	1,100	1,117	1,079	1,009	0,783	0,920	1,034	1,134	0,627	1,156
6.3	CanESM2	r3i1p1	45	1,071	1,084	1,093	1,064	1,088	1,005	0,882	0,916	0,965	1,025	0,839	1,080
6.4	CanESM2	r4i1p1	45	0,992	1,043	1,085	1,079	1,032	1,045	0,712	0,854	0,985	1,208	0,603	1,173
6.5	CanESM2	r5i1p1	45	1,003	1,047	1,089	1,224	1,027	1,037	0,818	0,922	1,013	1,081	0,706	1,129
6.1	CanESM2	r1i1p1	85	1,286	1,233	1,190	1,100	1,310	0,991	0,501	0,697	0,900	1,175	0,352	1,358
6.2	CanESM2	r2i1p1	85	1,256	1,250	1,249	1,272	1,280	1,016	0,453	0,670	0,902	1,216	0,282	1,420
6.3	CanESM2	r3i1p1	85	1,230	1,232	1,232	1,235	1,259	0,995	0,648	0,782	0,912	1,061	0,499	1,247
6.4	CanESM2	r4i1p1	85	1,167	1,197	1,227	1,341	1,165	1,030	0,621	0,768	0,920	1,272	0,507	1,232
6.5	CanESM2	r5i1p1	85	1,261	1,238	1,225	1,238	1,301	0,995	0,553	0,731	0,899	1,135	0,397	1,293
7.1	CCSM4	r1i1p1	26	1,062	1,032	1,013	1,050	1,118	0,968	0,884	0,953	1,006	1,017	0,803	1,074
7.2	CCSM4	r2i1p1	26	1,072	1,042	1,015	0,998	1,077	0,987	0,866	0,937	0,995	1,102	0,794	1,070
7.6	CCSM4	r6i1p1	26	1,048	1,029	1,007	0,897	1,079	0,984	0,887	0,941	0,986	1,085	0,841	1,048
7.1	CCSM4	r1i1p1	45	1,143	1,067	1,018	0,965	1,230	0,948	0,742	0,837	0,924	1,083	0,632	1,135
7.2	CCSM4	r2i1p1	45	1,061	1,079	1,092	1,173	1,056	1,014	0,822	0,950	1,051	1,167	0,707	1,116
7.6	CCSM4	r6i1p1	45	1,081	1,079	1,069	0,982	1,114	0,995	0,842	0,923	0,996	1,163	0,780	1,076
7.1	CCSM4	r1i1p1	60	1,081	1,047	1,023	1,009	1,113	0,976	0,734	0,879	0,992	1,082	0,573	1,169
7.2	CCSM4	r2i1p1	60	1,054	1,056	1,062	1,118	1,056	1,002	0,802	0,880	0,941	1,038	0,709	1,082
7.6	CCSM4	r6i1p1	60	1,028	1,057	1,078	1,066	0,992	1,027	0,844	0,918	0,977	1,097	0,749	1,077
7.1	CCSM4	r1i1p1	85	1,078	1,088	1,099	1,139	1,082	1,009	0,552	0,750	0,926	1,077	0,396	1,272
7.2	CCSM4	r2i1p1	85	1,056	1,100	1,138	1,256	1,010	1,040	0,608	0,787	0,947	1,197	0,462	1,220
7.6	CCSM4	r6i1p1	85	1,043	1,063	1,077	1,059	0,995	1,027	0,605	0,759	0,896	1,105	0,468	1,205
8.1	CMCC-CESM	r1i1p1	85	1,461	1,354	1,274	1,154	1,631	0,943	0,809	0,907	1,014	1,307	0,687	1,157
9.1	CMCC-CM	r1i1p1	45	0,853	0,917	0,977	1,089	0,832	1,056	0,640	0,832	0,994	1,099	0,489	1,236
9.1	CMCC-CM	r1i1p1	85	0,905	0,978	1,039	1,193	0,863	1,063	0,406	0,662	0,925	1,152	0,229	1,500
10.1	CMCC-CMS	r1i1p1	45	1,038	1,052	1,079	1,234	1,001	1,024	0,774	0,898	1,013	1,167	0,635	1,171
10.1	CMCC-CMS	r1i1p1	85	1,038	1,076	1,125	1,264	0,946	1,059	0,642	0,821	1,004	1,211	0,507	1,307
11.1	CNRM-CM5	r1i1p1	26	1,086	1,039	1,006	0,935	1,135	0,970	1,187	1,124	1,090	1,106	1,265	0,958
11.1	CNRM-CM5	r1i1p1	45	1,182	1,132	1,090	0,979	1,293	0,960	1,115	1,073	1,047	1,048	1,187	0,963
11.1	CNRM-CM5	r1i1p1	85	1,202	1,172	1,151	1,117	1,209	0,990	1,100	1,106	1,124	1,274	1,081	1,011
12.10	CSIRO-Mk3-6-0	r10i1p1	26	1,192	1,099	1,040	1,078	1,277	0,941	0,731	0,853	0,962	1,147	0,632	1,160
12.1	CSIRO-Mk3-6-0	r1i1p1	26	1,184	1,116	1,075	1,024	1,217	0,966	0,735	0,830	0,926	1,101	0,631	1,160
12.2	CSIRO-Mk3-6-0	r2i1p1	26	1,084	1,067	1,055	1,048	1,118	0,988	0,776	0,897	0,993	1,055	0,670	1,149
12.3	CSIRO-Mk3-6-0	r3i1p1	26	1,064	1,041	1,018	0,984	1,082	0,985	0,694	0,821	0,934	1,159	0,573	1,176
12.4	CSIRO-Mk3-6-0	r4i1p1	26	1,111	1,081	1,064	1,119	1,117	0,990	0,797	0,890	0,986	1,118	0,705	1,147
12.5	CSIRO-Mk3-6-0	r5i1p1	26	1,194	1,135	1,083	0,986	1,279	0,952	0,682	0,848	0,998	1,138	0,546	1,233
12.6	CSIRO-Mk3-6-0	r6i1p1	26	1,087	1,087	1,081	1,016	1,100	0,998	0,772	0,884	0,996	1,167	0,669	1,172
12.7	CSIRO-Mk3-6-0	r7i1p1	26	1,094	1,046	1,014	1,031	1,151	0,968	0,687	0,786	0,875	1,053	0,587	1,151
12.8	CSIRO-Mk3-6-0	r8i1p1	26	1,007	1,034	1,059	1,054	0,968	1,028	0,700	0,862	1,012	1,249	0,555	1,210
12.9	CSIRO-Mk3-6-0	r9i1p1	26	1,115	1,081	1,058	1,130	1,153	0,976	0,663	0,826	0,983	1,242	0,534	1,234
12.10	CSIRO-Mk3-6-0	r10i1p1	45	1,250	1,164	1,108	1,159	1,320	0,946	0,604	0,734	0,866	1,109	0,496	1,242
12.1	CSIRO-Mk3-6-0	r1i1p1	45	1,100	1,104	1,110	1,171	1,066	1,010	0,534	0,689	0,852	1,149	0,410	1,335
12.2	CSIRO-Mk3-6-0	r2i1p1	45	1,167	1,132	1,109	1,107	1,216	0,973	0,669	0,830	0,973	1,132	0,529	1,228
12.3	CSIRO-Mk3-6-0	r3i1p1	45	1,226	1,141	1,083	1,053	1,321	0,942	0,663	0,790	0,912	1,087	0,540	1,216
12.4	CSIRO-Mk3-6-0	r4i1p1	45	1,202	1,174	1,149	1,131	1,192	0,995	0,620	0,758	0,908	1,143	0,489	1,284
12.5	CSIRO-Mk3-6-0	r5i1p1	45	1,117	1,100	1,082	1,116	1,178	0,985	0,640	0,785	0,933	1,050	0,538	1,280
12.6	CSIRO-Mk3-6-0	r6i1p1	45	1,107	1,110	1,117	1,131	1,101	1,006	0,651	0,773	0,910	1,137	0,546	1,264
12.7	CSIRO-Mk3-6-0	r7i1p1	45	1,099	1,088	1,084	1,152	1,131	0,994	0,585	0,751	0,917	1,143	0,451	1,291
12.8	CSIRO-Mk3-6-0	r8i1p1	45	1,095	1,083	1,078	1,107	1,085	1,008	0,515	0,709	0,918	1,208	0,391	1,351
12.9	CSIRO-Mk3-6-0	r9i1p1	45	1,113	1,075	1,044	1,059	1,144	0,978	0,477	0,656	0,851	1,225	0,375	1,373
12.10	CSIRO-Mk3-6-0	r10i1p1	60	1,152	1,114	1,087	1,119	1,175	0,979	0,692	0,814	0,936	1,186	0,586	1,192
12.1	CSIRO-Mk3-6-0	r1i1p1	60	1,114	1,110	1,108	1,083	1,110	1,001	0,575	0,714	0,862	1,124	0,471	1,274
12.2	CSIRO-Mk3-6-0	r2i1p1	60	1,166	1,120	1,088	1,080	1,233	0,966	0,660	0,784	0,907	1,172	0,530	1,210
12.3	CSIRO-Mk3-6-0	r3i1p1	60	1,205	1,158	1,116	1,009	1,240	0,972	0,500	0,682	0,859	1,108	0,386	1,324
12.4	CSIRO-Mk3-6-0	r4i1p1	60	1,109	1,115	1,120	1,123	1,110	1,014	0,616	0,768	0,923	1,172	0,507	1,256
12.5	CSIRO-Mk3-6-0	r5i1p1	60	1,161	1,125	1,094	1,040	1,221	0,974	0,521	0,716	0,909	1,028	0,391	1,364
12.6	CSIRO-Mk3-6-0	r6i1p1	60	1,024	1,043	1,057	1,054	1,010	1,020	0,529	0,699	0,868	1,117	0,409	1,315
12.7	CSIRO-Mk3-6-0	r7i1p1	60	1,095	1,083	1,073	1,096	1,105	0,993	0,588	0,742	0,895	1,076	0,447	1,296
12.8	CSIRO-Mk3-6-0	r8i1p1	60	1,156	1,147	1,135	1,044	1,145	1,001	0,526	0,723	0,922	1,180	0,381	1,346
12.9	CSIRO-Mk3-6-0	r9i1p1	60	1,146	1,095	1,055	1,042	1,184	0,971	0,605	0,763	0,915	1,204	0,475	1,247
12.10	CSIRO-Mk3-6-0	r10i1p1	85	1,172	1,136	1,109	1,111	1,196	0,978	0,489	0,640	0,797	1,021	0,374	1,369
12.1	CSIRO-Mk3-6-0	r1i1p1	85	1,250	1,191	1,149	1,123	1,247	0,979	0,426	0,590	0,782	1,140	0,303	1,445
12.2	CSIRO-Mk3-6-0	r2i1p1	85	1,174	1,156	1,141	1,111	1,177	0,994	0,493	0,670	0,869	1,152	0,380	1,390

	12.3	CSIRO-Mk3-6-0	r3i1p1	85	1,159	1,137	1,116	1,046	1,148	0,998	0,423	0,631	0,858	1,196	0,278	1,460
	12.4	CSIRO-Mk3-6-0	r4i1p1	85	1,174	1,156	1,137	1,131	1,210	0,997	0,399	0,578	0,792	1,178	0,258	1,530
	12.5	CSIRO-Mk3-6-0	r5i1p1	85	1,246	1,191	1,148	1,056	1,293	0,970	0,525	0,672	0,843	1,032	0,412	1,405
	12.6	CSIRO-Mk3-6-0	r6i1p1	85	1,100	1,122	1,144	1,186	1,080	1,023	0,406	0,591	0,804	1,156	0,281	1,482
	12.7	CSIRO-Mk3-6-0	r7i1p1	85	1,218	1,139	1,079	1,022	1,287	0,953	0,443	0,603	0,783	0,999	0,334	1,430
	12.8	CSIRO-Mk3-6-0	r8i1p1	85	1,285	1,204	1,153	1,226	1,348	0,959	0,479	0,651	0,863	1,228	0,361	1,465
	12.9	CSIRO-Mk3-6-0	r9i1p1	85	1,212	1,165	1,128	1,115	1,232	0,979	0,388	0,577	0,808	1,166	0,270	1,554
	13.1	FGOALS-s2	r1i1p1	26	1,265	1,200	1,156	1,104	1,356	0,958	1,048	1,082	1,111	1,170	1,017	1,030
	13.1	FGOALS-s2	r1i1p1	45	1,420	1,325	1,245	1,042	1,498	0,954	0,623	0,865	1,086	1,166	0,440	1,311
	13.2	FGOALS-s2	r2i1p1	45	1,236	1,202	1,179	1,102	1,251	0,999	0,661	0,864	1,049	1,184	0,498	1,263
	13.3	FGOALS-s2	r3i1p1	45	1,295	1,230	1,188	1,133	1,350	0,979	1,035	1,060	1,108	1,110	0,933	1,095
	13.1	FGOALS-s2	r1i1p1	60	1,344	1,318	1,286	1,135	1,332	1,002	0,708	0,906	1,094	1,227	0,539	1,281
	13.1	FGOALS-s2	r1i1p1	85	1,296	1,316	1,316	1,117	1,255	1,034	0,607	0,837	1,066	1,205	0,415	1,376
	13.2	FGOALS-s2	r2i1p1	85	1,541	1,436	1,356	1,114	1,632	0,983	0,581	0,771	0,998	1,154	0,417	1,441
	13.3	FGOALS-s2	r3i1p1	85	1,479	1,433	1,413	1,382	1,433	1,019	0,739	0,818	0,926	1,139	0,607	1,263
	14.1	GFDL-CM3	r1i1p1	26	1,080	1,077	1,076	1,089	1,061	1,003	0,808	0,942	1,053	1,192	0,658	1,149
	14.1	GFDL-CM3	r1i1p1	60	1,062	1,082	1,105	1,204	1,026	1,026	0,686	0,887	1,074	1,262	0,519	1,270
	14.1	GFDL-CM3	r1i1p1	85	1,017	1,095	1,163	1,295	0,922	1,072	0,507	0,728	0,963	1,247	0,347	1,400
	15.1	GFDL-ESM2G	r1i1p1	26	0,997	1,010	1,023	1,080	0,988	1,014	0,888	0,944	0,993	1,086	0,815	1,059
	15.1	GFDL-ESM2G	r1i1p1	45	0,994	1,012	1,028	1,133	0,973	1,019	0,823	0,899	0,966	1,151	0,739	1,082
	15.1	GFDL-ESM2G	r1i1p1	60	1,045	1,072	1,092	1,101	1,008	1,030	0,745	0,857	0,962	1,206	0,607	1,147
	15.1	GFDL-ESM2G	r1i1p1	85	1,023	1,065	1,099	1,155	0,964	1,046	0,570	0,746	0,917	1,304	0,419	1,253
	16.1	GFDL-ESM2M	r1i1p1	26	1,253	1,194	1,138	0,942	1,308	0,966	0,976	1,011	1,038	1,063	0,926	1,045
	16.1	GFDL-ESM2M	r1i1p1	45	1,147	1,150	1,140	0,999	1,132	1,008	0,925	0,972	1,004	1,013	0,843	1,059
	16.1	GFDL-ESM2M	r1i1p1	60	1,184	1,180	1,167	1,018	1,156	1,006	0,757	0,869	0,960	1,026	0,632	1,144
	16.1	GFDL-ESM2M	r1i1p1	85	1,175	1,178	1,175	1,098	1,144	1,012	0,779	0,867	0,951	1,060	0,682	1,117
	17.6	GISS-E2-R	r6i1p1	45	0,973	0,999	1,016	0,984	0,927	1,031	0,893	0,975	1,036	1,062	0,815	1,075
	18.1	HadGEM2-CC	r1i1p1	45	1,039	1,053	1,060	1,033	1,046	1,022	0,559	0,760	0,950	1,144	0,412	1,318
	18.1	HadGEM2-CC	r1i1p1	85	1,048	1,087	1,125	1,200	1,045	1,047	0,399	0,582	0,827	1,192	0,288	1,617
	18.2	HadGEM2-CC	r2i1p1	85	0,815	0,955	1,106	1,615	0,688	1,143	0,354	0,536	0,775	1,189	0,240	1,584
	18.3	HadGEM2-CC	r3i1p1	85	0,916	1,054	1,189	1,303	0,825	1,141	0,518	0,651	0,840	1,119	0,438	1,476
	19.1	HadGEM2-ES	r1i1p1	26	0,903	1,013	1,111	1,126	0,802	1,124	0,850	0,958	1,070	1,205	0,814	1,134
	19.2	HadGEM2-ES	r2i1p1	26	0,918	0,980	1,032	1,055	0,864	1,065	0,658	0,800	0,934	1,210	0,520	1,215
	19.3	HadGEM2-ES	r3i1p1	26	1,106	1,069	1,037	0,957	1,136	0,976	0,766	0,813	0,862	0,974	0,697	1,083
	19.4	HadGEM2-ES	r4i1p1	26	1,088	1,068	1,068	1,223	1,130	0,983	0,986	0,999	1,021	1,062	0,964	1,033
	19.1	HadGEM2-ES	r1i1p1	45	1,036	1,095	1,151	1,296	0,965	1,056	0,699	0,834	0,966	1,104	0,612	1,216
	19.2	HadGEM2-ES	r2i1p1	45	1,059	1,074	1,084	1,109	1,030	1,023	0,592	0,756	0,917	1,125	0,466	1,305
	19.3	HadGEM2-ES	r3i1p1	45	1,015	1,057	1,092	1,120	0,982	1,031	0,520	0,698	0,857	1,012	0,376	1,283
	19.4	HadGEM2-ES	r4i1p1	45	1,069	1,075	1,076	1,074	1,067	1,008	0,729	0,852	0,971	1,113	0,602	1,224
	19.1	HadGEM2-ES	r1i1p1	60	0,957	1,019	1,072	1,206	0,906	1,062	0,625	0,780	0,946	1,173	0,529	1,294
	19.2	HadGEM2-ES	r2i1p1	60	1,054	1,099	1,124	1,059	1,018	1,038	0,565	0,705	0,861	1,130	0,479	1,321
	19.3	HadGEM2-ES	r3i1p1	60	1,009	1,060	1,099	1,075	0,966	1,040	0,581	0,740	0,882	1,039	0,433	1,289
	19.4	HadGEM2-ES	r4i1p1	60	1,043	1,066	1,089	1,197	0,982	1,033	0,589	0,730	0,881	1,069	0,475	1,348
	19.1	HadGEM2-ES	r1i1p1	85	0,945	1,065	1,173	1,300	0,821	1,110	0,507	0,679	0,882	1,164	0,384	1,468
	19.2	HadGEM2-ES	r2i1p1	85	0,986	1,066	1,142	1,249	0,915	1,072	0,411	0,573	0,806	1,175	0,292	1,674
	19.3	HadGEM2-ES	r3i1p1	85	0,941	1,046	1,137	1,238	0,868	1,095	0,346	0,529	0,748	1,025	0,227	1,600
	19.4	HadGEM2-ES	r4i1p1	85	0,988	1,061	1,136	1,388	0,904	1,068	0,366	0,555	0,773	1,021	0,238	1,565
	20.1	inmcm4	r1i1p1	45	1,010	1,005	1,003	1,004	0,998	1,004	0,684	0,753	0,811	0,895	0,592	1,100
	20.1	inmcm4	r1i1p1	85	0,999	1,032	1,061	1,108	0,933	1,036	0,582	0,686	0,783	0,935	0,468	1,171
	21.1	IPSL-CM5A-LR	r1i1p1	26	1,045	1,049	1,050	1,069	1,046	0,999	1,078	1,095	1,102	1,126	1,128	0,996
	21.2	IPSL-CM5A-LR	r2i1p1	26	1,054	1,060	1,064	1,020	1,011	1,014	0,984	1,031	1,058	1,010	0,939	1,039
	21.3	IPSL-CM5A-LR	r3i1p1	26	1,042	1,074	1,105	1,135	0,977	1,033	1,028	1,053	1,087	1,158	0,979	1,044
	21.4	IPSL-CM5A-LR	r4i1p1	26	1,048	1,047	1,048	1,072	1,043	0,998	1,131	1,099	1,081	1,106	1,156	0,979
	21.1	IPSL-CM5A-LR	r1i1p1	45	1,078	1,080	1,085	1,134	1,032	1,012	0,914	0,970	1,008	1,064	0,862	1,049
	21.2	IPSL-CM5A-LR	r2i1p1	45	1,129	1,103	1,082	1,004	1,134	0,985	0,963	0,994	1,019	1,091	0,890	1,040
	21.3	IPSL-CM5A-LR	r3i1p1	45	1,049	1,067	1,082	1,168	1,027	1,017	0,931	1,030	1,110	1,178	0,814	1,093
	21.4	IPSL-CM5A-LR	r4i1p1	45	0,884	0,968	1,038	1,072	0,796	1,078	0,736	0,875	0,994	1,171	0,587	1,171
	21.1	IPSL-CM5A-LR	r1i1p1	60	1,023	1,053	1,071	1,063	0,980	1,028	0,839	0,957	1,047	1,111	0,714	1,121
	21.1	IPSL-CM5A-LR	r1i1p1	85	1,064	1,096	1,132	1,281	0,975	1,042	0,695	0,849	0,986	1,161	0,530	1,207
	21.2	IPSL-CM5A-LR	r2i1p1	85	1,117	1,150	1,170	1,160	1,101	1,017	0,714	0,851	0,977	1,249	0,558	1,168
	21.3	IPSL-CM5A-LR	r3i1p1	85	1,165	1,156	1,155	1,205	1,186	0,995	0,771	0,901	1,030	1,328	0,624	1,179
	21.4	IPSL-CM5A-LR	r4i1p1	85	1,052	1,103	1,147	1,310	0,989	1,039	0,791	0,884	0,981	1,368	0,651	1,140
	22.1	IPSL-CM5A-MR	r1i1p1	26	1,059	1,086	1,114	1,039	1,010	1,029	1,006	1,027	1,050	1,067	0,953	1,038
	22.1	IPSL-CM5A-MR	r1i1p1	45	1,044	1,040	1,039	1,093	1,045	1,007	0,881	0,941	0,989	1,042	0,778	1,080
	22.1	IPSL-CM5A-MR	r1i1p1	60	1,128	1,134	1,142	1,130	1,090	1,015	0,698	0,855	0,982	1,052	0,517	1,202
	22.1	IPSL-CM5A-MR	r1i1p1	85	1,194	1,212	1,228	1,216	1,169	1,010	0,556	0,687	0,827	1,087	0,388	1,324
	23.1	IPSL-CM5B-LR	r1i1p1	45	1,070	1,106	1,141	1,140	1,018	1,036	1,476	1,292	1,196	1,118	1,683	0,897
	23.1	IPSL-CM5B-LR	r1i1p1	85	1,063	1,121	1,176	1,357	0,993	1,048	1,000	1,101	1,174	1,241	0,870	1,086
	24.1	MIROC-ESM	r1i1p1	26	1,168	1,138	1,114	1,070	1,207	0,978	1,131	1,192	1,222	1,177	1,072	1,043
	24.1	MIROC-ESM	r1i1p1	45	1,180	1,190	1,185	1,049	1,176	1,003	1,114	1,186	1,234	1,250	1,003	1,065
	24.1	MIROC-ESM	r1i1p1	60	1,117	1,123	1,124	1,096	1,090	1,011	1,080	1,157	1,214	1,281	0,980	1,067
	24.1	MIROC-ESM	r1i1p1	85	1,121	1,165	1,198	1,160	1,017	1,048	1,027	1,181	1,298	1,397	0,842	1,124
	25.1	MIROC-ESM-CHEM	r1i1p1	26	1,176	1,114	1,061	0,947	1,230	0,960	1,220	1,198	1,175	1,097	1,244	0,986
	25.1	MIROC-ESM-CHEM	r1i1p1	45	1,141	1,111	1,080	0,996	1,134	0,985	1,192	1,177	1,175	1,289	1,198	0,994
	25.1	MIROC-ESM-CHEM	r1i1p1	60	1,123	1,110	1,098	1,092	1,103	0,994	1,224	1,221	1,211	1,166	1,195	1,004
	25.1	MIROC-ESM-CHEM	r1i1p1	85	1,092	1,090	1,095	1,188	1,058	1,006	1,090	1,176	1,241	1,361	0,943	1,085
	26.1	MIROC5	r1i1p1	26	1,130	1,115	1,101	1,039	1,173	0,987	0,947	1,046	1,132	1,194	0,841	1,099
	26.2	MIROC5	r2i1p1	26	1,208	1,135	1,093	1,069	1,269	0,959	1,126	1,097	1,098	1,182	1,179	0,981
	26.3	MIROC5	r3i1p1	26	1,112	1,089	1,067	0,970	1,090	0,996	0,848	0,962	1,055	1,143	0,719	1,118
	26.1	MIROC5	r1i1p1	45	1,062	1,070	1,076	1,082	1,059	1,014	0,927	1,026	1,110	1,246	0,838	1,098
	26.2	MIROC5	r2i1p1	45	1,200	1,126	1,086	1,132	1,220	0,967	1,063	1,106	1,135	1,151	1,021	1,031
	26.3	MIROC5	r3i1p1	45	1,105	1,063	1,036	1,123	1,071	0,986	0,845	0,973	1,080	1,214	0,689	1,149
	26.1	MIROC5	r1i1p1	60	1,068	1,049	1,033	0,995	1,107	0,987	0,818	0,970	1,108	1,305	0,667	1,166
	26.1	MIROC5	r1i1p1	85	1,181	1,179	1,168	1,090	1,212	0,999	0,750	0,977	1,182	1,456	0,590	1,227
	26.2	MIROC5	r2i1p1	85	1,215	1,189	1,171	1,133	1,248	0,982	0,989	1,082	1,183	1,345	0,865	1,120
	26.3	MIROC5	r3i1p1	85	0,994	1,015	1,033	1,042	0,943	1,027	0,726	0,909	1,068	1,242	0,561	1,198
	27.1	MPI-ESM-LR	r1i1p1	26	1,039	1,044	1,042	0,936	1,037	1,011	1,052	1,049	1,053	1,055	1,070	0,999
	27.2	MPI-ESM-LR	r2i1p1	26	1,135	1,101	1,067	0,927	1,197	0,975	0,753	0,872	0,969	1,050	0,665	1,135
	27.3	MPI-ESM-LR	r3i1p1	26	1,106	1,042	1,022	1,179	1,152	0,979	1,013	0,982	0,970	0,985	1,057	0,985

	27.1	MPI-ESM-LR	r1i1p1	45	0,966	0,990	1,014	1,109	0,975	1,024	0,809	0,908	0,999	1,116	0,736	1,128
	27.2	MPI-ESM-LR	r2i1p1	45	1,220	1,132	1,060	0,869	1,359	0,934	0,746	0,872	0,965	1,001	0,627	1,152
	27.3	MPI-ESM-LR	r3i1p1	45	1,181	1,086	1,033	1,013	1,223	0,955	0,880	0,908	0,934	0,984	0,820	1,047
	27.1	MPI-ESM-LR	r1i1p1	85	1,080	1,080	1,084	1,151	1,076	1,010	0,616	0,772	0,929	1,204	0,488	1,296
	27.2	MPI-ESM-LR	r2i1p1	85	1,310	1,230	1,177	1,018	1,382	0,978	0,630	0,797	0,954	1,104	0,503	1,265
	27.3	MPI-ESM-LR	r3i1p1	85	1,100	1,074	1,072	1,140	1,100	1,012	0,538	0,701	0,867	1,053	0,425	1,322
	28.1	MPI-ESM-MR	r1i1p1	26	1,094	1,083	1,075	1,132	1,143	0,984	0,959	1,011	1,048	1,056	0,898	1,049
	28.1	MPI-ESM-MR	r1i1p1	45	0,974	1,053	1,114	1,123	0,895	1,066	0,726	0,883	1,008	1,053	0,561	1,181
	28.2	MPI-ESM-MR	r2i1p1	45	1,032	1,038	1,037	1,031	1,065	1,006	0,717	0,838	0,951	1,180	0,601	1,162
	28.3	MPI-ESM-MR	r3i1p1	45	0,997	1,027	1,052	1,114	1,010	1,022	0,793	0,879	0,951	0,994	0,688	1,119
	28.1	MPI-ESM-MR	r1i1p1	85	0,967	1,035	1,096	1,239	0,884	1,061	0,493	0,702	0,897	1,137	0,330	1,325
	29.1	MRI-CGCM3	r1i1p1	26	0,968	0,955	0,948	0,947	0,999	0,989	0,900	0,939	0,965	0,974	0,819	1,057
	29.1	MRI-CGCM3	r1i1p1	45	0,994	0,955	0,935	1,069	1,064	0,967	0,850	0,934	1,002	1,098	0,747	1,092
	29.1	MRI-CGCM3	r1i1p1	60	0,923	0,908	0,903	0,976	0,938	0,992	0,789	0,878	0,955	1,094	0,678	1,107
	29.1	MRI-CGCM3	r1i1p1	85	1,031	1,005	0,990	1,114	1,108	0,976	0,898	0,951	0,999	1,146	0,849	1,055
	30.1	NorESM1-M	r1i1p1	26	1,019	1,027	1,023	0,923	1,029	1,005	0,975	1,019	1,052	1,134	0,931	1,041
	30.1	NorESM1-M	r1i1p1	45	1,125	1,118	1,103	1,018	1,143	0,994	0,721	0,868	0,992	1,173	0,591	1,170
	30.1	NorESM1-M	r1i1p1	60	1,094	1,090	1,083	1,016	1,123	1,000	0,704	0,854	0,987	1,186	0,577	1,175
	30.1	NorESM1-M	r1i1p1	85	1,109	1,139	1,156	1,119	1,086	1,022	0,683	0,856	1,009	1,169	0,534	1,210
	EC.1	EC-EARTH	r1i1p1	85	1,194	1,152	1,119	1,053	1,267	0,969	0,754	0,872	0,985	1,186	0,648	1,190
	EC.2	EC-EARTH	r2i1p1	85	1,233	1,199	1,171	1,136	1,261	0,981	0,742	0,908	1,064	1,302	0,596	1,214
	EC.3	EC-EARTH	r3i1p1	85	1,244	1,177	1,140	1,173	1,373	0,970	0,772	0,919	1,054	1,206	0,642	1,198
	EC.4	EC-EARTH	r4i1p1	85	1,078	1,111	1,148	1,264	1,051	1,043	0,699	0,855	0,996	1,136	0,550	1,252
	EC.5	EC-EARTH	r5i1p1	85	1,048	1,116	1,158	1,099	1,000	1,046	0,737	0,877	0,995	1,148	0,619	1,167
	EC.6	EC-EARTH	r6i1p1	85	1,238	1,175	1,132	1,154	1,354	0,961	0,711	0,871	1,006	1,166	0,560	1,204
	EC.7	EC-EARTH	r7i1p1	85	1,146	1,213	1,259	1,206	1,083	1,045	0,674	0,836	0,976	1,202	0,522	1,216
	EC.8	EC-EARTH	r8i1p1	85	1,275	1,218	1,172	1,054	1,300	0,974	0,840	0,921	0,997	1,120	0,755	1,121

Summary statistics

		Winter						Summer					
		P30	P60	P90	E	a	b	P30	P60	P90	E	a	b
Overall	Mean	1,105	1,102	1,103	1,109	1,107	1,007	0,747	0,864	0,978	1,135	0,642	1,198
	Coefficient of variation	0,096	0,070	0,062	0,090	0,130	0,036	0,276	0,175	0,104	0,078	0,385	0,122
	Minimum	0,815	0,908	0,903	0,869	0,688	0,934	0,346	0,529	0,748	0,895	0,227	0,897
	1th Quartile	1,043	1,057	1,063	1,045	1,010	0,982	0,605	0,759	0,916	1,072	0,473	1,084
	Median	1,094	1,090	1,093	1,107	1,100	1,003	0,731	0,865	0,981	1,137	0,592	1,172
	3rd Quartile	1,168	1,136	1,139	1,155	1,197	1,027	0,883	0,958	1,044	1,183	0,814	1,282
	Maximum	1,541	1,436	1,413	1,615	1,632	1,143	1,476	1,292	1,298	1,456	1,683	1,674
RCP 2.6	Mean	1,091	1,073	1,061	1,046	1,112	0,992	0,913	0,973	1,028	1,106	0,854	1,080
	Coefficient of variation	0,070	0,045	0,037	0,078	0,104	0,032	0,167	0,107	0,069	0,062	0,240	0,069
	Minimum	0,903	0,955	0,948	0,897	0,802	0,941	0,658	0,786	0,862	0,974	0,520	0,958
	1th Quartile	1,046	1,042	1,033	0,985	1,031	0,971	0,773	0,886	0,986	1,057	0,669	1,034
	Median	1,088	1,069	1,063	1,049	1,118	0,985	0,926	0,985	1,040	1,102	0,841	1,054
	3rd Quartile	1,134	1,101	1,090	1,100	1,191	1,005	1,027	1,048	1,067	1,155	1,008	1,144
	Maximum	1,265	1,200	1,156	1,223	1,356	1,124	1,220	1,198	1,222	1,249	1,265	1,234
RCP 4.5	Mean	1,090	1,085	1,083	1,093	1,097	1,004	0,786	0,892	0,990	1,115	0,686	1,158
	Coefficient of variation	0,090	0,061	0,048	0,070	0,119	0,031	0,239	0,144	0,086	0,067	0,344	0,090
	Minimum	0,853	0,917	0,935	0,869	0,796	0,934	0,477	0,656	0,811	0,895	0,375	0,897
	1th Quartile	1,032	1,053	1,052	1,042	1,027	0,985	0,661	0,808	0,933	1,064	0,538	1,080
	Median	1,078	1,080	1,084	1,107	1,068	1,007	0,742	0,879	0,989	1,118	0,627	1,152
	3rd Quartile	1,143	1,111	1,108	1,133	1,144	1,022	0,882	0,970	1,032	1,166	0,815	1,236
	Maximum	1,420	1,325	1,245	1,296	1,498	1,078	1,476	1,292	1,234	1,289	1,683	1,373
RCP 6.0	Mean	1,095	1,095	1,094	1,079	1,089	1,006	0,699	0,836	0,964	1,131	0,574	1,215
	Coefficient of variation	0,073	0,060	0,054	0,056	0,090	0,024	0,228	0,151	0,099	0,072	0,302	0,079
	Minimum	0,923	0,908	0,903	0,976	0,906	0,966	0,500	0,682	0,859	0,994	0,381	1,004
	1th Quartile	1,047	1,058	1,072	1,041	1,012	0,992	0,588	0,741	0,898	1,071	0,475	1,152
	Median	1,095	1,096	1,091	1,078	1,101	1,002	0,689	0,834	0,944	1,121	0,530	1,211
	3rd Quartile	1,142	1,120	1,119	1,118	1,140	1,027	0,759	0,880	0,986	1,185	0,626	1,293
	Maximum	1,344	1,318	1,286	1,206	1,332	1,062	1,224	1,221	1,214	1,305	1,195	1,364
RCP 8.5	Mean	1,131	1,141	1,153	1,181	1,118	1,021	0,617	0,774	0,938	1,176	0,483	1,311
	Coefficient of variation	0,119	0,081	0,061	0,088	0,166	0,041	0,297	0,201	0,128	0,087	0,389	0,119
	Minimum	0,815	0,955	0,990	1,018	0,688	0,943	0,346	0,529	0,748	0,935	0,227	1,011
	1th Quartile	1,048	1,080	1,119	1,114	0,989	0,991	0,489	0,670	0,843	1,135	0,347	1,198
	Median	1,117	1,137	1,144	1,155	1,101	1,017	0,605	0,768	0,926	1,169	0,462	1,272
	3rd Quartile	1,215	1,189	1,173	1,238	1,248	1,046	0,737	0,871	0,999	1,228	0,590	1,441
	Maximum	1,541	1,436	1,413	1,615	1,632	1,143	1,100	1,181	1,298	1,456	1,081	1,674

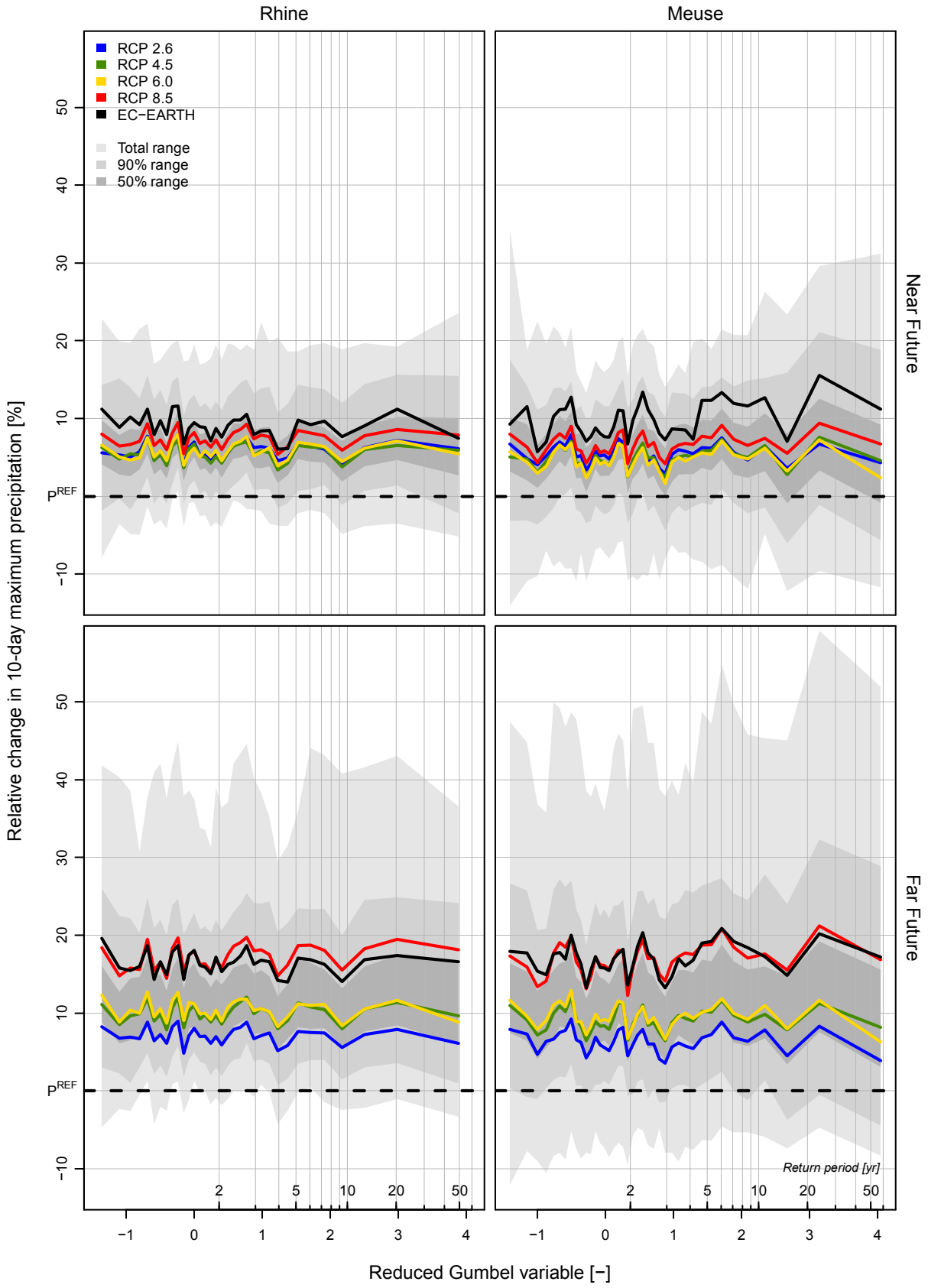

Figure B.1: Basin-averaged equivalent of Figure 19.

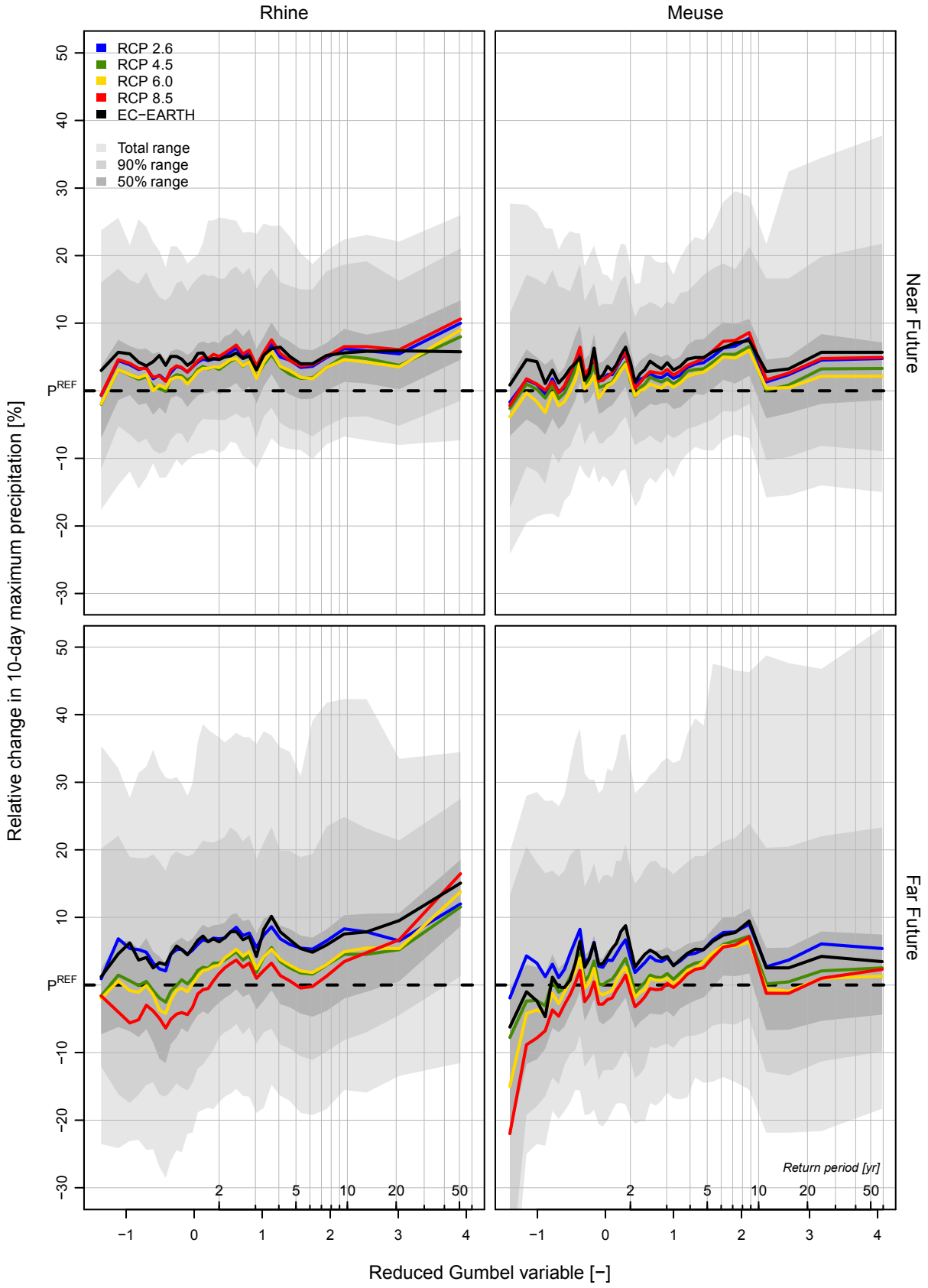

Figure B.2: Basin-averaged equivalent of Figure 21.

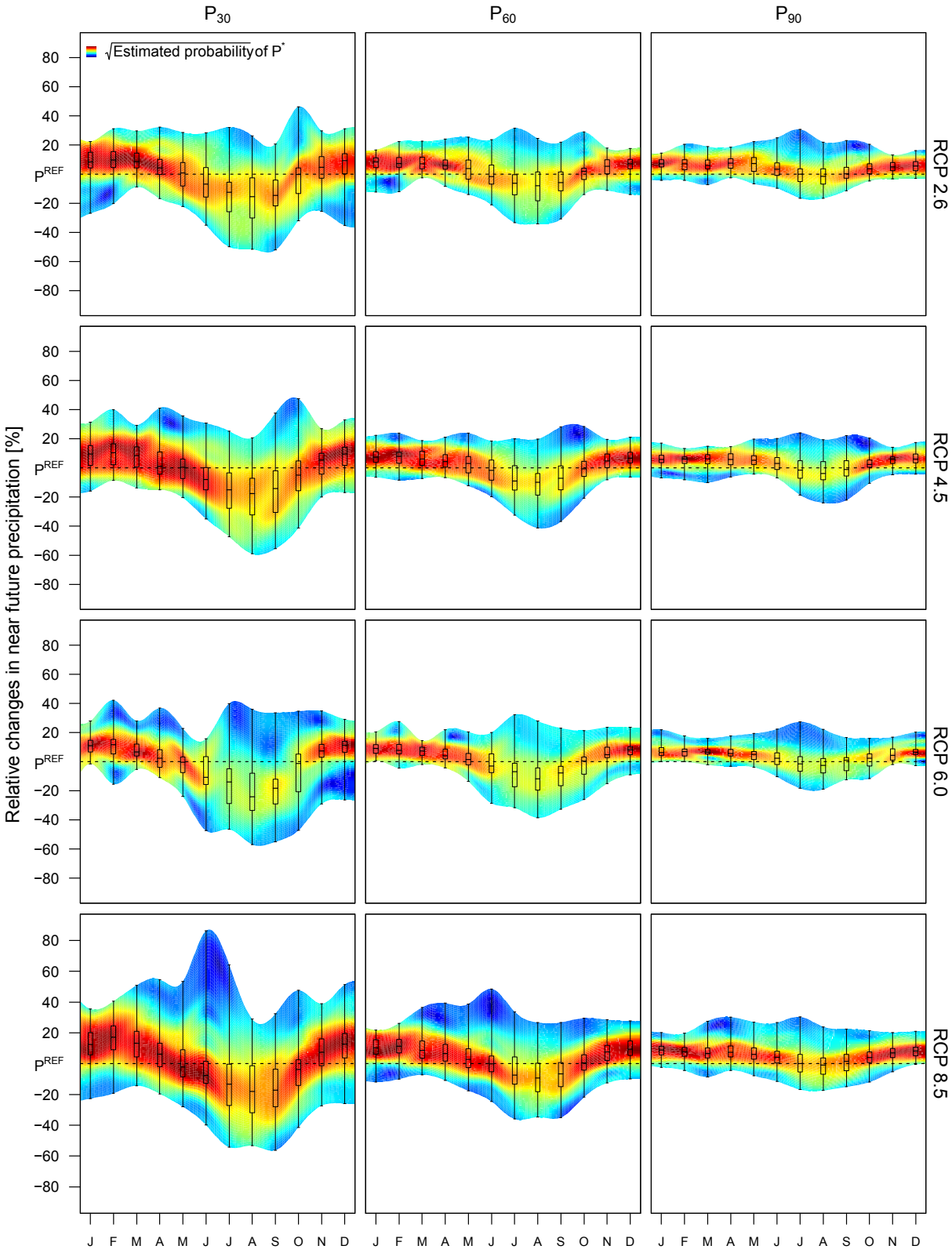

Figure C.1: Near future equivalent of Figure 16.

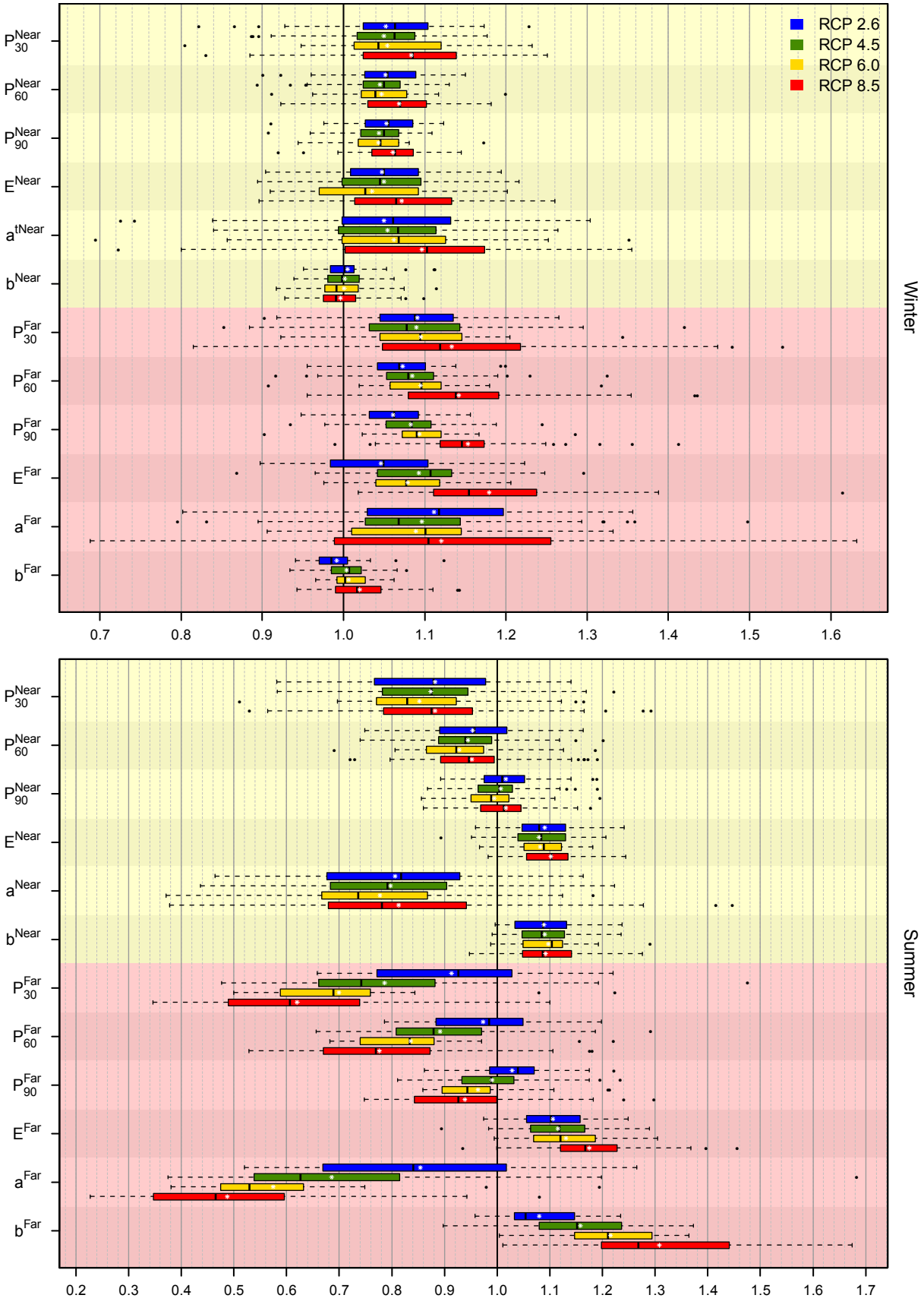

Figure D.1: Meuse basin equivalent of Figure 17.

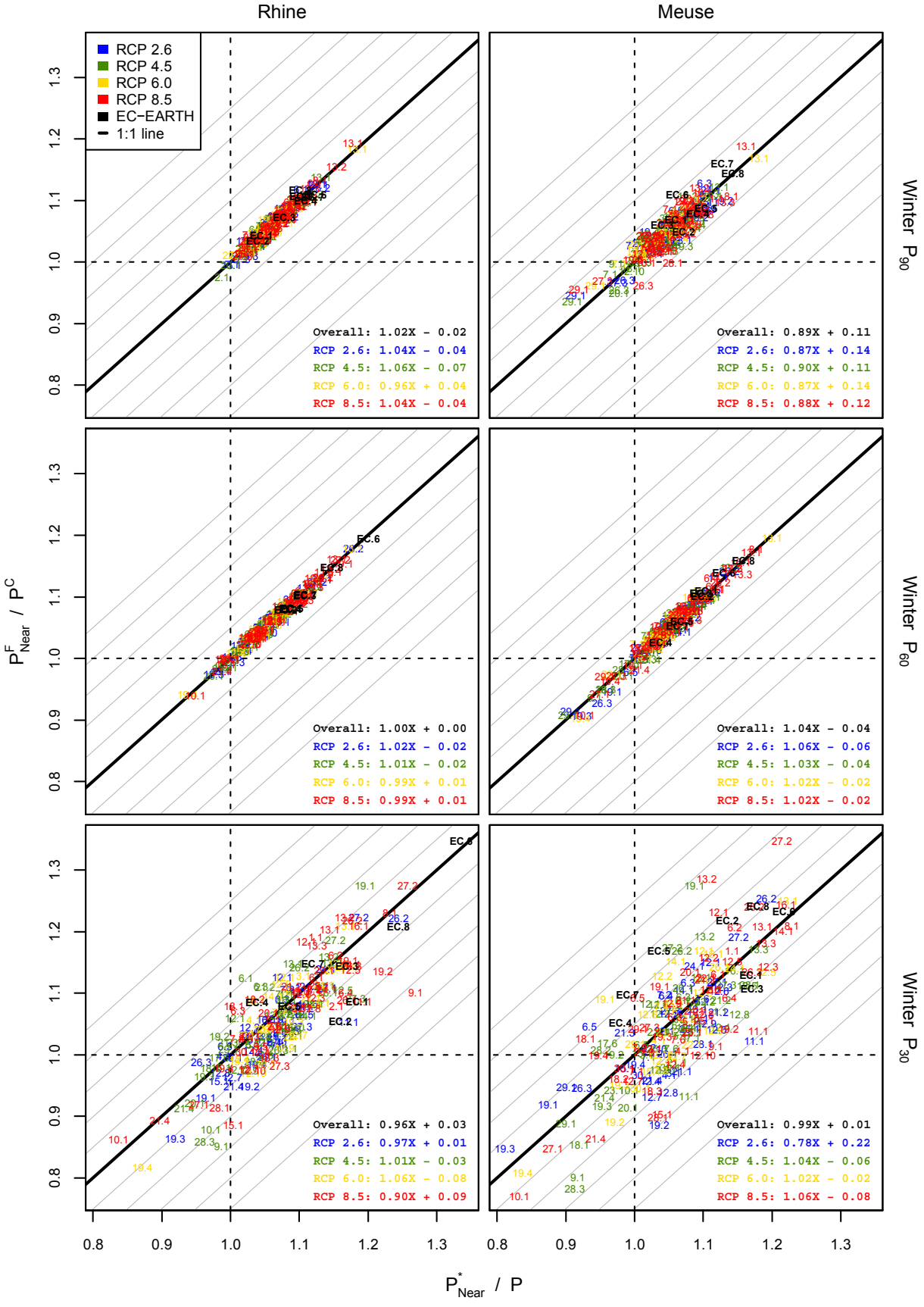

Figure E.1: Near future equivalent of Figure 12.

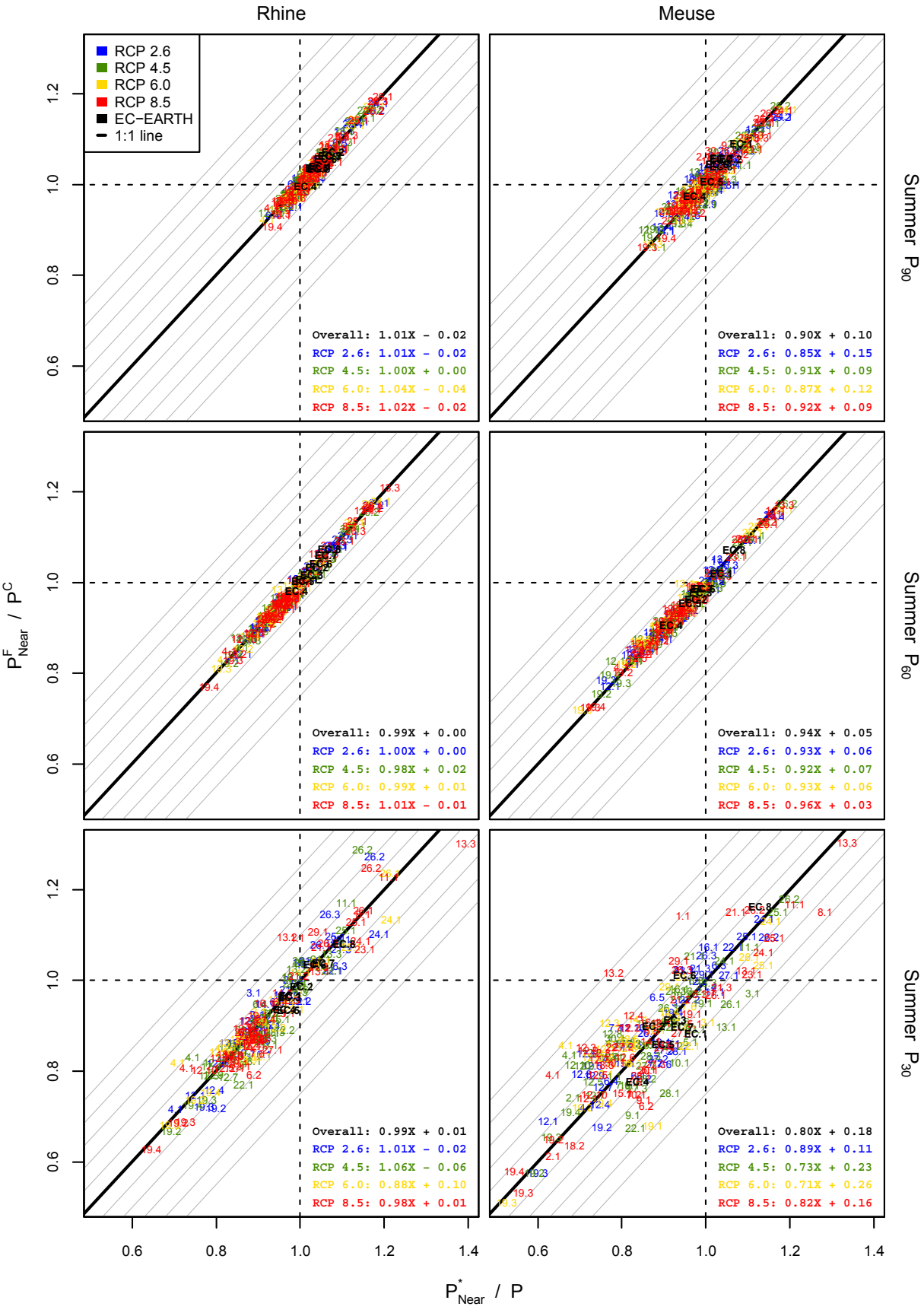

Figure E.2: Near future equivalent of Figure 13.

KNMI
Advanced Delta Change method

Application Manual

March 2013

Philip Kraaijenbrink
Royal Netherlands Meteorological Institute

Alena Pavlásková
Czech University of Life Sciences

Royal Netherlands
Meteorological Institute
Ministry of Infrastructure and the Environment

TABLE OF CONTENTS

1. Introduction

1.1. The delta change method

The delta change method is a transformation that scales historical precipitation time series to obtain series that are representative for a future climate. The coefficients required in the transformation are obtained from a global climate model (GCM) climate change signal. For precipitation this signal is essentially the relative difference in precipitation between a control period of the GCM, i.e. the same period as the historical time series, and a future period. As the historical data and GCM data is usually present on very different spatial scales, a linkage between the two scales is required. This is performed by the use of a common grid to which the observation data is aggregated and the GCM data is interpolated.

The advanced delta change (ADC) method (van Pelt et al., 2012) is a revised delta change method that uses a non-linear transformation of observed precipitation data. By using a non-linear transformation changes in the distribution of precipitation are taken into account. This specific revision focusses on details in the high end of the distribution to improve for example the use of the transformed data for extreme discharge modelling, as it is based on the 60% and 90% quantiles (P_{60} and P_{90}) of the precipitation distribution. Inherent to the method is a correction for the biases of P_{60} and P_{90} that exist between the control period of the GCM and the historical reference period.

1.2. Transformation calculations

The equations involved with the ADC method are described in Van Pelt et al. (2012). The exact method for which this manual is applicable is an extension to Van Pelt's method developed by Kraaijenbrink (2013). In Kraaijenbrink's report the pre-processing steps, data and exact calculations are extensively described. For further information about the process and definitions of the terms used in this manual, please consult this report.

The ADC method can be split in two main parts. The first part determines the transformation coefficients *a* and *b* and the ratio between the means of future and control excesses. The second part of the ADC method is the application of the transformation parameters to observation datasets. A flowchart of the calculations involved in the second part is shown in Figure 1. To provide a service to end-users, it is chosen to provide the pre-determined transformation parameters to the community. They are determined for a large part of Europe and for two future periods. This way end-users do not have to occupy themselves with the first step and can apply the parameters to their own datasets directly.

For hydrological modelling purposes temperature data is often required besides precipitation data. Therefore a separate linear transformation of temperature is performed as well (Kraaijenbrink, 2013).

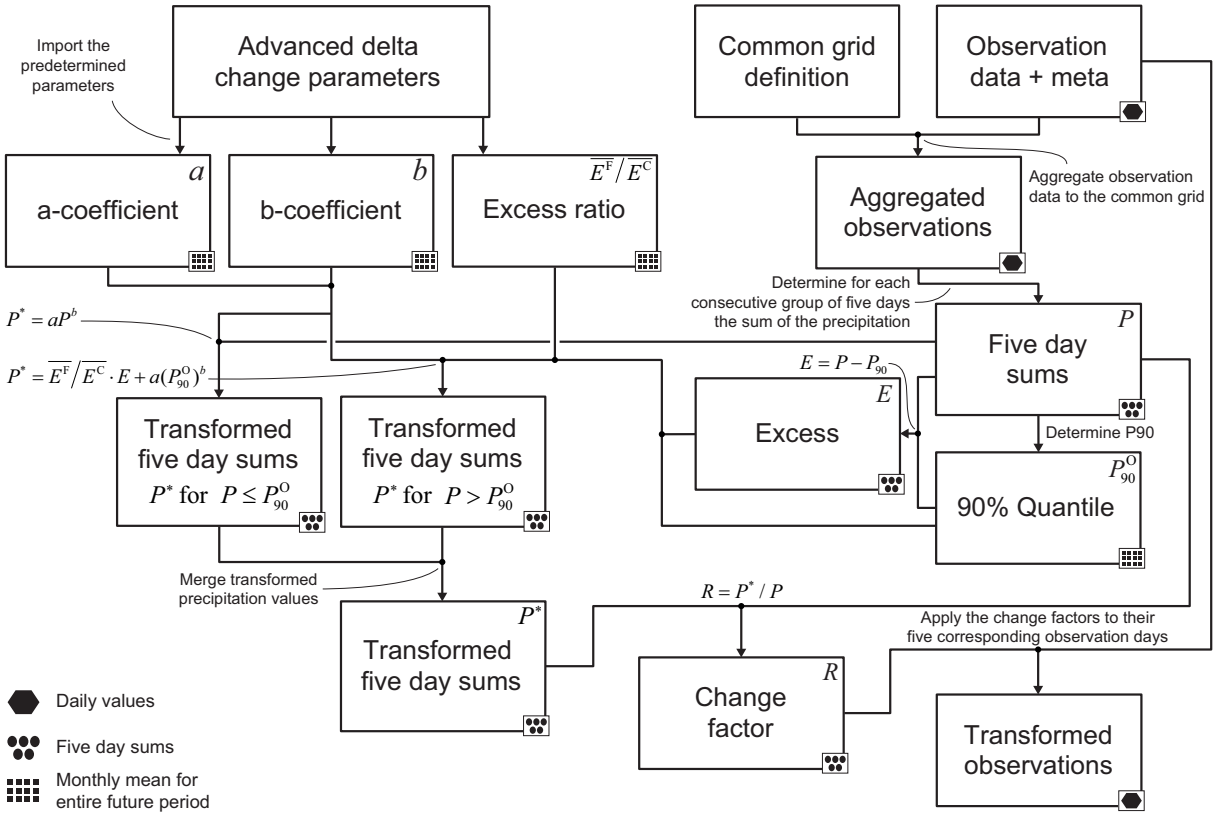

Figure 1: Flowchart of the transformation of the observation time series, or "application of the coefficients".

2. Available GCM data

The GCM data from which the ADC transformation parameters are determined originate from the Coupled Model Intercomparison Project Phase 5 (CMIP5). This set of models is based on four different climate forcings, the so called Representative Concentration Pathways (RCPs), that have forcings in W/m^2 at the top of the atmosphere of 2.6, 4.5, 6.0 and 8.5 by the year 2100. The time slices that were selected from the GCMs comprise one control period (1961-1995), a near future period (2021-2050) and a far future period (2071-2100).

As many CMIP5 GCMs as possible were used. Their final number was limited by availability of daily precipitation and temperature data as well as the presence of errors or missing data within the selected time slices. Additionally to the GCMs from the CMIP5 archive, eight model runs from the EC-EARTH model (version 2.3 extra) were included, a model partly developed and parameterized by the KNMI. This is a slightly different version of the EC-EARTH model that can be found as part of CMIP5. The final list of included models and number of runs per RCP are presented in Table 1.

Model (n=31)	**Model realizations**	**RCP 2.6 runs**	**RCP 4.5 runs**	**RCP 6.0 runs**	**RCP 8.5 runs**	**Total runs**
ACCESS1-0	1	-	1	-	1	2
ACCESS1-3	1	-	1	-	1	2
bcc-csm1-1	1	1	1	1	1	4
bcc-csm1-1-m	1	1	1	1	1	4
BNU-ESM	1	1	1	-	1	3
CanESM2	5	5	5	-	5	15
CCSM4	3	3	3	3	3	12
CMCC-CESM	1	-	-	-	1	1
CMCC-CM	1	-	1	-	1	2
CMCC-CMS	1	-	1	-	1	2
CNRM-CM5	1	1	1	-	1	3
CSIRO-Mk3-6-0	10	10	10	10	10	40
FGOALS-s2	3	1	3	1	3	8
GFDL-CM3	1	1	-	1	1	3
GFDL-ESM2G	1	1	1	1	1	4
GFDL-ESM2M	1	1	1	1	1	4
GISS-E2-R	1	-	1	-	-	1
HadGEM2-CC	3	-	1	-	3	4
HadGEM2-ES	4	4	4	4	4	16
inmcm4	1	-	1	-	1	2
IPSL-CM5A-LR	4	4	4	1	4	13
IPSL-CM5A-MR	1	1	1	1	1	4
IPSL-CM5B-LR	1	-	1	-	1	2
MIROC-ESM	1	1	1	1	1	4
MIROC-ESM-CHEM	1	1	1	1	1	4
MIROC5	3	3	3	1	3	10
MPI-ESM-LR	3	3	3	-	3	9
MPI-ESM-MR	3	1	3	-	1	5
MRI-CGCM3	1	1	1	1	1	4
NorESM1-M	1	1	1	1	1	4
EC-EARTH	8	-	-	-	8	8
Total	69	46	57	30	66	**199**

Table 1: Models, realizations and runs per RCP for which ADC transformation parameters are determined. For all entries both near future and far future parameters are available.

3. Available spatial extent

The defined common grid (Fig. 2), on which all transformation calculations are performed, has an extent that ranges from 14° W to 36° E and from 32° N to 62° N. The grid cell dimensions are 1.25° latitude by 2° longitude. In total there are 411 cells for which the transformation parameters could be determined. All cells are indexed using 4 digits in the form YY.XX, using y and x indices as shown in the figure.

Vector data of the common grid map in the form of an ArcGIS shapefile (ESRI, 2010) is included in the processing package. This, together with spatial data of the dataset that is to be transformed, can be used to visualise the location of the data with respect to the common grid, for instance for presentation in a report.

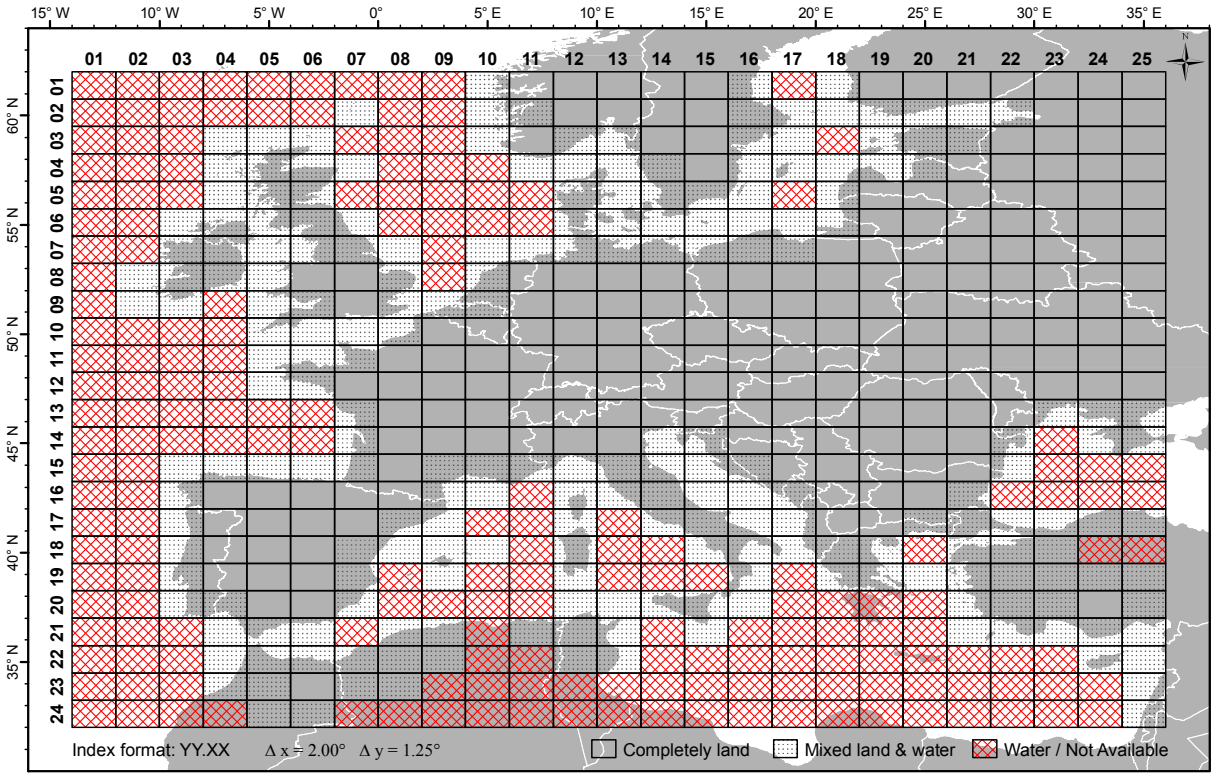

Figure 2: The common grid used in in transformation.

In the coastal areas the common grid cells, as a result of interpolation of the GCMs to the common grid, comprise a mixture of land and sea characteristics that can be quite different for precipitation and temperature. Usability of these cells is therefore limited. A quantification of the per cell usability is shown in Figure 3. See Kraaijenbrink (2013) for further details on this quantification. The usability data is included as an attribute of the common grid shapefile and in the parameter NetCDF files as a variable.

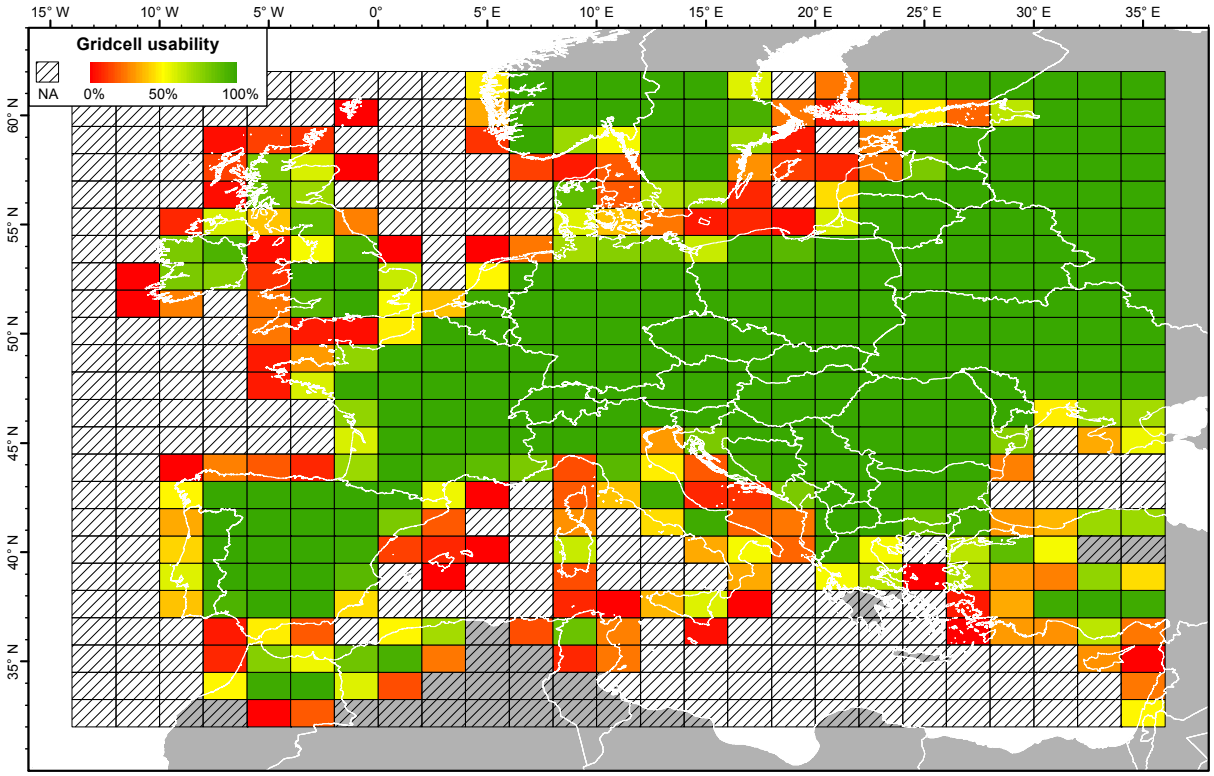

Figure 3: The quantified usability of the common grid cells in the ADC method.

4. Required software

4.1. R

All transformation calculations are perfomed by scripts written for R (R Development Core Team, 2008), a free software package for statistical computing and graphing. It runs on a wide variety of UNIX distributions, Windows and MacOS. The software can be downloaded from *http://www.r-project.org/*. R comes with a command line interface and on Windows and MacOS also with its standard graphical user interface (GUI). There are many third party GUIs developed for R such as RStudio, Rkward and R Commander, which some users might find easier to use. Execution of the provided scripts however, does not require advanced R usage so the command line or standard GUI should suffice.

4.2. R-packages

Additionally to R three R-packages are required for the scripts to work, namely *RNetCDF, tcltk2* and *stringr*. They are resprectively used to load NetCDF data, provide a graphical progress bar during processing and to perform string manipulation. The packages can be downloaded from the Comprehensive R Archive Network (CRAN) via the menus of the GUI of preference or by using the following syntax on the R command line:

```
install.packages(c("RNetCDF","tcltk2","stringr"), dependencies=TRUE);
```

4.3. Notepad++

All R-scripts were developed on a UNIX distribution and therefore the end of line (EOL) convention that is used in the scripts is the convention used on UNIX and MacOS. On Windows machines another EOL convention is used and text editors such as notepad will not display the scripts correctly, i.e. no line breaks will be visible. When working on a Windows operating system it is therefore recommended to open and edit the scripts in a R GUI or by using a text editor that can deal with different EOL conventions. An example of a versatile editor with that capability is Notepad++, available for free online at *http://notepad-plus-plus.org/*.

5. Input data requirements

As it is unknown which daily precipitation and/or temperature data end-users will transform, it is chosen to provide the method for input observation data of different spatial definitions. These can for instance be vector representations such as sub-basins, (ir)regular gridded datasets or meteostation datasets. However, for representativity of the input data it is important that the spatial resolution of the input data is not coarser than that of the common grid.

To be able to handle the different datatypes, they all have to be provided to the scripts in a similar ASCII table format. Furthermore, a descriptive metadata table must be provided. After processing, the scripts output a table in the exact same format. It is therefore required that users convert their data of choice to the table format for processing and, if necessary, convert the output back to the original form after processing.

5.1. Time period of input data

The reference period for which the transformation parameters are determined is 1961-01-01 to 1995-31-12. It is not required that the input data of choice mimics this period exactly, although it is advisable to use a period that is considered to have a corresponding climate. The reference period of the input data of choice thus may vary in length and position in time. It is impossible to give precise guidelines, but any period with a length of 20 to 45 years within the timeframe 1950-2005 possibly produces representative results. It may however be valuable to evaluate the differences between the exact reference period used for the parameters and the period intended by the user. Note that it is however required that the start and end of the chosen time period corresponds to the beginning and end of a calendar year and that the series must not have any missing dates.

5.2. Input data format

Input data tables for precipitation and temperature must have daily values on the first dimension (rows) and the different areas, cells or stations on the second dimension (columns). Important is that the first column must contain the dates in a numeric YYYYMMDD form. It is also required to provide column headers in the first row. The table columns must be delimited by a single space (" ") and the values must use a point (".") as decimal separator. Input precipitation and temperature data must have values in respectively mm and °C. An example subset of a correct input data table:

```
"date" "area_1" "area_2" "area_3" "area_4"
19610101 0.5 0.3 0.6 0.2
19610102 0.9 0.1 0.1 0
19610103 0.6 0.1 0.2 0.1
19610104 2.6 1 1.3 0.7
19610105 5.6 5.2 4.8 4.1
```

5.3. Input metadata format

The metadata table must contain rows that represent the areas/cells/stations and columns that represent their characteristics. The rows must have the same top to bottom order as the left to right order of the columns in the input data table. The column order and contents must be exactly as follows: area/cell/station index, longitude of centroid (degrees E), latitude of centroid (degrees N) and surface area (any unit). After these mandatory columns extra columns with metadata may be present,

these will not be used during processing. Again, the table columns must be delimited by a single space (" "), the values must use a point (".") as decimal separator and column headers must be present. An example subset of a correct input metadata table (mandatory colums are in regular font, additional colums in italic):

```
"index" "centroid_x" "centroid_y" "area" "name" "KNMI_order"
1 5.699 48.3932 2614 "Meuse (St. Mihiel)" 1
2 5.5186 49.5007 2211 "Chiers" 3
3 5.3354 49.179 1299 "Meuse (St. Mihiel-Stenay)" 2
4 4.7574 49.7428 2271 "Meuse (Stenay-Chooz)" 4
```

5.4. Area-weighted data aggregation

The input data is automatically aggregated to the common grid during processing. This is performed by the calculation of a area-weighted mean of the areas/cells/stations that have their centroids within a specific common grid cell. This area-weighted averaging is only meaningful if the input data comprises areas of different size, which can be the case with vector or irregular gridded datasets. For regular gridded or meteostation datasets the surface area input for all cells or stations can be set to equal values, e.g. 1. If one would like to assign weights to different cells or stations the surface area entries in the metadata table can be set accordingly.

5.5. Automatic grid cell assigment overrides

It might be that some common grid cells are only covered by a few input areas/cells/stations. Examples of this are shown in Figure 4 for the grid cells 11.13, 9.15, 10.17 and 11.17. This is undesirable as such a small area is less representative for the precipitation or temperature of a whole common grid cell. In these cases the user can override the automatic grid cell assignment and assign all areas/cells/stations in a specific grid cell to another grid cell of their choice. How to implement such an override is explained in section 6.1.4. If desired to distribute areas/cells/stations in a specific grid cell over multiple other grid cells, which for example might be desired for the basins in cell 09.12 of Figure 4, it is easiest to alter their coordinates in the metadata table.

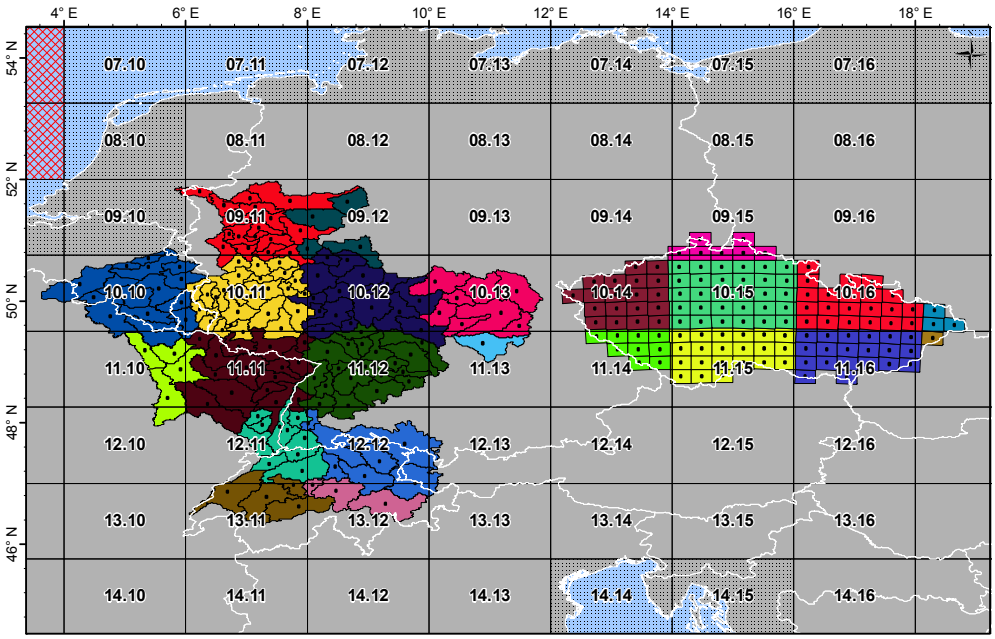

Figure 4: Example of the automatic grid cell assignment of vector sub-basins (left) and a regular gridded dataset (right).

6. Contents of the processing package

6.1. Main scripts

6.1.1. SETTINGS_apply_delta.r

This script is used to define variables that are required in the transformation scripts. Here the input data, input metadata, parameter data, and output directory must be specified. Note that the output directory must exist before processing, otherwise R will give an error.

6.1.2. apply_delta_precipitation.r and apply_delta_temperature.r

These scripts perform the transformation calculation for respectively precipitation and temperature data. They are designed as independent scripts because not every user will require both and/or may not have both types of data. When the input data and metadata is correctly formatted and the settings script contains the correct paths, the scripts should work. They automatically aggregate the input data to the common grid, perform the transformation and store disaggregated transformed data in the output directory. No edits have to be made by the user in these two scripts.

6.1.3. obtain_modellist.r

For the scripts to run correctly a table is required in the root directory of the processing package. The table, *models_to_process.csv*, contains a list of model runs that must be processed along with some characteristics of the runs. The table is not present at default and must be created first using the script *obtain_modellist.r*.

The script uses the filenames of the NetCDFs parameter filenames to create the table. By default it recreates the entire model table, i.e. a table of all available combinations of models, runs, RCPs and future periods (n=398). By adding lines of code it is easy to make subsets of the table, for instance to use only a specific period or RCP. This provides an easy and powerful way of managing the model runs that will be processed. In the script it is indicated were to put these lines. Some examples:

```
# select only single model:
models <- models[which(models$model == "HadGEM2-ES"),]

# select all IPSL-CM5A-MR, IPSL-CM5A-LR and IPSL-CM5B-LR models:
models <- models[grep("IPSL-CM",models$model),]

# select only the far future (2071-2100) and RCP 8.5 (note that the values for RCPs
# used in the script comprise the original W/m2 multiplied by 10)
models <- models[which(models$startyear == 2071 & models$rcp == 85),]

# remove RCP 2.6 entries from the table
models <- models[-which(models$rcp == 26),]
```

Once created, *models_to_process.csv* can also be edited manually. Note that table format and the model and run names must be completely similar as those in the original *models_to_process.csv*, otherwise the parameter files cannot be located correctly and processing will yield errors. If editing manually, it is preferable to use a text editor (e.g. notepad++, gedit) rather than spreadsheet software (e.g. MS Excel, Libre Office Calc) or word processors (e.g. MS Word, wordpad) as these can alter the formatting of the CSV-file harmfully.

6.1.4. determine_gridcells.r

This script is used to determine which common grid cells encompass the input data. It does so by using the coordinates of the common grid cells and those of the centroids provided in the metadata

table. It is not required to edit this script. Running this script generates two files in the processing package root directory:

- PDF-file called *gridcell_assignment.pdf* that contains a plot that shows the position of the centroids with respect to the common grid. The centroids that are assigned to each grid cell are randomly coloured. As they are randomly coloured it can be that the colours are indistinct, in that case run the script again. The plot can be used to determine if it would be better to override the automatic grid cell assignment for some cells. An example of the plot is shown in Figure 5.
- A text file called *gridcell_assignment.txt* that contains two columns: "original" and "target". Both columns initially contain equal values, i.e. all the indices of the grid cells that encompass the input data. If it is desired to override any of the automatically assigned grid cells, the indices of the cells that should be overridden must be changed to the indices of the grid cells that one would like to override them with. The indices must be changed in the "target" column, the "original"-column must remain as it is. In the transformation scripts the indices that are present in the text file are loaded to achieve the override, therefore this file must not be deleted.

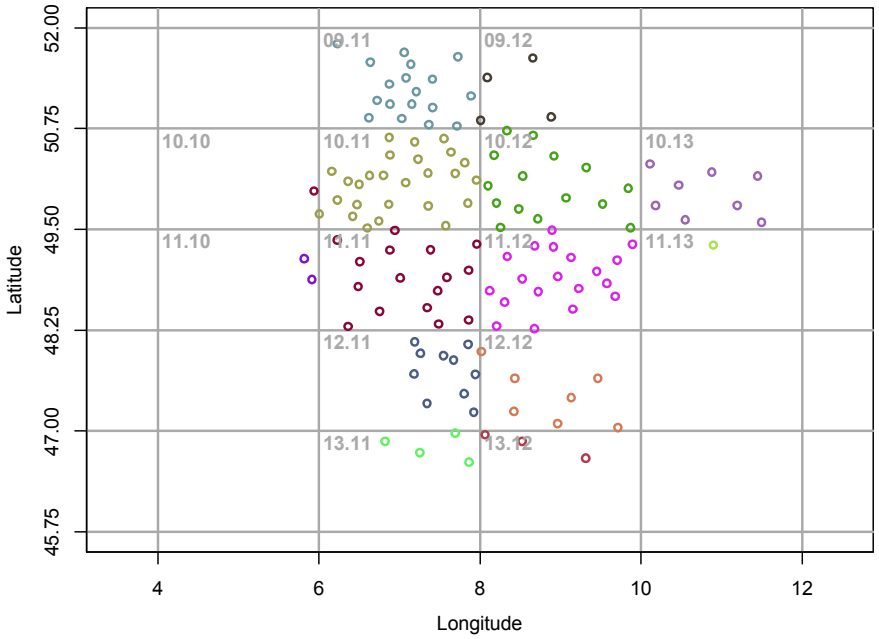

Figure 5: Example of a plot that *determine_gridcells.r* will produce.

6.2. Shared scripts and files

6.2.1. date_vector_and_leap_days.r

This auxiliary script is used to determine the leap days that are present in the input dataset. These are removed from the data, treated separately and reinserted later. The script also produces a vector of month assignments. The latter is used by the precipitation transformation scripts, as the month definition used in the ADC method is not equal to normal Gregorian months. The ADC method acts on five day sums of which there are 73 in a 365-day year. These 73 five day sums are distributed over the 12 months by using 6 five day sums for January-November and 7 five day sums for December. This script should not be edited.

6.2.2. common_grid_definition.r

This script generates tables that contain information about the common grid and the grid cells chosen by the user. This is used in the main scripts to automatically aggregate the input data and to form a bridge between spatial and tabular representations the data. This script should not be edited.

6.2.3. all_available_grid_indices.txt

This file contains a list with all the 411 common grid cells for which parameters are determined. The file is used in *common_grid_definition.r* to correctly generate the variables that define the common grid. This file should not be edited.

6.2.4. Parameter NetCDFs

The NetCDF parameter files, located in "`./data/parameters/`", contain the transformation parameters used in the transformation of precipitation and temperature. Besides the parameters, additional data is present such as the 30%, 60% and 90% quantiles of the control and future period as well as mean precipitation and temperature. Also the grid cell usability quantification is included. Note that all parameters and data comprise monthly values over the entire period, i.e. 12 values per gridcell. In the scripts the parameter data is loaded automatically so there is no need to extract any data from the NetCDF manually, unless further analysis of the additional data, which is not needed for ADC processing, is intended. The NetCDF header of one of the parameter files is presented as appendix A, which shows the contents present in each NetCDF parameter file.

6.2.5. Shapefiles and maps

The vector representation of the common grid is included as a shapefile which can be opened in ArcGIS and most other GIS software packages as well as in R using the R-packages *rgdal* and *maptools*. The shapefile consist of multiple files with the same base name and different extensions (.shp, .shx, .dbf etc.) that must be kept together. The very same map as Figure 2 is included as a mxd-file, which can only be opened in ArcGIS. To correctly display the map, a shapefile with the country outlines is included as well. The files are located in "`./data/shapefiles/`".

6.3. Literature and figures

The original paper on the ADC method of Van Pelt et al. (2012) that appeared in Hydrology and Earth System Sciences, the report of Kraaijenbrink (2013) and this manual are included as PDF-files in the folder "`./reference`". These documents should provide sufficient background knowledge for the ADC method and the scripts in this processing package. The paper and the report present further analyses of transformed datasets that can provide ideas of what is possible analysis-wise. Kraaijenbrink's report presents evaluations of the differences in transformation results for the Rhine and Meuse basins when using the different models and RCPs described in chapter 2. This can be useful to determine which models and/or model runs one would like to use to transform input data. Furthermore, PDF-files of the common grid map and the flowchart (Figure 1 and 2) as well as a spreadsheet with the model list (Table 1) are included in the folder "`./reference/figures/`".

7. Stepwise processing guide

1. Install R and the required R-packages described in section 4.2 on your computer. If working on a Windows OS consider installing Notepad++.

2. Extract the *ADC_processing_package* directory in the provided zip-archive to a location on your harddrive. The path to this directory must be the working directory used in R. Every time R is started to run any of the provided scripts this working directory must be set manually first on the R command line, otherwise the relative paths defined in the scripts cannot locate the required auxiliary files. The working directory can be set using the following syntax. Note that R always uses forward slashes in paths.

   ```
   setwd("path/to/the/extracted/ADC_processing_package")
   ```

   It is advisable to not alter the structure of the processing package, as this causes the relative paths defined in the scripts to become broken.

3. Convert the daily historical precipitation and/or temperature data of choice to the necessary table format described in section 5.2**Error! Reference source not found.**.

4. Create a metadata table for the areas/cells/stations of your data in the required format described in section 5.3.

5. Open *SETTINGS_apply_delta.r* in a text editor and set the correct the path to the input data and metadata as well as the desired output directory (must pre-exist!). Note that if all available NetCDF parameter files are used the input data will be transformed 398 times, hence enough disk space is required at the output location to store 398 times the size of the input data table.

6. Run *determine_gridcells.r* by pressing a "run" button in the R GUI of preference or by using the `source` command on the R command line as follows:

   ```
   source("./determine_gridcells.r")
   ```

   Open *gridcell_assignment.pdf* that is created by the script in the root of the working directory. Inspect the plot and determine if overrides of the automatic grid cell assignment are needed. If so, apply these overrides in the text file *gridcell_assignment.txt* using the method described in section 6.1.4, bullet 2.

7. Generate *models_to_process.csv* by running *obtain_modellist.r*. If desired create a subset of the table using the methods described in section 6.1.3.

8. Run the script *apply_delta_precipitation.r* or *apply_delta_temperature.r* to start transforming the daily input data. A window will pop up that shows the script's progress. When finished the transformed daily data is present in the chosen output directory. The output data filenames follow the CMIP5 naming convention with a *P_trans* or *T_trans* prefix, indicating resp. transformed precipitation or temperature files.

In case of any questions about the processing or the ADC method please contact Jules Beersma at *jules.beersma@knmi.nl*.

References

ESRI. (2010), ArcGIS 10. Redlands, CA, USA:

Kraaijenbrink P. D. A. (2013). Advanced delta change method: extension of an application to CMIP5 GCMs. De Bilt: KNMI.

R Development Core Team. (2008), R: A language and environment for statistical computing. R Foundation for Statistical Computing, Vienna, Austria.

van Pelt, S., J. Beersma, T. Buishand et al. (2012), Future changes in extreme precipitation in the Rhine basin based on global and regional climate model simulations. Hydrol. Earth Syst. Sci. 16, pp.4517-4530.

Appendix A: Contents of a parameter NetCDF file

```
netcdf ADCparams61-95_ACCESS1-0_rcp45_r1i1p1_20710101-21001231 {
dimensions:
        latitude = 24 ;
        longitude = 25 ;
        month = 12 ;
variables:
        double longitude(longitude) ;
                longitude:description = "The x-coordinates of the gridcell center" ;
                longitude:units = "degrees E" ;
                longitude:_FillValue = -9999. ;
        double latitude(latitude) ;
                latitude:description = "The y-coordinates of the gridcell center" ;
                latitude:units = "degrees N" ;
                latitude:_FillValue = -9999. ;
        double P30_obs(month, longitude, latitude) ;
                P30_obs:description = "Temporally smoothed 30% percentile of precipitation
(observations)" ;
                P30_obs:units = "mm" ;
                P30_obs:_FillValue = -9999. ;
        double P60_obs(month, longitude, latitude) ;
                P60_obs:description = "Temporally smoothed 60% percentile of precipitation
(observations)" ;
                P60_obs:units = "mm" ;
                P60_obs:_FillValue = -9999. ;
        double P90_obs(month, longitude, latitude) ;
                P90_obs:description = "Temporally smoothed 90% percentile of precipitation
(observations)" ;
                P90_obs:units = "mm" ;
                P90_obs:_FillValue = -9999. ;
        double Pmean_obs(month, longitude, latitude) ;
                Pmean_obs:description = "Unsmoothed means of precipitation (observations)" ;
                Pmean_obs:units = "mm" ;
                Pmean_obs:_FillValue = -9999. ;
        double Pstdev_obs(month, longitude, latitude) ;
                Pstdev_obs:description = "Unsmoothed standard deviation of precipitation
(observations)" ;
                Pstdev_obs:units = "mm" ;
                Pstdev_obs:_FillValue = -9999. ;
        double P30_con(month, longitude, latitude) ;
                P30_con:description = "Temporally smoothed 30% percentile of precipitation
(control run)" ;
                P30_con:units = "mm" ;
                P30_con:_FillValue = -9999. ;
        double P60_con(month, longitude, latitude) ;
                P60_con:description = "Temporally smoothed 60% percentile of precipitation
(control run)" ;
                P60_con:units = "mm" ;
                P60_con:_FillValue = -9999. ;
        double P90_con(month, longitude, latitude) ;
                P90_con:description = "Temporally smoothed 90% percentile of precipitation
(control run)" ;
                P90_con:units = "mm" ;
                P90_con:_FillValue = -9999. ;
        double Pmean_con(month, longitude, latitude) ;
                Pmean_con:description = "Unsmoothed means of precipitation (control run)" ;
                Pmean_con:units = "mm" ;
                Pmean_con:_FillValue = -9999. ;
        double Pstdev_con(month, longitude, latitude) ;
                Pstdev_con:description = "Unsmoothed standard deviation of precipitation
(control run)" ;
                Pstdev_con:units = "mm" ;
                Pstdev_con:_FillValue = -9999. ;
        double P30_fut(month, longitude, latitude) ;
                P30_fut:description = "Temporally smoothed 30% percentile of precipitation
(future run)" ;
                P30_fut:units = "mm" ;
                P30_fut:_FillValue = -9999. ;
        double P60_fut(month, longitude, latitude) ;
                P60_fut:description = "Temporally smoothed 60% percentile of precipitation
(future run)" ;
                P60_fut:units = "mm" ;
                P60_fut:_FillValue = -9999. ;
        double P90_fut(month, longitude, latitude) ;
                P90_fut:description = "Temporally smoothed 90% percentile of precipitation
(future run)" ;
                P90_fut:units = "mm" ;
                P90_fut:_FillValue = -9999. ;
        double Pmean_fut(month, longitude, latitude) ;
                Pmean_fut:description = "Unsmoothed means of precipitation (future run)" ;
                Pmean_fut:units = "mm" ;
                Pmean_fut:_FillValue = -9999. ;
        double Pstdev_fut(month, longitude, latitude) ;
```

```
                Pstdev_fut:description = "Unsmoothed standard deviation of precipitation
(future run)" ;
                Pstdev_fut:units = "mm" ;
                Pstdev_fut:_FillValue = -9999. ;
        double a(month, longitude, latitude) ;
                a:description = "Transformation coefficient (a = P60f / (P60c)^b * g1^(1-b)" ;
                a:units = "factor" ;
                a:_FillValue = -9999. ;
        double b(month, longitude, latitude) ;
                b:description = "Transformation coefficient (b = log((g2*P90f)/(g1*P60f)) /
log((g2*P90c)/(g1*P60c)))" ;
                b:units = "factor" ;
                b:_FillValue = -9999. ;
        double excess_con(month, longitude, latitude) ;
                excess_con:description = "Part of precipitation above P90 (E = P-P90), for
control period" ;
                excess_con:units = "mm" ;
                excess_con:_FillValue = -9999. ;
        double excess_fut(month, longitude, latitude) ;
                excess_fut:description = "Part of precipitation above P90 (E = P-P90), for
future period" ;
                excess_fut:units = "mm" ;
                excess_fut:_FillValue = -9999. ;
        double excess_factor(month, longitude, latitude) ;
                excess_factor:description = "Temporally and spatially smoothed delta excess
(Ef/Ec)" ;
                excess_factor:units = "factor" ;
                excess_factor:_FillValue = -9999. ;
        double EOBS_NA_fraction(longitude, latitude) ;
                EOBS_NA_fraction:description = "Fraction of original 0.25 degree E-OBS cells
that were NaN and were used for the aggregation of a \'common grid\' E-OBS cell" ;
                EOBS_NA_fraction:units = "fraction" ;
                EOBS_NA_fraction:_FillValue = -9999. ;
        double T_mean_con(month, longitude, latitude) ;
                T_mean_con:description = "Mean of temperature (control run)" ;
                T_mean_con:units = "Kelvin" ;
                T_mean_con:_FillValue = -9999. ;
        double T_mean_fut(month, longitude, latitude) ;
                T_mean_fut:description = "Mean of temperature (future run)" ;
                T_mean_fut:units = "Kelvin" ;
                T_mean_fut:_FillValue = -9999. ;
        double T_stdev_con(month, longitude, latitude) ;
                T_stdev_con:description = "Temporally smoothed st.dev of temperature (control
run)" ;
                T_stdev_con:units = "Kelvin" ;
                T_stdev_con:_FillValue = -9999. ;
        double T_stdev_fut(month, longitude, latitude) ;
                T_stdev_fut:description = "Temporally smoothed st.dev of temperature (future
run)" ;
                T_stdev_fut:units = "Kelvin" ;
                T_stdev_fut:_FillValue = -9999. ;

// global attributes:
                :title = "Parameters used in the Advanced Delta Change method to transform
historical timeseries (with a reference period of approx. 1961-1995) to a future period" ;
                :institution = "Royal Netherlands Meteorological Insititute (KNMI)" ;
                :transformation_reference_data = "E-OBS 0.25 degree gridded dataset, part of
the European Climate Assessment & Dataset project (http://www.ecad.eu/), regridded to common
grid." ;
                :transformation_reference_period = "1961-01-01 to 1995-12-31" ;
                :transformation_common_grid = "xmin=14W, xmax=36E, ymin=32N, ymax=62N,
delta_x=2, delta_y=1.25 (Coordinate system: latlon, Datum: WGS84)" ;
                :transformation_method = "Advanced Delta Change (ADC) method. Non-linear
precipitation transformation, linear temperature transformation." ;
                :transformation_GCM_project = "Climate Model Intercomparison Project 5 (CMIP5)"
;
                :transformation_GCM_model = "ACCESS1-0" ;
                :transformation_GCM_modelrun = "r1i1p1" ;
                :transformation_GCM_rcp = "RCP 4.5" ;
                :transformation_GCM_future_period = "2071-2100" ;
                :references = "The advanced delta change method is presentend in: van Pelt, S.
C., Beersma, J. J., Buishand, T. A., van den Hurk, B. J. J. M., and P. Kabat (2012). Future
changes in extreme precipitation in the Rhine basin based on global and regional climate model
simulations, Hydrol. Earth Syst. Sci., 16, 1-14." ;
                :comment = "This NetCDF file has been generated using the RNetCDF library in R"
;
                :creator = "P.D.A. Kraaijenbrink (KNMI & Utrecht University)" ;
                :disclaimer = "Copyright Royal Netherlands Meteorological Insititute (KNMI)" ;
                :history = "Original NetCDF file created on 2013-03-27" ;
}
```

A complete list of all KNMI-publications (1854 – present) can be found on our website

www.knmi.nl/knmi-library/knmipub_en.html

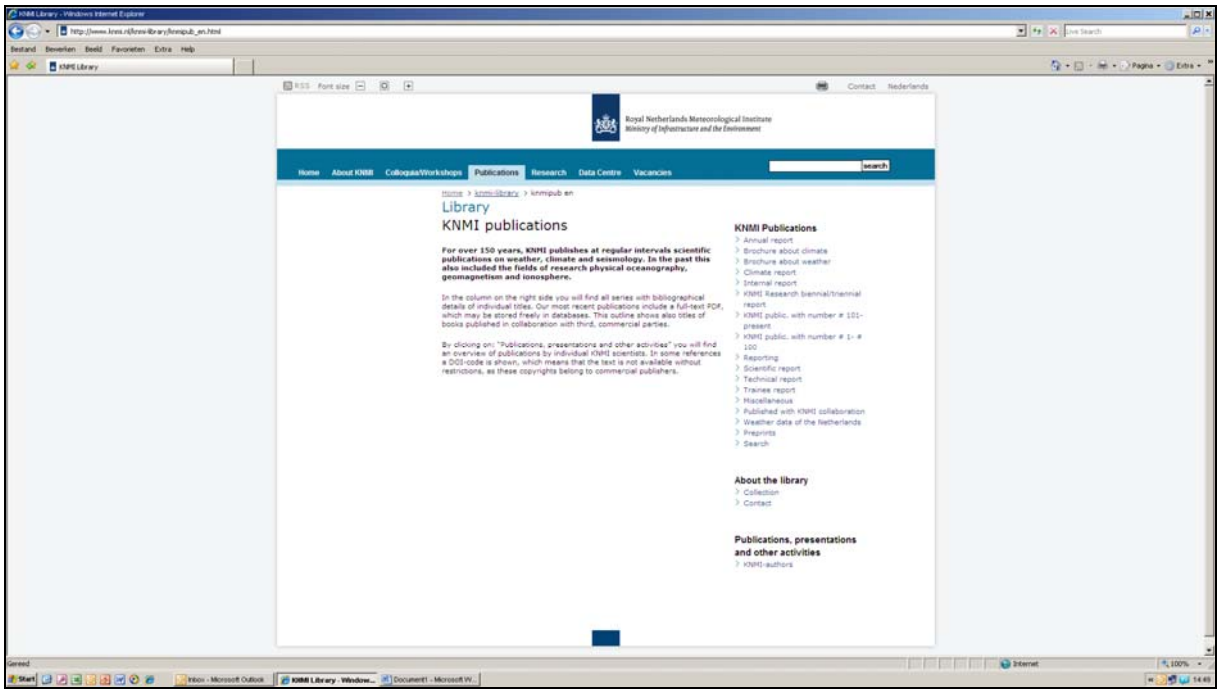

The most recent reports are available as a PDF on this site.